

# **The role of microtubules in initial neuronal polarization**

**Dissertation zur Erlangung des Doktorgrades der Naturwissenschaften**

**an der Fakultät für Biologie  
der Ludwig–Maximilians–Universität  
München**

**Angefertigt am Max-Planck-Institut für Neurobiologie  
in der Arbeitsgruppe 'Axonales Wachstum und Regeneration'**

**Vorgelegt von  
Harald Witte**

**München, 15. April 2008**



**Erstgutachter:**

**Prof. Dr. Rüdiger Klein**

**Zweitgutachter:**

**PD Dr. Angelika Böttger**

**Tag der mündlichen Prüfung:**

**09. Juli 2008**



### **Ehrenwörtliche Versicherung:**

Ich versichere hiermit ehrenwörtlich, dass ich die Dissertation mit dem Titel "The role of microtubules in initial neuronal polarization" selbständig und ohne unerlaubte Hilfe angefertigt habe. Ich habe mich dabei keiner anderen als der von mir ausdrücklich bezeichneten Hilfen und Quellen bedient.

### **Erklärung:**

Hiermit erkläre ich, dass ich mich nicht anderweitig einer Doktorprüfung ohne Erfolg unterzogen habe. Die Dissertation wurde in ihrer jetzigen oder ähnlichen Form bei keiner anderen Hochschule eingereicht und hat noch keinen sonstigen Prüfungszwecken gedient.

München, 15. April 2008

Harald Witte



Die vorliegende Arbeit wurde in der Arbeitsgruppe für „Axonales Wachstum und Regeneration“ von Dr. Frank Bradke am Max-Planck-Institut für Neurobiologie in Martinsried angefertigt.



***Für meine Familie***



<b>Table of Contents</b>	<b>I</b>
Table of Figures.....	V
Index of Tables .....	VII
Abbreviations.....	IX
<b>Summary</b>	<b>1</b>
<b>1. Introduction</b>	<b>3</b>
1.1 Neuronal polarity .....	3
1.2 Primary neuronal cultures .....	5
1.2.1 Characteristics of <i>in vitro</i> neuronal cultures .....	5
1.2.2 Dissociated hippocampal neurons in culture .....	6
1.3 Polarity regulation and the neuronal cytoskeleton .....	8
1.3.1 Signaling pathways involved in the specification of neuronal polarity .....	8
1.3.2 The actin cytoskeleton .....	13
1.3.3 Microtubules – More than just supporting actors? .....	16
1.4 Objectives of this study .....	20
<b>2. Results</b>	<b>21</b>
2.1 Microtubule turnover in neuronal cells .....	21
2.1.1 Microtubule turnover is decreased in axons .....	21
2.1.2 A reduction of microtubule turnover precedes axon formation.....	23
2.1.3 Differences in posttranslational modifications reflect an actual stability difference of microtubules .....	25
2.2 Microtubule turnover is changed in neurons whose polarity is affected by manipulation of polarity regulators .....	27
2.2.1 Microtubule turnover is reduced in supernumerary axons induced by inhibition of GSK-3 $\beta$ .....	28
2.2.2 Inhibition of GSK-3 $\beta$ leads to microtubule stabilization before axon formation .....	29
2.2.3 Polarization of microtubule stability is lost in SAD A / SAD B knockout neurons .....	30
2.3 Moderate microtubule destabilization selectively reduces the formation of minor neurites .....	31
2.4 Microtubule stabilization is sufficient to induce axon formation .....	33
2.4.1 Microtubule stabilization promotes neurite outgrowth.....	34
2.4.2 Taxol-induced processes show axonal characteristics.....	36
2.4.3 Microtubule acetylation alone is not sufficient to induce axon formation .....	38
2.5 Taxol application rapidly stabilizes microtubules and shifts dynamic microtubules to the tips of processes .....	40

2.6	<b>Local microtubule stabilization is sufficient to bias the site of axon formation.....</b>	<b>43</b>
<b>3.</b>	<b>Discussion</b>	<b>47</b>
3.1	<b>Microtubule stability correlates with the identity of neuronal processes.....</b>	<b>48</b>
3.1.1	Axonal microtubules show increased stability .....	48
3.1.2	Interfering with regulators of neuronal polarity results in altered microtubule stability... ..	48
3.2	<b>Microtubule stabilization causes axon formation .....</b>	<b>49</b>
3.2.1	Global pharmacological microtubule stabilization induces the formation of multiple axons.....	49
3.2.2	MAPs, microtubule stabilization and axon formation.....	50
3.3	<b>Microtubule stabilization precedes axon formation .....</b>	<b>53</b>
3.3.1	Microtubule stabilization and axon formation - Sequential events .....	53
3.3.2	Regulation of microtubule stabilization during neuronal polarization .....	53
3.3.3	Microtubule stability, posttranslational modifications and axonal transport.....	57
3.3.4	Local microtubule stabilization and feedback loops.....	59
<b>4.</b>	<b>Outlook</b>	<b>63</b>
<b>5.</b>	<b>Materials and Methods</b>	<b>65</b>
5.1	<b>Materials .....</b>	<b>65</b>
5.1.1	Chemicals .....	65
5.1.2	Drugs .....	66
5.1.3	Commercial kits.....	66
5.1.4	Enzymes and DNA markers .....	67
5.1.5	Equipment.....	67
5.1.6	Consumables.....	69
5.1.7	Media and standard solutions .....	71
5.1.7.1	Buffers and standard solutions.....	71
5.1.7.2	Media and supplements for primary cell culture .....	72
5.1.7.3	Media and antibiotics for bacterial culture .....	74
5.1.8	Antibodies.....	74
5.1.8.1	Primary antibodies.....	74
5.1.8.2	Secondary antibodies.....	75
5.1.9	Other dyes.....	76
5.1.10	Bacteria.....	76
5.1.11	Plasmids.....	76
5.1.12	Oligonucleotides.....	77
5.2	<b>Methods.....</b>	<b>77</b>
5.2.1	Cell Culture.....	77
5.2.1.1	Primary culture of hippocampal neurons.....	77
5.2.1.2	Primary culture of glia cells.....	78

5.2.1.3	Transfection of hippocampal neurons.....	78
5.2.1.4	Drug treatment.....	79
5.2.1.5	Microtubule stability assay.....	79
5.2.2	Microscopy.....	79
5.2.2.1	Image acquisition.....	79
5.2.2.2	Time lapse imaging (Video microscopy).....	80
5.2.2.3	Image Analysis and Quantification.....	80
5.2.2.4	Scion image macros for image acquisition and analysis.....	80
5.2.2.5	Focal photoactivation of caged taxol.....	81
5.2.2.6	Fluorescence recovery after photo-bleaching (FRAP).....	81
5.2.3	Immunocytochemistry.....	82
5.2.3.1	Fixation methods.....	82
5.2.3.2	Immunostaining.....	82
5.2.4	Molecular Biology.....	82
5.2.4.1	Culturing of <i>E. coli</i> .....	82
5.2.4.2	Transformation of <i>E. coli</i> .....	83
5.2.4.3	Preparation of plasmid DNA.....	83
5.2.4.4	Handling of nucleic acids.....	84
5.2.4.5	Genotyping.....	84
5.2.5	Transgenic mice.....	86
5.2.6	Data analysis.....	86
<b>6.</b>	<b><u>References</u></b> .....	<b>87</b>
<b>7.</b>	<b><u>Appendix – Source codes of Scion Image macros</u></b> .....	<b>103</b>
7.1	Triple stain image acquisition.....	103
7.2	Intensity or ratio measurements.....	106
7.3	Shutter control during uncaging experiments.....	108
7.4	Time lapse imaging.....	113
7.5	Kymograph building and analysis.....	117
<b>8.</b>	<b><u>Acknowledgements</u></b> .....	<b>123</b>
<b>9.</b>	<b><u>Curriculum vitae</u></b> .....	<b>125</b>



## **Table of Figures**

<b>Figure 1-1:</b> Neuronal polarity and function .....	4
<b>Figure 1-2:</b> Development of dissociated hippocampal neurons in culture .....	7
<b>Figure 1-3:</b> Rho GTPase effectors and cytoskeletal dynamics .....	10
<b>Figure 1-4:</b> Regulation of Rho GTPases .....	11
<b>Figure 1-5:</b> Actin - Structure and dynamics .....	14
<b>Figure 1-6:</b> Microtubules – Structure and dynamics.....	17
<b>Figure 2-1:</b> Differential distribution of acetylated and tyrosinated microtubules in polarized hippocampal neurons.....	22
<b>Figure 2-2:</b> Growth cones display higher microtubule turnover than neurite shafts.....	23
<b>Figure 2-3:</b> Differential distribution of acetylated and tyrosinated microtubules in unpolarized hippocampal neurons.....	24
<b>Figure 2-4:</b> Stable microtubules are enriched in axons.....	26
<b>Figure 2-5:</b> Microtubule stability and posttranslational modifications of $\alpha$ -tubulin.....	27
<b>Figure 2-6:</b> Supernumerary axons induced by inhibition of GSK-3 $\beta$ show increased microtubule stability .....	28
<b>Figure 2-7:</b> Loss of neuronal polarity in SAD A/B knockout neurons is associated with loss of polarized microtubule stability.....	30
<b>Figure 2-8:</b> Moderate microtubule destabilization selectively blocks the formation of minor neurites .	32
<b>Figure 2-9:</b> Taxol-induced microtubule stabilization triggers the formation of multiple axons .....	34
<b>Figure 2-10:</b> Taxol induces the formation of axon-like processes with reduced microtubule turnover and increased stability .....	35
<b>Figure 2-11:</b> Taxol-induced processes show axonal characteristics.....	36
<b>Figure 2-12:</b> Multiaxonal neurons mature and form neuronal networks.....	37
<b>Figure 2-13:</b> Acetylation of microtubules alone is not sufficient to induce axon formation. ....	38
<b>Figure 2-14:</b> Treatment with deacetylase inhibitors does not alter the distribution of specific microtubule associated proteins. ....	39
<b>Figure 2-15:</b> Taxol induces the protrusion of polymerizing dynamic microtubules to the growth cone periphery .....	40
<b>Figure 2-16:</b> High concentrations of taxol abolish microtubule dynamics .....	41
<b>Figure 2-17:</b> Taxol directs growing microtubule plus ends toward the tips of processes.....	42
<b>Figure 2-18:</b> Dynamic microtubules in polarizing neurons .....	43
<b>Figure 2-19:</b> Local microtubule stabilization promotes axon formation.....	44
<b>Figure 2-20:</b> Local microtubule stabilization shifts dynamic microtubules to the growth cone periphery .....	46
<b>Figure 5-1:</b> Wiring diagram for dual-control shutter cable .....	80



## **Index of Tables**

<b>Table 1:</b> Chemicals .....	65
<b>Table 2:</b> Drugs .....	66
<b>Table 3:</b> Commercial kits .....	66
<b>Table 4:</b> Enzymes and DNA markers .....	67
<b>Table 5:</b> Equipment.....	67
<b>Table 6:</b> Consumables .....	69
<b>Table 7:</b> Buffers and standard solutions .....	71
<b>Table 8:</b> Stock solutions.....	72
<b>Table 9:</b> N2 supplements .....	73
<b>Table 10:</b> Cell culture media .....	73
<b>Table 11:</b> Bacterial media .....	74
<b>Table 12:</b> Antibiotic stocks .....	74
<b>Table 13:</b> Primary antibodies .....	74
<b>Table 14:</b> Secondary antibodies .....	75
<b>Table 15:</b> Other dyes .....	76
<b>Table 16:</b> Plasmids .....	76
<b>Table 17:</b> Oligonucleotides .....	77
<b>Table 18:</b> PCR mix for SAD A/B genotyping:.....	85



## Abbreviations

<b>acet.</b>	acetylated	<b>GSK-3<math>\beta</math></b>	glycogen synthase kinase-3 $\beta$
<b>ADF</b>	actin depolymerizing factor	<b>GTP</b>	guanosine triphosphate
<b>ADP</b>	adenosine diphosphate	<b>h</b>	hour(s)
<b>APC</b>	adenomatous polyposis coli protein	<b>HBSS</b>	Hank's balanced salt solution
<b>aPKC</b>	atypical protein kinase C	<b>HDAC</b>	histone deacetylase
<b>Arp</b>	actin-related protein	<b>Hepes</b>	4-(2-Hydroxyethyl)piperazine-1-ethanesulfonic acid
<b>Asef</b>	APC-stimulated exchange factor	<b>HS</b>	heat-inactivated horse serum
<b>ATP</b>	adenosine triphosphate	<b>ILK</b>	integrin-linked kinase
<b>BDNF</b>	brain-derived neurotrophic factor	<b>IRS-1</b>	insulin receptor substrate-1
<b>Borax</b>	sodium tetraborate	<b>IRSp53</b>	insulin receptor substrate of 53 kDa
<b>BSA</b>	bovine serum albumin	<b>JIP1</b>	JNK-interacting protein 1
<b>Cdc42</b>	cell division cycle 42	<b>JNK</b>	c-Jun N-terminal kinase
<b><i>C. elegans</i></b>	<i>Caenorhabditis elegans</i>	<b>KIF</b>	kinesin heavy chain isoform
<b>CLASP</b>	CLIP-associated protein	<b>LB</b>	Luria-Bertani
<b>CLIP</b>	cytoplasmic linker protein	<b>LIMK</b>	Lin-11, Isl-1, and Mec-3 kinase
<b>CRMP-2</b>	collapsin response mediator protein 2	<b>MAP</b>	microtubule-associated protein
<b>DIV</b>	days <i>in vitro</i>	<b>MARK</b>	MAP/microtubule affinity regulating kinase
<b>DMSO</b>	dimethyl sulfoxide	<b>mDia</b>	Diaphanous-related formin (of mouse, <i>Mus musculus</i> )
<b><i>E. coli</i></b>	<i>Escherichia coli</i>	<b>MEM</b>	minimal essential medium
<b>EB3</b>	end binding protein 3	<b>MEM-HS</b>	MEM supplemented with 10% heat-inactivated horse serum
<b>EDTA</b>	ethylenediamine-tetraacetic acid	<b>min</b>	minute(s)
<b>EGFP</b>	enhanced green fluorescent protein	<b>MLC</b>	myosin light chain
<b>EGTA</b>	ethylene glycol-bis(2-aminoethylether)-tetraacetic acid	<b>MLCK</b>	myosin light chain kinase
<b>En</b>	embryonic day n	<b>MLCP</b>	myosin light chain phosphatase
<b>F-actin</b>	filamentous actin	<b>MTOC</b>	microtubule organizing center
<b>G-actin</b>	globular actin	<b>n</b>	number
<b>GAKIN</b>	guanylate kinase-associated kinesin	<b>NgCAM</b>	neuron–glia cell adhesion molecule
<b><math>\gamma</math>-TURC</b>	$\gamma$ (gamma)-tubulin ring complex	<b>NGF</b>	nerve growth factor
<b>GAP</b>	GTPase-activating protein	<b>NT3</b>	neurotrophin 3
<b>GDI</b>	guanine nucleotide exchange inhibitor	<b>N-terminus</b>	amino terminus
<b>GDP</b>	guanosine diphosphate	<b>OD<sub>x</sub></b>	optical density at $\lambda=x$ nm
<b>GEF</b>	guanine nucleotide exchange factor	<b>p</b>	probability
<b>GFP</b>	green fluorescent protein	<b>PAK</b>	p21-activated kinase

<b>Par</b>	partitioning defective	<b>UV</b>	ultra-violet
<b>PBS</b>	phosphate-buffered saline	<b>WASP</b>	Wiskott-Aldrich syndrome protein
<b>PK1</b>	phosphoinositide-dependent protein kinase 1	<b>WAVE</b>	WASP family Verprolin-homologous protein
<b>PFA</b>	paraformaldehyde	<b>WNT</b>	acronym for Wingless / INT (Wingless type mouse mammary tumor virus integration site family)
<b>PH domain</b>	pleckstrin homology domain	<b>WT</b>	wild type
<b>PI3K</b>	phosphoinositide 3-kinase		
<b>PIP<sub>3</sub></b>	Phosphatidylinositol (3,4,5)-trisphosphate		
<b>Pipes</b>	1,4-piperazine-diethanesulfonic acid		
<b>PKB</b>	protein kinase B (also called Akt kinase)		
<b>PSD-95</b>	postsynaptic density protein 95		
<b>PSP</b>	postsynaptic potential		
<b>PTEN</b>	phosphatase and tensin homologue deleted on chromosome 10		
<b>Rac1</b>	ras-related C3 botulinum toxin substrate 1		
<b>Rap1B</b>	Ras-related protein 1B		
<b>RhoA</b>	ras homolog gene family, member A		
<b>ROCK</b>	Rho kinase		
<b>rpm</b>	rounds per minute		
<b>RT</b>	room temperature		
<b>SAD</b>	synapses of amphids defective		
<b>SDS</b>	sodium dodecyl sulfate		
<b>sec</b>	second(s)		
<b>SEM</b>	standard error of the mean		
<b>sif</b>	<i>still life</i>		
<b>STEF</b>	SIF and Tiam1-like exchange factor		
<b>TAE</b>	Tris-acetate EDTA		
<b>TBE</b>	Tris-borate EDTA		
<b>Tiam1</b>	T-lymphoma and metastasis 1		
<b>Tris</b>	Tris[hydroxymethyl]aminomethane		
<b>Trk</b>	tyrosine receptor kinase		
<b>TSA</b>	trichostatin A		
<b>t-test</b>	Student's t-test		
<b>TX-100</b>	Triton X-100		
<b>tyr.</b>	tyrosinated		
<b>U</b>	unit(s)		

## **Summary**

Neurons are highly polarized cells with two structurally and functionally distinct compartments, axons and dendrites. This dichotomy is the basis for unidirectional signal propagation, the quintessential function of neurons. During neuronal development, the formation of the axon is the initial step in breaking cellular symmetry and the establishment of neuronal polarity. Although a number of polarity regulators involved in this process have been identified, our understanding of the intracellular mechanisms underlying neuronal polarization still remains fragmentary.

In my studies, I addressed the role of microtubule dynamics in initial neuronal polarization. To this end I aimed to investigate the following issues: 1) How do microtubule dynamics and stability change during initial neuronal development? 2) Do microtubules play an instructive role in axon formation? 3) What are possible regulators mediating changes in microtubule dynamics during axon formation?

Using hippocampal neurons in culture as a model system for neuronal polarization I first addressed the dynamics of microtubules in early developmental stages of neurons. Assessing posttranslational modifications of tubulin which serve as markers of microtubule turnover I found that microtubule stability is increased in a single neurite already before axon formation and in the axon of morphologically polarized cells. This polarized distribution of microtubule stability was confirmed by testing the resistance of neuronal microtubules to pharmacologically induced depolymerization. The axon of polarized neurons and a single neurite in morphologically unpolarized cells showed increased microtubule stability. Thus, I established a correlation between the identity of a process and its microtubule stability.

By manipulating specific regulators of neuronal polarity, SAD kinases and GSK-3 $\beta$ , I analyzed a possible relation between a polarization of microtubule stability and neuronal polarity. I found that a loss of polarity correlated with a loss of polarized microtubule stability in neurons defective for SAD A and SAD B kinases. In marked contrast, the formation of multiple axons, induced by the inhibition of GSK-3 $\beta$ , was associated with increased microtubule stability in these supernumerary axons. These

results suggested that SAD kinases and GSK-3 $\beta$  regulate neuronal polarization –at least in part– by modulating microtubule dynamics.

To establish a possible causal relation between microtubule dynamics and axon formation I assessed the effects of specific pharmacological alterations of microtubule dynamics on neuronal polarization. I found that application of low doses of the microtubule destabilizing drug nocodazole selectively reduced the formation of future dendrites. Conversely, low doses of the microtubule stabilizing drug taxol led to the formation of multiple axons. I also studied microtubule dynamics in living neurons transfected with GFP-tagged EB3, a protein binding specifically to polymerizing microtubule plus ends. In line with my previous observations I found that microtubules are stabilized along the shaft of the growing axons while dynamic microtubules enrich at the tip of the growing process, suggesting that a well-balanced shift of microtubule dynamics towards more stable microtubules is necessary to induce axon formation. By uncaging a photoactivatable analog of taxol I induced a local stabilization of microtubules at the neurite tip of an unpolarized neuron which was sufficient to favor the site of axon formation. This indicates that a transient stabilization of microtubules is sufficient to trigger axon formation.

In summary, my data allow the following conclusions: 1) Microtubule stability correlates with the identity of a neuronal process. 2) Microtubule stabilization causes axon formation. 3) Microtubule stabilization precedes axon formation. I therefore deduce that microtubules are actively involved in the process of axon formation and that local microtubule stabilization in one neuronal process is a physiological signal specifying neuronal polarization.

# **1. Introduction**

Neurons are highly polarized cells, a characteristic that enables them to form the cellular basis of neuronal networks, one of the most refined structures found in nature. Typically, mature neurons have one thin, long process to transmit information, the axon, and several tapered, shorter processes to receive information, the dendrites. Newly generated neurons gradually develop these clear-cut polar structures, thereby laying the foundation for unidirectional signal propagation. The formation of the axon is a crucial hallmark of this process of neuronal polarization, as it marks the first break in symmetry during neuronal development. Accommodating the importance of neuronal polarization for the function of nerve cells, one of the key questions of neurobiology is how a neuron acquires and maintains its polarity.

## **1.1 Neuronal polarity**

The polarity of nerve cells takes shape in three different levels: Morphology, molecular composition and function. Eye-catching, axons and dendrites differ at the level of morphology. Axons are usually long and slender, in contrast to the shorter, tapered, highly branched morphology of dendrites. On the level of molecular composition, neuronal polarity is reflected in the distinct machinery of axons and dendrites for signal transmission and reception, respectively (Bear *et al.*, 2007). Axons are equipped to actively conduct electrical signals in the form of action potentials —generated at their initial segment, the so-called ‘axon hillock’ (reviewed in Catterall, 2000)— down to their terminals (see Figure 1-1 A; Bear *et al.*, 2007).

When an action potential reaches the presynaptic axon terminal it promotes the release of neurotransmitters into the synaptic cleft (see Figure 1-1 B). By this mechanism an electrical signal (the action potential) is converted to a chemical signal and passed on via a (chemical) synapse to a postsynaptic cell, e.g. an adjacent neuron or other target tissues like muscles or secretory glands. [Signal transmission via electrical synapses is described in (Bennett and Zukin, 2004).] In contrast to axons, dendrites are fitted to receive signals (Bear *et al.*, 2007). Receptors in their postsynaptic membrane bind the neurotransmitter molecules released by the axon

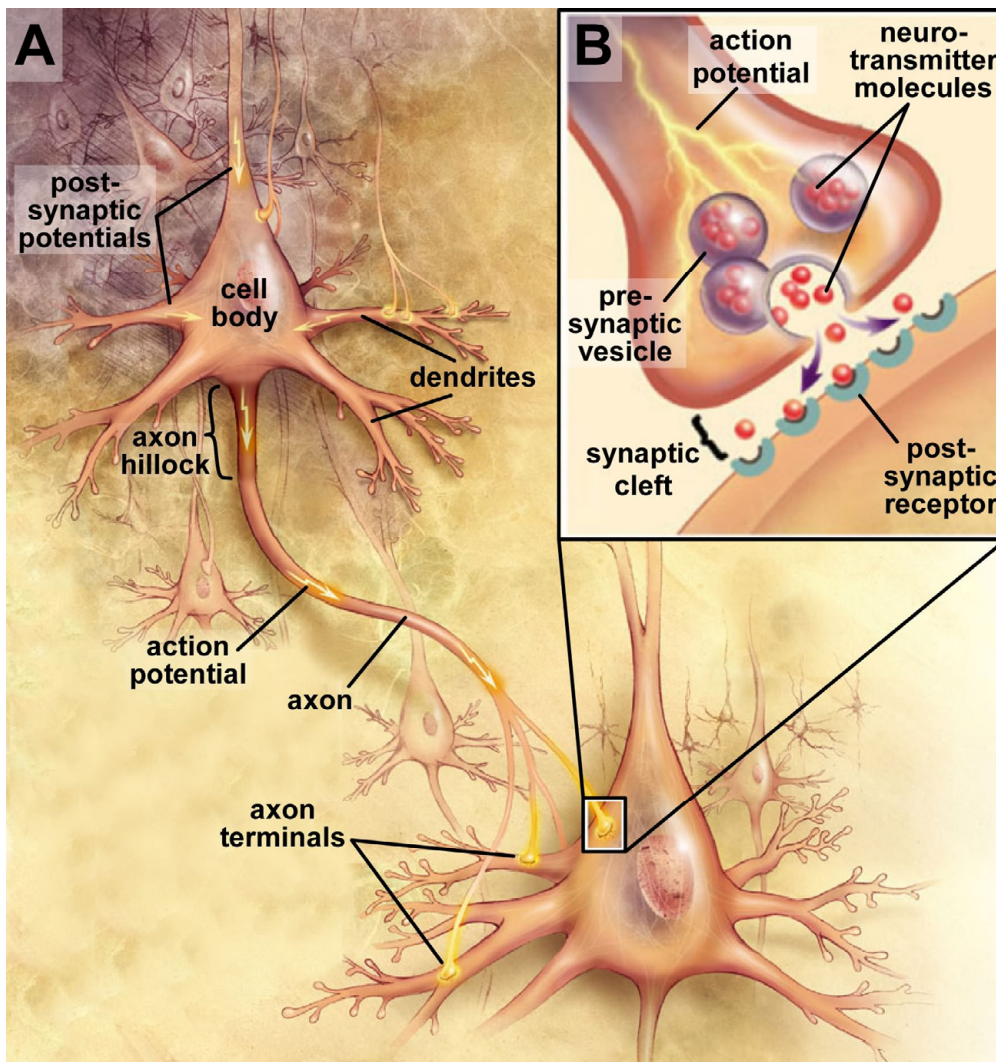


**Figure 1-1: Neuronal polarity and function**

Neurons generate action potentials at the initial segment of the axon (the axon hillock) which are subsequently conducted down the axon to the axon terminals (A). There the action potentials trigger the release of neurotransmitter molecules from presynaptic vesicles into the synaptic cleft (B). Neurotransmitters bind to postsynaptic receptors (B) and thereby evoke or modulate postsynaptic potentials (PSPs) which are integrated in dendrites and the cell body (A). If the summarized PSPs exceed a certain threshold in the receiving neuron they stimulate voltage-gated sodium channels at the axon hillock to induce a new action potential. Image from <http://www.nia.nih.gov/> (National Institute of Ageing).

which evokes or modulates postsynaptic potentials (PSPs; reviewed in Südhof, 2008). Depending on the type of receptor, PSPs may be excitatory or inhibitory; they are summarized in the dendrites and the cell body and may in turn generate a new action potential at the axon hillock of the receiving cell (Bear *et al.*, 2007).

Selective targeting and retention establishes the compartmentalized distribution of axonal (Gu *et al.*, 2003; Sampo *et al.*, 2003; Stowell and Craig, 1999; Wisco *et al.*, 2003; Yap *et al.*, 2008) and dendritic (Rosales *et al.*, 2005; Stowell and Craig, 1999;

West *et al.*, 1997) proteins. Once set up, a membrane diffusion barrier at the axonal initial segment maintains this polarity by preventing the diffusional mixing of axonal and somatodendritic membrane proteins (Nakada *et al.*, 2003).

In summary, the morphological and molecular polarity of neurons reflects the different functions of axons and dendrites, with the axon transmitting signals over long distances and the extensively branched dendrites receiving and integrating signals.

## **1.2 Primary neuronal cultures**

Given the complexity of neuronal development, a molecular understanding of neuronal polarization requires studying at least part of the process *in vitro*, where, in principle, one can both control the cellular environment and manipulate individual neurons.

### **1.2.1 Characteristics of *in vitro* neuronal cultures**

Several *in vitro* cell culture techniques have been successfully employed to address specific cell biological or functional questions and provide a common means to systematically study the complex nervous system (Harry *et al.*, 1998; Saneto and de Vellis, 1987; Shahar *et al.*, 1989). Although not considered absolute alternatives to *in vivo* experiments, *in vitro* methods are invaluable to address specific issues of neuronal development in a more isolated context under controlled conditions. In principle, the simplification of the culture system allows the dissection and analysis of individual aspects of developmental processes which as a whole are too complex to scrutinize.

Importantly, *in vitro* cultures of embryonic neural tissues such as organotypic cultures, re-aggregate cultures, and dissociated primary cell cultures recapitulate many aspects of the neural *in vivo* development, including polarization (Dotti *et al.*, 1988), maturation (Bartlett and Banker, 1984a; Mains and Patterson, 1973; Seeds and Haffke, 1978; Trapp *et al.*, 1979) and synaptogenesis (Bartlett and Banker,

1984b; Bornshein and Model, 1972; Trenkner and Sidman, 1977; Yavin and Yavin, 1977). Moreover, the time course of their development often parallels the one displayed by neurons *in situ* (Kozak, 1977; Mains and Patterson, 1973; Spitzer and Lamborghini, 1976; Yavin and Yavin, 1977).

Primary cultures make individual living neurons more easily accessible to both manipulation and observation. For instance, neurons can be readily transfected at different developmental stages (Kaech and Banker, 2006; Zeitelhofer *et al.*, 2007). By this means it is possible to overexpress certain proteins or to knock down the expression of specific genes (reviewed in Zeringue and Constantine-Paton, 2004) to study their function. Moreover, fluorescently tagged proteins can be introduced to explore the subcellular localization and trafficking of proteins inside living neurons (Jacobson *et al.*, 2006; Stepanova *et al.*, 2003) or as reporters for intracellular processes (Heim *et al.*, 2007; Hüttelmaier *et al.*, 2005). The analysis of neuronal cultures prepared from knockout animals in addition offers the possibility to analyze the effects of specific gene disruptions. Furthermore, it allows investigating postnatal aspects of neural development of knockout animals that die at or shortly after birth from systemic defects.

### **1.2.2 Dissociated hippocampal neurons in culture**

Dissociated hippocampal neurons are among the best-characterized model systems to study neuronal polarity (Dotti *et al.*, 1988). Since the first description of this system by Banker and Cowan (Banker and Cowan, 1977) it has been considerably refined (de Hoop *et al.*, 1997; Goslin and Banker, 1991). Dissociated hippocampal neurons grow and mature under controlled growth conditions, mainly free of unspecified external cues. Although this on the one hand deprives them of their *in vivo* environment it offers on the other hand the chance to study their cell-autonomous polarization program. Such insights in turn provide entry points to analyze which extracellular signals regulate the intracellular mechanisms underlying polarization. Several particularities account for the widespread popularity of dissociated hippocampal neurons as a model system. Firstly, the population of nerve cells in the hippocampus is relatively homogeneous, with pyramidal cells accounting for

approximately 90 % of the neurons and interneurons making up the rest (Benson *et al.*, 1994). Since hippocampal cultures are routinely prepared from late-stage rodent embryos the tissue also contains relatively few 'contaminating' glial cells and is easy to dissociate.

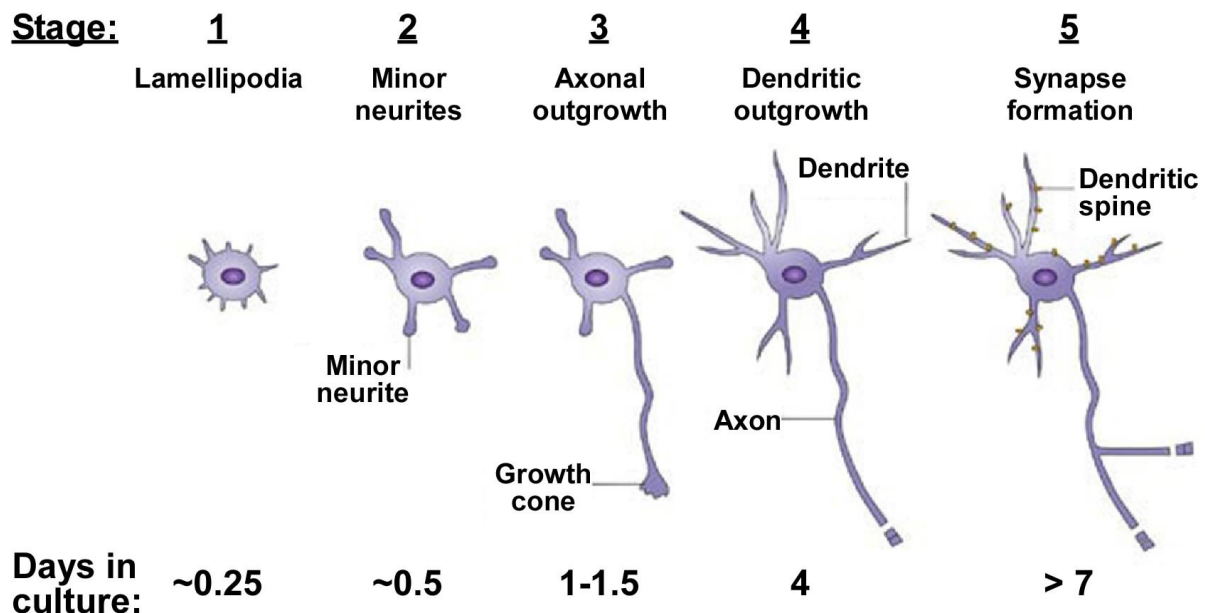


**Figure 1-2: Development of dissociated hippocampal neurons in culture**

Dissociated hippocampal neurons develop in culture in a stereotyped manner, recapitulating neuronal polarization and maturation. For details see text. Scheme modified from Dotti *et al.*, 1988 and Arimura and Kaibuchi, 2007.

Secondly, cultured hippocampal neurons reliably polarize *in vitro* forming one axon and several dendrites. Later in development they also mature and form synaptic contacts (Bartlett and Banker, 1984a; Bartlett and Banker, 1984b), just like their *in vivo* counterparts. The polarization of cultured hippocampal neurons follows a highly stereotyped sequence of developmental events which can be divided into five stages (Dotti *et al.*, 1988 see Figure 1-2). Shortly after plating in serum-supplemented medium, hippocampal neurons attach to the substrate and start to form lamellipodia, dynamic membrane ruffles, around their cell body (stage 1). Subsequently, after 6-18 hours in culture, the lamellipodia condense to 4-5 short processes, the so-called 'minor neurites' (stage 2). By this time, the neurons are transferred to serum-free medium in culture dishes containing an astrocyte feeder layer to promote growth and differentiation (de Hoop *et al.*, 1997). Towards the end of stage 2 membrane organelles as well as cytosolic proteins become concentrated

in one of the – seemingly identical – minor neurites (Bradke and Dotti, 1997). This process then starts to grow out quickly to become the axon (stage 3; after 1-1.5 days in culture). This first morphological sign of axon formation is a crucial hallmark of neuronal polarization, as it marks the initial break in symmetry during neuronal development (Craig and Banker, 1994). The remaining processes start to elongate with a delay of several days and also grow at a much slower rate to form the cell's dendrites (stage 4; after ~4 days in culture). Axonal and dendritic proteins are segregated in stage 4 (Bradke and Dotti, 2000a), indicating the molecular polarization of axons and dendrites. By stage 5 (>7 days in culture) the neurons have formed functional synaptic contacts and generate electric currents (Bartlett and Banker, 1984b; Segal, 1983) – they have now reached functional polarization.

To summarize, preparations of dissociated hippocampal neurons recapitulate neuronal polarization *in vitro*. The decisive step in this process is the formation of the axon since it represents the cornerstone for all further polarization events.

### **1.3 Polarity regulation and the neuronal cytoskeleton**

During the last years various molecular regulators of neuronal polarization have been identified (reviewed in Arimura and Kaibuchi, 2007). Although these studies have largely improved our knowledge about the specific signaling pathways mediating neuronal polarity, our understanding of most of the intracellular mechanisms underlying neuronal polarization has remained fragmentary. The next sections will provide an overview of polarity regulators, their complex interconnections and their relation to the neuronal cytoskeleton, a cellular structure crucial for neuronal polarization.

#### **1.3.1 Signaling pathways involved in the specification of neuronal polarity**

Phosphoinositide 3-kinase (PI3K) has recently been shown to be a central player in the establishment of neuronal polarity (Menager *et al.*, 2004; Shi *et al.*, 2003). PI3K is activated by upstream regulators such as Ras (Huang and Reichardt, 2003; Oinuma *et al.*, 2007; Yoshimura *et al.*, 2006) or insulin receptor substrate-1 (IRS-1; Yamada

*et al.*, 1997) in response to stimulation by neurotrophic factors. Active PI3K produces the phospholipid phosphatidylinositol-(3,4,5)-trisphosphate (PIP<sub>3</sub>) at the plasma membrane which was reported to promote neurite outgrowth and axon specification (Menager *et al.*, 2004). Phosphatase and tensin homologue deleted on chromosome 10 (PTEN), in contrast, represents an antagonist of PI3K which decreases PIP<sub>3</sub> levels at the leading edge of neurites and disrupts the development of polarity (Shi *et al.*, 2003). Proteins with pleckstrin homology (PH) domains bind PIP<sub>3</sub> with high affinity (reviewed in Saraste and Hyvonen, 1995), hence active PI3K recruits such factors to the plasma membrane.

For example, the membrane localization of phosphoinositide-dependent protein kinase 1 (PDK1; Alessi *et al.*, 1997), integrin-linked kinase (ILK; Oinuma *et al.*, 2007) and their target Akt kinase (also called protein kinase B/PKB; reviewed in Cantley, 2002; Lawlor and Alessi, 2001) depends on PIP<sub>3</sub>. Elevated PIP<sub>3</sub>-levels bring Akt, PDK1 and ILK into close proximity at the plasma membrane which facilitates phosphorylation and thereby activation of Akt (reviewed in Cantley, 2002; Lawlor and Alessi, 2001). The expression of constitutively active forms of PI3K or Akt induces the formation of multiple axons in cultured hippocampal neurons (Yoshimura *et al.*, 2006), likely because Akt regulates another key player of neuronal polarization, the constitutively active glycogen synthase kinase-3 $\beta$  (GSK-3 $\beta$ ). When phosphorylated by Akt, GSK-3 $\beta$  is inactivated (Cross *et al.*, 1995).

GSK-3 $\beta$  is implicated in the regulation of neuronal polarization but also a multitude of other processes, including the control of metabolism, gene expression, cytoskeletal dynamics, intracellular vesicular transport and apoptosis. This variety of functional implications reflects its broad spectrum of targets which includes metabolic, signaling, and structural proteins (reviewed in Doble and Woodgett, 2003; Grimes and Jope, 2001; Zhou and Snider, 2005). It is not yet fully understood how a seemingly 'promiscuous' enzyme that has as many proposed substrates as GSK-3 $\beta$  can confer signal-dependent specificity. Possible regulatory mechanisms include selective activation and inhibition through specific tyrosine and serine phosphorylations, binding to scaffolding proteins to facilitate substrate interaction, and targeting of GSK-3 $\beta$  to different subcellular localizations (Doble and Woodgett, 2003). Moreover,

targets of GSK-3 $\beta$  vary in their requirement for pre-phosphorylation by other kinases at a 'priming' residue to allow phosphorylation by GSK-3 $\beta$  (Fiol *et al.*, 1987). Active GSK-3 $\beta$  mainly inhibits its targets (Doble and Woodgett, 2003). During neuronal polarization GSK-3 $\beta$  therefore needs to be inactivated (Jiang *et al.*, 2005; Yoshimura *et al.*, 2005). Together with adenomatous polyposis coli protein (APC), GSK-3 $\beta$  is implicated in targeting partitioning defective 3 (Par-3) to the nascent axon (Shi *et al.*, 2004). Par-3 is part of the Par-3 / Par-6 / atypical protein kinase C (aPKC) polarity complex which provides a link between GSK-3 $\beta$  and Rho GTPases (see below).

Rho GTPases (in full small GTPases of the Rho family) and their effectors are among the best-studied regulators of the actin cytoskeleton (reviewed in Govek *et al.*, 2005; Witte and Bradke, 2005; see Figure 1-3). They have been implicated in the establishment of neuronal polarity (reviewed in Arimura and Kaibuchi, 2007; Govek *et al.*, 2005) and a broad variety of other processes, including polarization of other cell types, microtubule dynamics, gene transcription, cell cycle progression, and vesicle transport (reviewed in Etienne-Manneville and Hall, 2002).

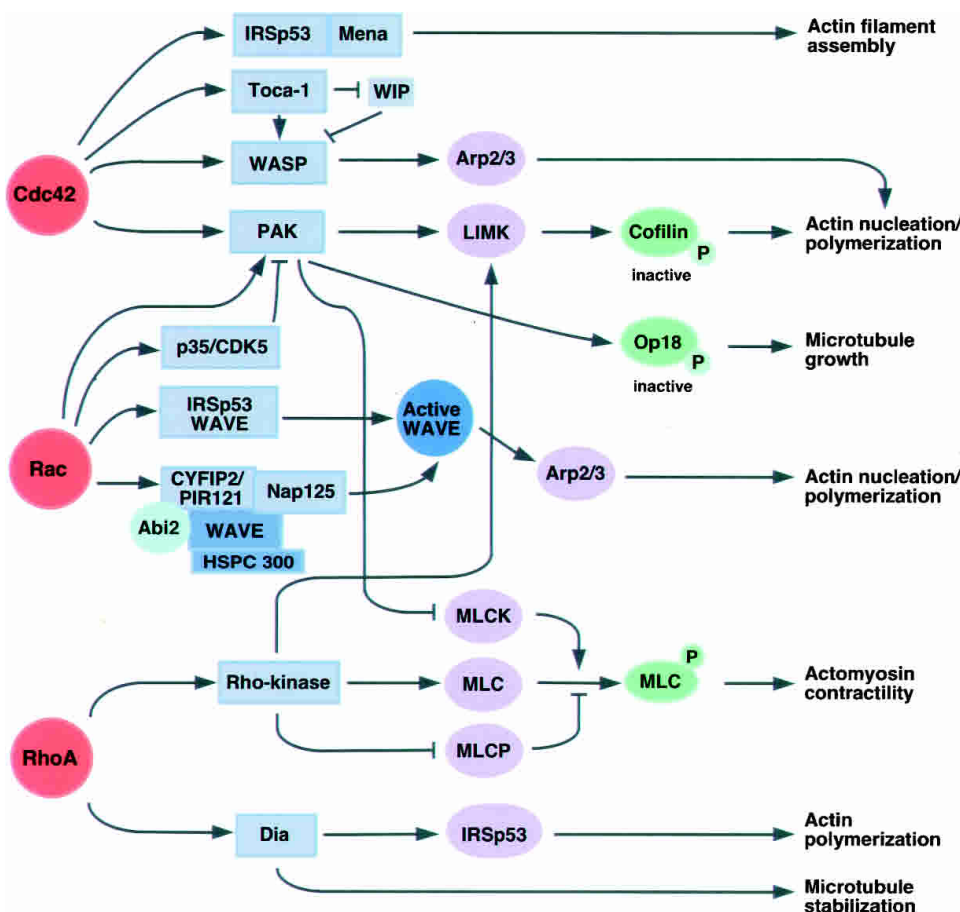


**Figure 1-3: Rho GTPase effectors and cytoskeletal dynamics**

Rho GTPases control a multitude of effectors to modulate the dynamics of the actin cytoskeleton and microtubules. They regulate the nucleation and assembly of actin filaments, the contractility of actomyosin and the stabilization of microtubules. Scheme from Govek *et al.*, 2005.

Rho GTPases cycle between an active GTP-bound and an inactive GDP-bound state (Nobes and Hall, 1995); their activity is mainly controlled by guanine nucleotide exchange factors (GEFs), GTPase-activating proteins (GAPs), and guanine nucleotide exchange inhibitors (GDIs; see Figure 1-4).

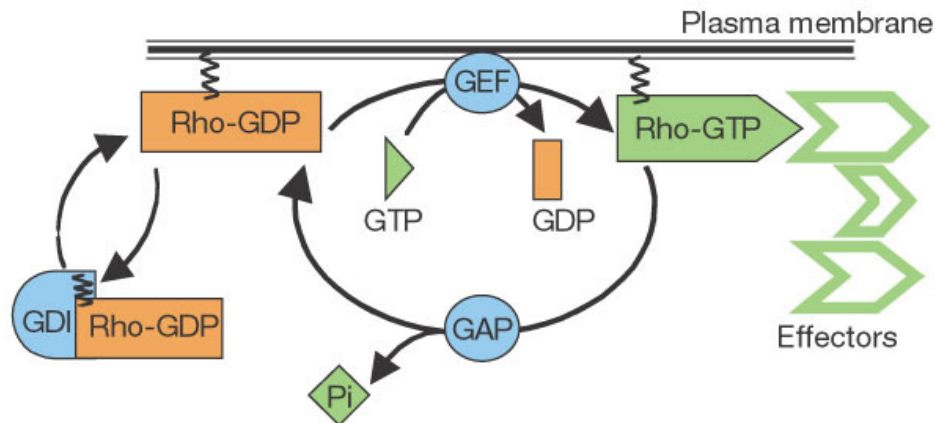


**Figure 1-4: Regulation of Rho GTPases**

Rho GTPases cycle between an inactive (GDP-bound) and an active (GTP-bound) state (Nobes and Hall, 1995) in which they interact with their target proteins (effectors). The Rho GTPase cycle is tightly controlled by three types of regulators: (1) Guanine nucleotide exchange factors (GEFs) activate Rho GTPases by catalyzing the nucleotide exchange of GDP to GTP. (2) GTPase-activating proteins (GAPs) inactivate Rho GTPases by stimulating GTP hydrolysis. (3) Guanine nucleotide exchange inhibitors (GDIs) are involved in subcellular targeting of inactive GTPases and controlling the access to GEFs and GAPs. All Rho GTPases are essentially prenylated at their C-terminus. Scheme from Etienne-Manneville and Hall, 2002.

At present more than 20 Rho GTPase have been identified, with RhoA (ras homolog gene family, member A), Cdc42 (cell division cycle 42) and Rac1 (ras-related C3 botulinum toxin substrate 1) being the most extensively characterized members. In neuroblastoma cells, the activation of Cdc42 or Rac1 enhances neurite elongation, whereas the activation of RhoA is associated with the inhibition of neurite formation (Kozma *et al.*, 1997). In morphologically unpolarized hippocampal neurons, Cdc42 and another small GTPase, Ras-related protein 1B (Rap1B) localize to a single neurite during development, most likely promoting the specification of the future axon (Schwamborn and Püschel, 2004). Interestingly, their function depends on PIP<sub>3</sub>, with Rap1B acting upstream of Cdc42, presumably via activating a Cdc42-GEF (Schwamborn and Püschel, 2004). The restriction of Rap1B to a single neurite of unpolarized cells is mediated by ubiquitin/proteasome-dependent degradation of inactive Rap1B in all but one neurite (Schwamborn *et al.*, 2007). Strikingly, neurotrophin receptor TrkA (tyrosine receptor kinase A) which is activated at the tip of

growing axons (Da Silva *et al.*, 2005) recruits guanine nucleotide exchange factors of Rap1 (York *et al.*, 1998). Rap1 activated in this way may escape the destruction by the ubiquitin/proteasome-system and promote axon formation.

Cdc42 also interacts with Par-3 in the aforementioned Par-3 / Par-6 / aPKC polarity complex. In this context, Cdc42 mediates the activation of Rac via its guanine nucleotide exchange factors STEF/Tiam1 (Nishimura *et al.*, 2005). Active Rac1 seems able to stimulate PI3K (Keely *et al.*, 1997; Tolia *et al.*, 1995) which closes a positive feedback loop consisting of PI3K, PIP<sub>3</sub>, Rap1B, Cdc42, Par-3 / Par-6 / aPKC and Rac1. Such a feedback loop may be able to drive continuous axon outgrowth (reviewed in Arimura and Kaibuchi, 2007). An “exit” for such a circle may be provided by the PIP<sub>3</sub>-degrading PTEN or specific GTPase-activating proteins which could inactivate either Cdc42 or Rac1. The localized distribution of Rap1B may restrict the axon-inducing effect of a positive feedback loop to a single neurite. Consequently, overexpression of constitutively active Rap1B or a hyperactivated form of Cdc42 which overrides the restricted localization induces the formation of multiple axons (Schwamborn and Püschel, 2004).

Recent work has shown that also activated c-Jun N-terminal kinase (JNK), so far known to be implicated in the regulation of gene transcription, cell death and survival (reviewed in Krens *et al.*, 2006), plays a decisive role in axon formation (Oliva *et al.*, 2006). JNK targets a wide variety of nuclear and cytoplasmic proteins, including transcription factors and proteins that regulate the dynamics of actin or microtubules (Bjorkblom *et al.*, 2005; Chang *et al.*, 2003; Reynolds *et al.*, 2000; Ricos *et al.*, 1999; Yoshida *et al.*, 2004). Interestingly, the JNK pathway seems to interact with several other signaling cascades involved in neuronal polarization. JNK, for instance, mediates the inhibition of GSK-3 $\beta$  together with Dishevelled, a scaffold protein of the Wingless / INT (WNT)-signaling pathway (Ciani *et al.*, 2004; Ciani and Salinas, 2007), thus forming a connection to GSK-3 $\beta$ - and WNT-signaling. Along those lines, JNK interacting protein 1 (JIP1) associates with p190rhoGEF, an activator of RhoA signaling (Meyer *et al.*, 1999), thereby linking JNK and Rho GTPase signaling.

This brief overview already gives an idea about how complex and interconnected the signaling network is that regulators of neuronal polarity form. Moreover, the

described signaling pathways can trigger a multitude of intracellular events, quite likely not all of which are involved in axon formation. In this respect, local instability of the actin cytoskeleton and enhanced membrane traffic into one minor neurite are known to play pivotal roles in axon formation (Bradke and Dotti, 1997; Bradke and Dotti, 1999; Jareb and Banker, 1997). As a consequence, efforts have mainly focused to establish connections between polarity regulators and the regulation of actin dynamics.

### **1.3.2 The actin cytoskeleton**

Actin microfilaments consist of two helically twisted strands of filamentous actin (F-actin; see Figure 1-5 A, page 14) and are with a diameter of approximately 7 nm the thinnest fibers of the cytoskeleton. Regulators of the actin cytoskeleton modulate various processes, including 'de novo' nucleation of filaments, crosslinking/bundling, severing, depolymerization and ADP/ATP exchange to fine-tune the dynamic properties of the actin cytoskeleton (Figure 1-5 B; (reviewed in Pollard and Borisy, 2003). Due to their polar structure actin microfilaments serve as tracks for myosin motor proteins which mediate directed transport of organelles and macromolecules (reviewed in Krendel and Mooseker, 2005). Myosin motors also drive the transport of actin filaments centripetally from the leading edge towards the center of the growth cones where actin bundles are depolymerized, a phenomenon called retrograde flow (Forscher and Smith, 1988; Lin *et al.*, 1996).

One hallmark of the future axonal growth cone in unpolarized hippocampal neurons is a reduced stability of its actin cytoskeleton which may cause a reduction in outgrowth obstruction (Bradke and Dotti, 1999). Such local actin instability manifests itself in a higher susceptibility of the actin cytoskeleton to extraction using detergents (Bradke and Dotti, 1999) and increased dynamics of the growth cone (Bradke and Dotti, 1997; Bradke and Dotti, 1999). Regulators of actin dynamics –which may mediate such actin instability—are the effectors of several signaling pathways involved in axon formation. For instance, neurons treated with toxin B, an inhibitor of Rho GTPases (Just *et al.*, 1995) form multiple axons instead of one (Bradke and Dotti, 1999), a phenotype that is equally observed upon treatment of neurons with

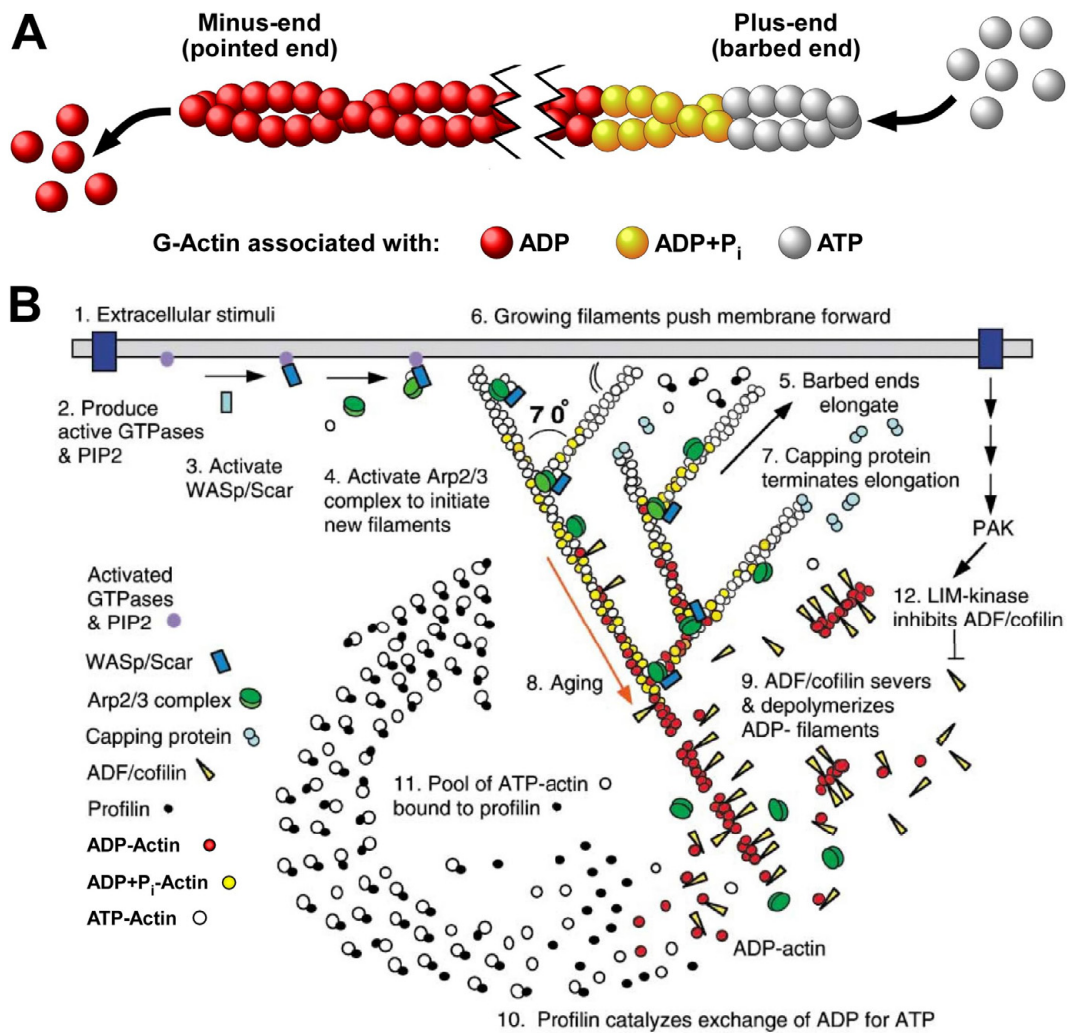


**Figure 1-5: Actin - Structure and dynamics**

(A) Actin microfilaments consist of two helically intertwined strands of F-actin which is itself composed of polymerized subunits of globular actin (G-actin). G-actin subunits are arranged head-to-tail in the actin filament which creates two ends with distinct dynamic properties. At the so-called plus- or 'barbed' end addition of G-actin prevails (i.e. polymerization), making it the faster-growing end. At the minus- or 'pointed' end loss of subunits, i.e. depolymerization, dominates, it thus grows slowly. Polymerizing G-actin is associated with ATP (white subunits) which is then hydrolyzed upon ageing in the filament (yellow subunits). Inorganic phosphate ( $P_i$ ) is released slowly from G-actin (red subunits).

(B) Simplified actin cycle. Extracellular signaling leads to the activation of WASp/Scar proteins which in turn induce actin nucleation and branching by the Arp2/3 complex. Capping proteins terminate polymerization at the barbed end of the filament. Formins, in contrast, favor actin polymerization by protecting barbed ends from capping proteins. ADF/cofilin –which may be inhibited by PAK and LIM kinase– promotes dissociation of the inorganic phosphate, severs ADP-actin filaments and promotes dissociation of ADP-actin from filament ends. Profilin catalyzes the ADP/ATP exchange of actin, thereby reconverting ADP-associated G-actin to the ATP-bound form. Moreover, profilin sequesters ATP-actin to rapidly release it just upon stimulation by WASP/Scar proteins. Scheme modified from Pollard and Borisy, 2003.

cytochalasin D, an actin destabilizing drug (Bradke and Dotti, 1999; Schwamborn and Püschel, 2004). Correspondingly, the active form of actin-depolymerizing factor cofilin (see Figure 1-5 B) is enriched in axonal growth cones of hippocampal neurons

which may account for a local actin instability (Garvalov *et al.*, 2007). Interestingly, neurons derived from mice deficient in the Rho GTPase Cdc42 show an increased inactivation of cofilin, which thus seems to be a physiological downstream effector of Cdc42 in the process of neuronal polarization (Garvalov *et al.*, 2007). Cdc42 itself is likely to be regulated by Rap1B (Schwamborn and Püschel, 2004; see section 1.3.1 above).

Suggesting an involvement of Rac1 in the establishment of neuronal polarity, overexpression of T-lymphoma and metastasis 1 (Tiam1) protein, a GEF activating Rac1, induces the formation of several axon-like neurites in hippocampal neurons (Kunda *et al.*, 2001). Suppression of Tiam1, in contrast, prevents axon formation, presumably since neurons fail to reorganize the actin cytoskeleton. This in turn blocks the invasion of microtubules into selected growth cones to drive neurite outgrowth. Pharmacological destabilization of the actin cytoskeleton can rescue this inability, leading to the formation of multiple axons in cells lacking Tiam1 (Kunda *et al.*, 2001).

Along those lines, the actin regulator profilin is also involved in the establishment of neuronal polarization. Profilin stimulates the ADP/ATP exchange of G-actin (see Figure 1-5 B), thus refilling the pool of ATP-associated G-actin which in turn promotes actin polymerization (Goldschmidt-Clermont *et al.*, 1992; Kang *et al.*, 1999). In hippocampal neurons, the brain-specific profilin IIa mediates actin stabilization and inhibits neurite sprouting (Da Silva *et al.*, 2003). Normal neuronal polarity can be rescued by actin destabilizing using cytochalasin D (Da Silva *et al.*, 2003). During neuronal polarization, the inhibition of profilin IIa via RhoA and its downstream effector Rho kinase (ROCK) indirectly promotes such a destabilization of the actin cytoskeleton (Da Silva *et al.*, 2003) which allows neurite formation.

In spite of its importance for initial neuronal polarization, the regulation of actin dynamics does not seem to be the primary target of all signaling pathways involved in axon formation. Several recently discovered pathways, although modulating numerous cellular events, seem to have another common denominator:

The regulation of microtubule dynamics.

### 1.3.3 Microtubules – More than just supporting actors?

Microtubules are hollow cylinders (about 25 nm in diameter) composed of stable heterodimers of  $\alpha$ - and  $\beta$ -tubulin (Weisenberg et al., 1968; Figure 1-6 A). These  $\alpha/\beta$ -tubulin heterodimers polymerize in a head-to-tail fashion to form polar protofilaments (Amos and Klug, 1974), 13 of which form the helical microtubule wall (Evans et al., 1985). The two ends of a microtubule show different polymerization rates; the faster growing end is designated the plus-end while the slower growing end is called the minus-end (Allen and Borisy, 1974; Figure 1-6 B). In most non-neuronal cells microtubules are oriented radially with the plus ends extending out from a central microtubule organizing center (MTOC) during interphase (Piehl and Cassimeris, 2003). However, in neurons the situation is somewhat different: In axons, microtubules have been reported to be all oriented with the plus ends outward, while microtubules in dendrites may have a mixed polarity (Baas et al., 1989; Baas et al., 1988). Microtubule ends alternate between prolonged phases of polymerization and depolymerization, a phenomenon called 'dynamic instability' (Mitchison and Kirschner, 1984). The transition from polymerization to depolymerization is referred to as 'catastrophe', whereas the opposite transition from depolymerization to polymerization is referred to as 'rescue' (Walker et al., 1991; Figure 1-6 C).

The assembly, dynamics and organization of microtubules is regulated by a variety of microtubule-associated proteins (MAPs; for detailed review see Cassimeris and Spittle, 2001). Specific MAPs stabilize microtubules, for instance by stimulating the addition of tubulin subunits to the microtubule polymer, by blocking catastrophes, or by promoting rescue events. Stabilization is also achieved by cross-linking protofilaments (Chapin and Bulinski, 1992; Gustke et al., 1994) or bundling of microtubules (Kanai et al., 1992; Masson and Kreis, 1993; Preuss et al., 1997). On the other hand, some MAPs destabilize microtubules by promoting catastrophes and inhibiting rescues, by severing microtubules, sequestering tubulin subunits and weakening lateral interactions between protofilaments (see Cassimeris and Spittle, 2001). Most MAPs are rendered inactivate by phosphorylation, e.g. by MAP/microtubule affinity regulating kinases (MARKs; Trinczek et al., 1995), GSK-3 $\beta$  (Zumbrunn et al., 2001) or JNK (Yoshida et al., 2004).

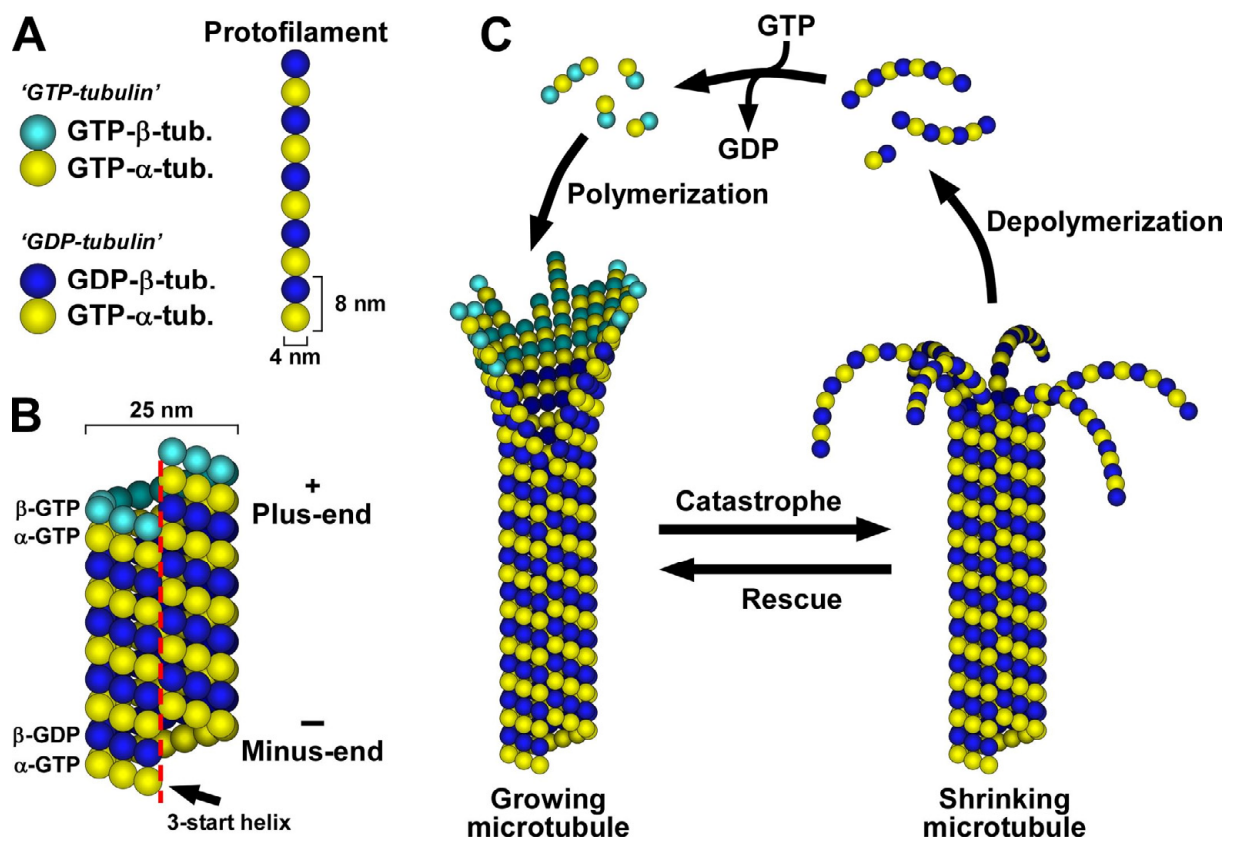


**Figure 1-6: Microtubules – Structure and dynamics**

(A) Heterodimers of  $\alpha$ - and  $\beta$ -tubulin are the building blocks of microtubules. Both  $\alpha$ - and  $\beta$ -tubulin bind one molecule of guanine nucleotide (Weisenberg *et al.*, 1968).  $\alpha$ -tubulin is associated with GTP which is neither exchanged nor hydrolyzed. The helical microtubule wall typically consists of 13 parallel protofilaments (A) with each turn of the helix spanning 3 tubulin monomers (B, see Desai and Mitchison, 1997; Mandelkow *et al.*, 1986). This arrangement results in a lattice seam on one side of the microtubule wall (B, red dashed line). Presumably, the structure of the microtubule is determined by the  $\gamma$ -tubulin ring complex ( $\gamma$ -TURC) at the MTOC. Microtubules are nucleated by the binding of  $\alpha/\beta$ -tubulin heterodimers to the  $\gamma$ -tubulin ring complex and start elongating by the addition of dimers at the plus-end (for review see Raynaud-Messina and Merdes, 2007). The binding, hydrolysis and exchange of GDP/GTP on the  $\beta$ -tubulin monomer is the driving force for switching between polymerization (assembly) and depolymerization (disassembly) of microtubules (C), yet it is not required for microtubule assembly itself (Hyman *et al.*, 1992). Scheme modified from Akhmanova and Steinmetz, 2008.

$\alpha/\beta$ -tubulin heterodimers are subject to various post-translational modifications including acetylation/deacetylation, tyrosination/detyrosination, generation of  $\Delta 2$ -tubulin, polyglutamylation, polyglycylation, palmitoylation and phosphorylation (reviewed in Westermann and Weber, 2003). Mainly, the carboxy-terminal tails of tubulin are modified. As yet, the functions of most posttranslational tubulin modifications have remained rather elusive. Some modifications are used as markers for microtubule longevity (reviewed in Westermann and Weber, 2003). For instance,

acetylation of  $\alpha$ -tubulin or enzymatic removal of its C-terminal tyrosine residue (detyrosination) gradually occurs in the microtubule polymer and is therefore found in long-lived, stable microtubules, i.e. microtubules with a low turnover which undergo few catastrophic events. In contrast, the presence of tyrosinated  $\alpha$ -tubulin in microtubules which has not undergone detyrosination yet, denotes a recent assembly, i.e. tyrosinated  $\alpha$ -tubulin is found in dynamic microtubules with a high turnover.

The intrinsic polarity of microtubules qualifies them as well-suited tracks for directed intracellular transport. Using various microtubule-dependent motor proteins of the kinesin and dynein superfamilies, cells specifically transport macromolecules, vesicles and organelles along microtubules (reviewed in Goldstein and Yang, 2000; Vale, 2003). Apart from few exceptions, most kinesins move toward the plus-ends of microtubules. By contrast, all dyneins discovered so far target microtubule minus-ends. It is still not fully understood how neurons achieve compartment-specific transport to axons and dendrites, but selective delivery, retention and vesicle fusion (reviewed in Tang, 2001), target-specific motor proteins (Setou *et al.*, 2000) and posttranslational modifications of microtubules (Reed *et al.*, 2006) seem to be involved in regulating this process.

In the context of neuronal polarization, microtubules have drawn little attention only. That is somewhat surprising since microtubules are necessary for process formation in neuronal and non-neuronal cells (Daniels, 1972; Edson *et al.*, 1993; Joshi *et al.*, 1985), growth cone steering (Buck and Zheng, 2002; Suter *et al.*, 1998) as well as migration of neuronal (Rakic *et al.*, 1996) and non-neuronal cells (Kole *et al.*, 2005; Liao *et al.*, 1995). Microtubules have mostly been considered to be passive players controlled by actin restraint (Forscher and Smith, 1988; Suter *et al.*, 1998; Waterman-Storer and Salmon, 1997; also see section 1.3.2 above).

Recently, a growing number of studies has identified polarity regulators that appear to act through processes independent of actin dynamics, including synapses of amphids defective (SAD) kinases (Kishi *et al.*, 2005), collapsin response mediator protein 2 (CRMP-2; Inagaki *et al.*, 2001) and GSK-3 $\beta$  (Jiang *et al.*, 2005; Yoshimura

*et al.*, 2005). This underscores the notion that additional intracellular mechanisms underlie neuronal polarization. Although these non-actin regulating proteins are involved in multiple processes, one common denominator appears to be their direct or indirect involvement in the control of microtubule dynamics. GSK-3 $\beta$ , for example, a multitarget protein kinase regulating many metabolic, signaling, and structural proteins (reviewed in Doble and Woodgett, 2003) is involved in the establishment and maintenance of neuronal polarity (Jiang *et al.*, 2005; Yoshimura *et al.*, 2005). Among its many functions GSK-3 $\beta$  also modulates microtubule dynamics, e.g. by phosphorylating MAPs (Doble and Woodgett, 2003; Goold *et al.*, 1999), whose binding to microtubules is essential for neurite formation (Caceres and Kosik, 1990). It is worth noting that some MAPs, including adenomatous polyposis coli protein (APC), are inhibited by GSK-3 $\beta$  phosphorylation while others, including MAP1B, are activated (Doble and Woodgett, 2003; Goold *et al.*, 1999). Consistent with the complex effects on MAPs, GSK-3 $\beta$  can either support or inhibit axonal growth depending on the extent of its inhibition (Kim *et al.*, 2006). Overexpression of CRMP-2, another target of GSK-3 $\beta$  implicated in the regulation of microtubule dynamics and endocytosis, induces multiple axons in later developmental stages, suggesting a role for CRMP-2 in axon formation and maintenance (Inagaki *et al.*, 2001). Another example are the SAD kinases, homologs of the conserved Par-1 serine/threonine kinase which acts in a variety of polarity events in species ranging from nematodes and flies to mammals (reviewed in Wodarz, 2002). SAD kinases are required for neuronal polarization (Kishi *et al.*, 2005) and modulate presynaptic vesicle clustering (Crump *et al.*, 2001) but also phosphorylate MAPs (Kishi *et al.*, 2005). Recent work also suggests a role for activated JNK, so far known to be implicated in the regulation of gene transcription, cell death and survival (reviewed in Bogoyevitch and Kobe, 2006) in axon formation (Oliva *et al.*, 2006). JNK target microtubule associated proteins —among a wide variety of other nuclear and cytoplasmic proteins, including transcription factors and actin regulating proteins (Bjorkblom *et al.*, 2005; Chang *et al.*, 2003; Reynolds *et al.*, 2000; Ricos *et al.*, 1999; Yoshida *et al.*, 2004).

In summary, several identified regulators of neuronal polarity appear to indirectly or directly act on microtubules. Therefore the possibility arises that, in addition to the

well-established function of the actin cytoskeleton, microtubules may play a pivotal role in axon formation.

#### **1.4 Objectives of this study**

Despite the wealth of polarity regulators identified in the past years our knowledge regarding the intracellular mechanisms that establish neuronal polarization has remained fragmentary. While efforts so far mainly have focused on the role of the actin cytoskeleton in axon formation, the task of microtubules in the establishment of neuronal polarity has remained unclear and is still poorly understood. The work presented in this thesis therefore aims to characterize the role of microtubules in neuronal polarization. To this end I addressed the following issues: 1) How do microtubule dynamics and stability change during initial neuronal development? 2) Do microtubules play an instructive role in axon formation? 3) What are possible regulators mediating changes in microtubule dynamics during axon formation? I report here that the future axon has more stable microtubules in its shaft, and that stabilization of microtubules is sufficient to induce axon formation. The data shows that microtubules and the regulation of their stability play an instructive role in the initial polarization of neuronal cells.

## **2. Results**

### **2.1 Microtubule turnover in neuronal cells**

Previous studies have yielded divergent results concerning the distribution of long-lived, stable microtubules in developing neuronal cells (Arregui *et al.*, 1991; Dotti and Banker, 1991), leaving it unclear whether microtubule turnover was different in axons and minor neurites. As an entry point to study the role of microtubules in initial neuronal polarization the differential distribution of microtubule turnover in neurons was reanalyzed. To that end cultured rodent hippocampal neurons (Dotti *et al.*, 1988) were used as a model system.

Some posttranslational modifications of  $\alpha$ -tubulin are a good read-out for turnover of microtubules (see section 1.3.3 on page 17), therefore acetylation and tyrosination levels of  $\alpha$ -tubulin were used as markers for stable and dynamic microtubules, respectively (reviewed in Westermann and Weber, 2003). While acetylated  $\alpha$ -tubulin is confined to microtubules, tyrosinated  $\alpha$ -tubulin is found both polymerized in microtubules and unpolymerized in the cytoplasm. To remove unpolymerized tubulin subunits, i.e. to assess polymerized microtubules only, cells were extracted during fixation. Thereafter, cells were stained for different posttranslational modifications of  $\alpha$ -tubulin and their distribution evaluated.

#### **2.1.1 Microtubule turnover is decreased in axons**

To examine potential differences in the microtubule turnover of axons and minor neurites, morphologically polarized neurons (stage 3) were scrutinized. Expectedly, tyrosinated microtubules were predominant in the growth cones of all processes regardless of their identity, reflecting their dynamic state required for steering and extension (Tanaka *et al.*, 1995; Figure 2-1 C, D).

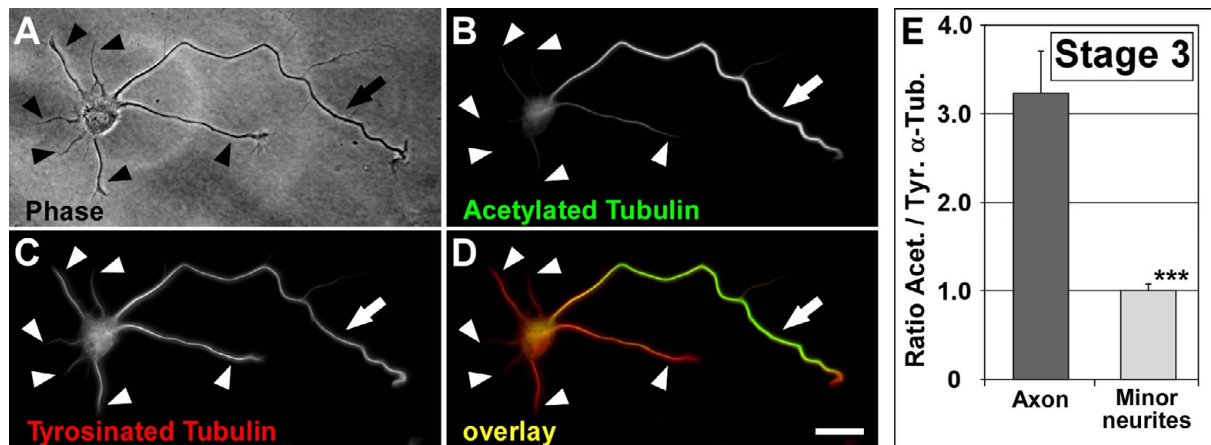


**Figure 2-1: Differential distribution of acetylated and tyrosinated microtubules in polarized hippocampal neurons**

(A-D) Polarized stage 3 rat hippocampal neurons stained for acetylated (B) and tyrosinated (C)  $\alpha$ -tubulin (arrow, axon; arrowheads, minor neurites). Cells were permeabilized during fixation to remove unpolymerized tubulin subunits, therefore only tubulin incorporated in microtubules is assessed. In stage 3 neurons, a high ratio of acetylated to tyrosinated  $\alpha$ -tubulin is found in microtubules in the axonal shaft (D, arrow) in comparison to microtubules of minor neurites (D, arrowheads, and E). Scale bar: 20  $\mu$ m.

(E) Ratio quantification of fluorescence intensities of acetylated and tyrosinated  $\alpha$ -tubulin in microtubules of stage 3 neurons (mean $\pm$ SEM; n>105 neurons from 3 independent experiments; \*\*\*, p-value<0.001 by t-test). Values are normalized to the mean of non-axonal processes.

When we analyzed fluorescence recovery after photo-bleaching (FRAP) using neurons transfected with  $\alpha$ -tubulin fused to GFP, we found that the GFP signal recovered faster in the growth cone compared to the axonal shaft. This reinforces the concept of a high turnover of microtubules in the growth cones (Figure 2-2).

The axonal shaft of stage 3 neurons (Figure 2-1 A), however, showed an enrichment of stable acetylated microtubules compared to the shafts of minor neurites in 83.5 $\pm$ 1.0% of the cases (mean $\pm$ SEM; n=709 neurons from 3 independent experiments; Figure 2-1 B, D). On average of all stage 3 neurons, the axonal shaft showed a 3.2-fold  $\pm$ 0.5 ratio increase of the fluorescence intensities of acetylated versus tyrosinated microtubules compared to the shafts of minor neurites (Figure 2-1 E; n=106 neurons from 3 independent experiments; p-value<0.001 by t-test).

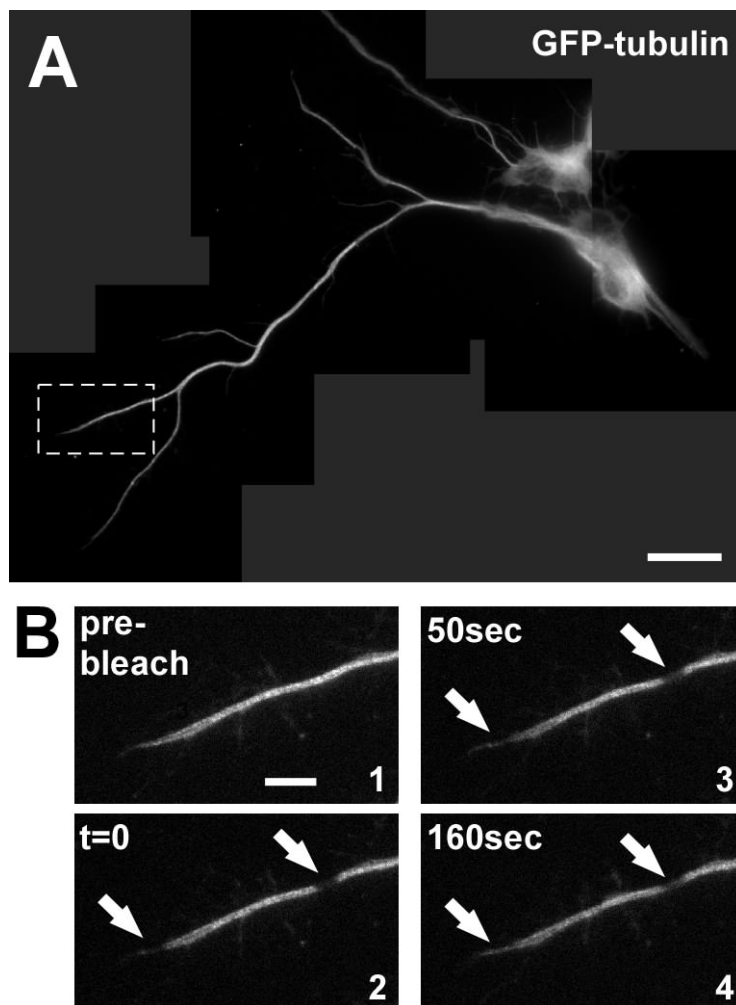


**Figure 2-2: Growth cones display higher microtubule turnover than neurite shafts**

(A) Rat hippocampal neuron (2 days *in vitro*), transfected with  $\alpha$ -tubulin-GFP.

(B) Panels 1 to 4 show a higher magnification of the area boxed in (A). The signal of  $\alpha$ -tubulin GFP was simultaneously bleached in two regions in the growth cone and the neurite shaft (arrows) and fluorescence recovery was followed afterwards.

Scale bars: 20  $\mu$ m (A); 5  $\mu$ m (B).

### 2.1.2 A reduction of microtubule turnover precedes axon formation

The above analysis had shown a correlation between axonal identity and reduced microtubule turnover in the axon. The next question was when this change in microtubule dynamics occurs: Is it a consequence of axon formation itself or does it happen already before the establishment of the axon?

For detailed analysis of the microtubule turnover in stage 2 neurons (Figure 2-3 A), the ratios of acetylated to tyrosinated  $\alpha$ -tubulin in the medial part of all neurites of a cell were measured and compared using the Hampel outlier test. In  $35.0 \pm 6.1\%$  of all stage 2 neurons one neurite had singled out and exhibited a significantly higher ratio of acetylated to tyrosinated  $\alpha$ -tubulin than the remaining neurites (Figure 2-3 B-D, arrowhead with asterisk; F, arrow; G;  $p$ -value < 0.05 by Hampel outlier test,  $n=107$

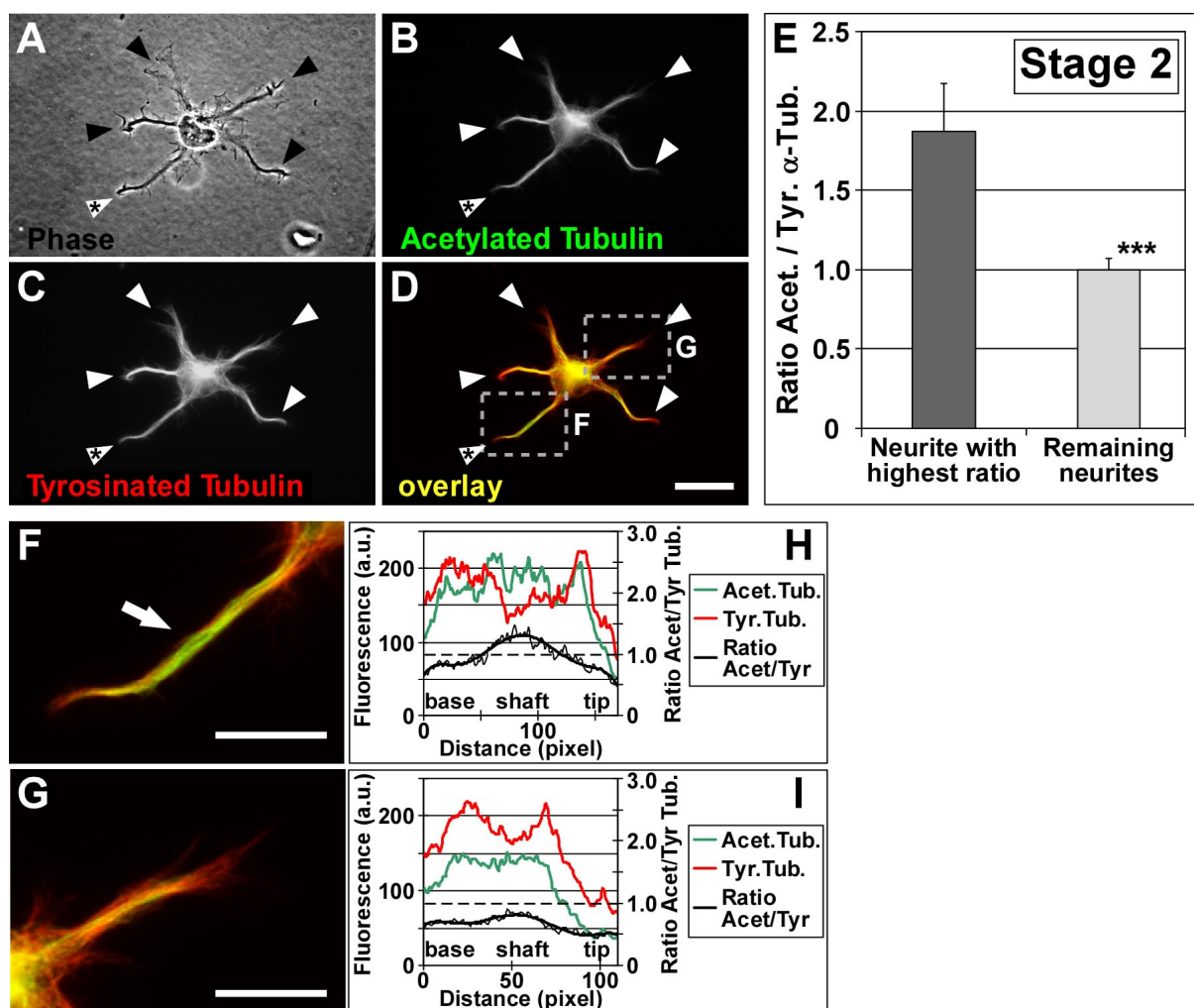


**Figure 2-3: Differential distribution of acetylated and tyrosinated microtubules in unpolarized hippocampal neurons**

(A-D) Morphologically unpolarized stage 2 rat hippocampal neurons stained for acetylated (B) and tyrosinated (C)  $\alpha$ -tubulin (compare Figure 2-1; arrowheads, minor neurites). In  $35.0 \pm 6.1\%$  of morphologically unpolarized stage 2 neurons, the ratio acetylated/tyrosinated  $\alpha$ -tubulin is significantly increased in one of the minor neurites (D, white arrowhead with asterisk) ( $p < 0.05$  by Hampel outlier test). The areas boxed in (D) are shown in higher magnification in panels (F) and (G). Scale bars: 20  $\mu\text{m}$ .

(E) Ratio quantification of fluorescence intensities of acetylated and tyrosinated  $\alpha$ -tubulin in microtubules of stage 2 neurons (mean  $\pm$  SEM;  $n > 105$  neurons from 3 independent experiments; \*\*\*,  $p$ -value  $< 0.001$  by t-test). Values are normalized to the mean of non-maximal processes.

(F-I) Higher magnification (F, G) and profiles of immunofluorescence intensity (arbitrary units) (H, I) of acetylated (green channel) and tyrosinated (red channel)  $\alpha$ -tubulin of the neurites marked in (D). Scale bars: 10  $\mu\text{m}$ .

neurons from 3 independent experiments). On average of all stage 2 neurons, the ratio of acetylated vs. tyrosinated  $\alpha$ -tubulin was increased 1.9-fold  $\pm 0.3$  in the minor neurite with the highest ratio compared to the average of the other neurites ( $p$ -value  $< 0.001$  by t-test; Figure 2-3 E) and also significantly different from the neurite with the second-highest ratio alone ( $p$ -value  $< 0.001$  by t-test). The increase of the

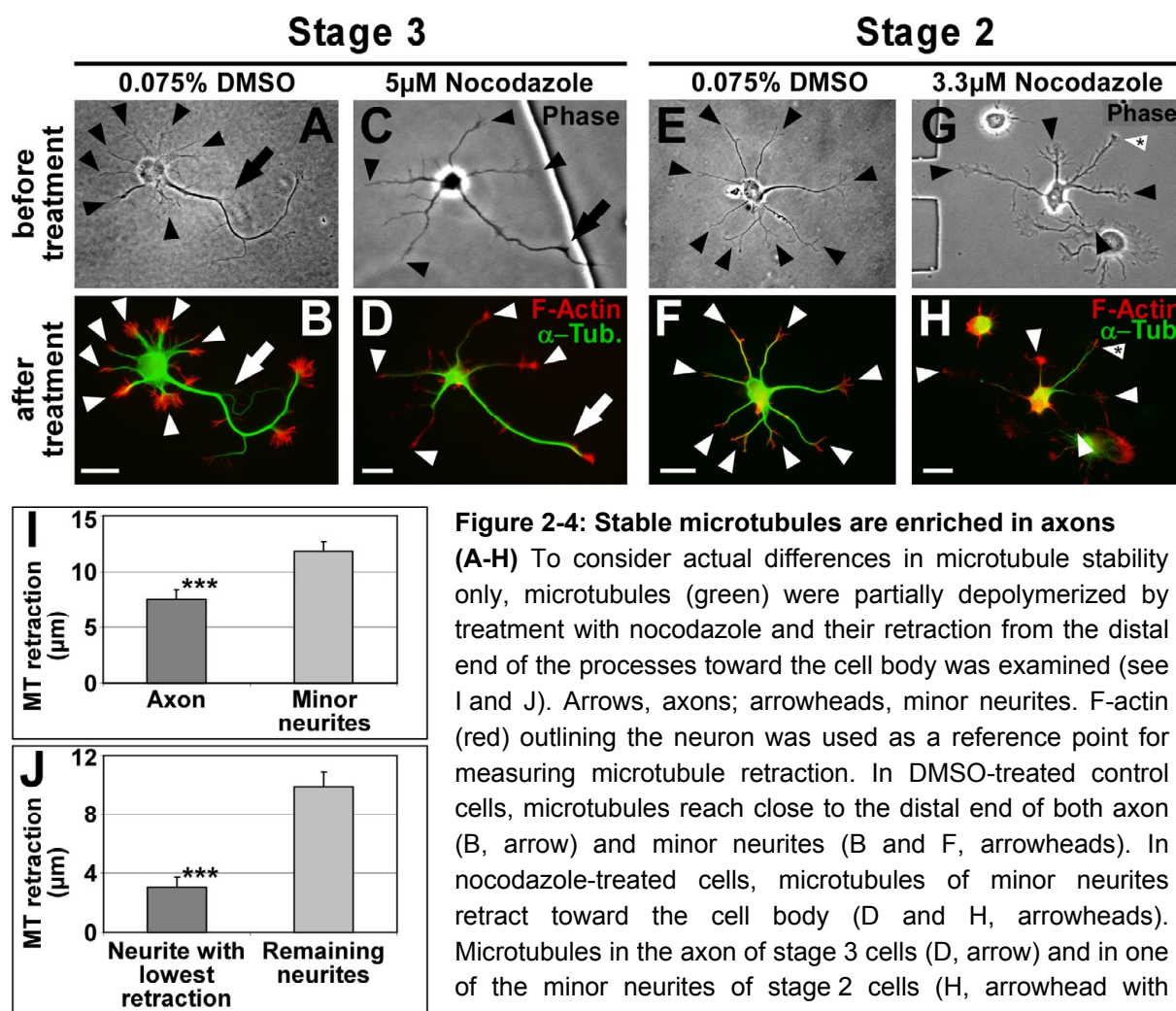
ratio was due to a relative increase of acetylated  $\alpha$ -tubulin over tyrosinated or total  $\alpha$ -tubulin within the process (Figure 2-3 H, I) and indicates that microtubule stabilization in one neurite precedes axon formation in morphologically still unpolarized cells.

### **2.1.3 Differences in posttranslational modifications reflect an actual stability difference of microtubules**

Posttranslational modifications of microtubules are widely used as markers for microtubule dynamics and stability (reviewed in Westermann and Weber, 2003). Altered microtubule dynamics, however, are not a result of the modifications themselves (Khawaja *et al.*, 1988). Therefore the next step was to address whether the observed differential distribution of posttranslational modifications reflects an actual stability difference of microtubules in axons and minor neurites.

To assess their stability microtubules were partially depolymerized by treatment with the microtubule destabilizing drug nocodazole (Hoebeke *et al.*, 1976) and their retraction at the distal end of processes was examined. To this end unpolarized cells (stage 2; 1 day *in vitro* (DIV)) and polarized cells (stage 3; 2 DIV) grown on a coverslip containing a relocation grid were located, imaged (Figure 2-4 A,C,E,G) and treated with 3.3-5 $\mu$ M nocodazole for 5 mins. Subsequently, cells were fixed and simultaneously extracted to remove tubulin monomers. Then  $\alpha$ -tubulin was labeled to assess microtubules and F-actin to better visualize the outline of the cells.

In 81.8 $\pm$ 5.9% (n=119 neurons from 5 independent experiments) of polarized neurons (stage 3), briefly treated with nocodazole for 5 min, microtubules of minor neurites retracted more than axonal microtubules (Figure 2-4 C, D, I; 7.6 $\pm$ 0.9  $\mu$ M and 11.9 $\pm$ 0.8  $\mu$ M in axons and minor neurites, respectively; p <0.001 by t-test). Treatment with vehicle (DMSO; Figure 2-4 A, B, E, F) showed no effect, microtubules extended close to the distal end of all processes (Figure 2-4 B, F). Thus, the differential distribution of posttranslational modifications also reflects an actual stability difference of microtubules in axons compared to minor neurites.



**(I and J)** Microtubule retraction after nocodazole treatment in polarized stage 3 (I) and morphologically unpolarized stage 2 (J) neurons (mean $\pm$ SEM; n=119 and 50 neurons from five and three independent experiments, respectively; \*\*\*, P<0.001 by t-test).

Similar to polarized neurons, morphologically unpolarized neurons (stage 2) showed a distinct difference between microtubule retraction in one neurite compared to the remaining neurites ( $3.1\pm 0.7 \mu\text{m}$  and  $9.9\pm 1.0 \mu\text{m}$ , respectively; n=50 neurons from 3 independent experiments; p-value<0.001 by t-test; Figure 2-4 G, H, J; compare with control neurons in Figure 2-4 E, F), thus suggesting an early polarization of stabilized microtubules during neuronal development.

Doublestaining for acetylated and tyrosinated  $\alpha$ -tubulin revealed that microtubules which resisted depolymerization were acetylated (Figure 2-5 A, B, D), whereas tyrosinated microtubules had vanished after nocodazole treatment (Figure 2-5 A, C, D). This is in agreement with previous studies (e.g. Baas and Black, 1990) and

confirms that acetylation and tyrosination of microtubules are indeed markers for microtubule stability. The ratio of acetylated to tyrosinated microtubules was subsequently used to rate microtubule stability.

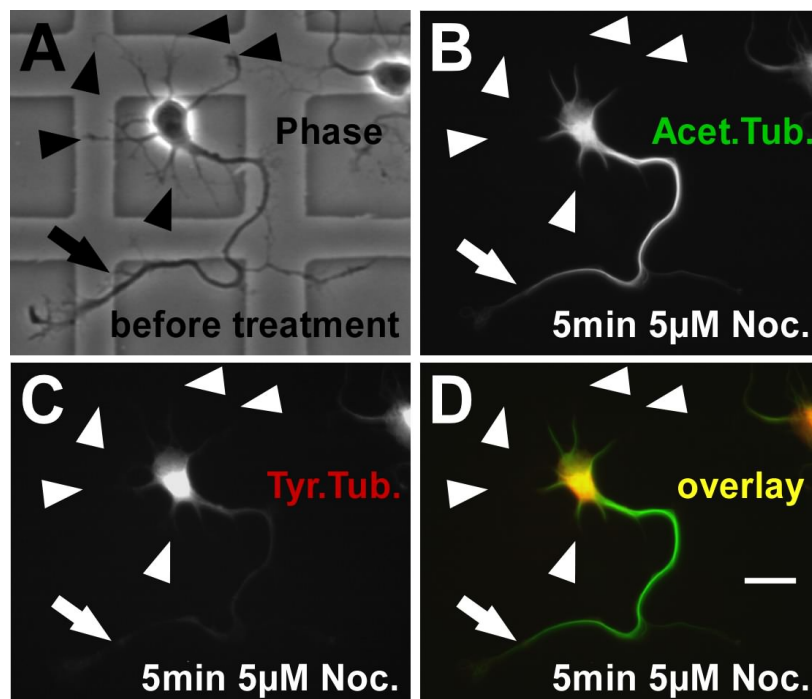


**Figure 2-5: Microtubule stability and posttranslational modifications of  $\alpha$ -tubulin**

Polarized rat hippocampal neurons with one axon (arrow) and several minor neurites (arrowheads) after 2 DIV before (A) and after (B-D) treatment with nocodazole ( $5 \mu\text{M}$  for 5 min). Tyrosinated (C; D, red channel) and acetylated (B; D, green channel) microtubules are assessed. Scale bar:  $20 \mu\text{m}$ .

Taken together, these results indicate that the axon of stage 3 neurons and one minor neurite of a subpopulation of stage 2 neurons show markers of lower microtubule turnover. Moreover, these differences in posttranslational modifications reflect a stability difference of microtubules in morphologically polarized and unpolarized neurons.

## **2.2 Microtubule turnover is changed in neurons whose polarity is affected by manipulation of polarity regulators**

In recent years a number of molecular players has been identified which are involved in the regulation of neuronal polarity (reviewed in Arimura and Kaibuchi, 2007). To assess whether such regulators potentially affect microtubule turnover in polarizing

neurons two examples with opposing polarity phenotypes –formation of multiple axons and loss of polarity– were analyzed.

### 2.2.1 Microtubule turnover is reduced in supernumerary axons induced by inhibition of GSK-3 $\beta$

First, the relation of microtubule turnover and GSK-3 $\beta$ , one of the central regulators of neuronal polarity, was investigated. Inhibition of GSK-3 $\beta$  has been reported to induce the formation of multiple axons (Jiang *et al.*, 2005; Yoshimura *et al.*, 2005) and therefore provided a means to analyze a multiple axon-phenotype. In this study, the GSK-3 $\beta$  inhibitor SB415286 (Meijer *et al.*, 2004 and references therein) was used.

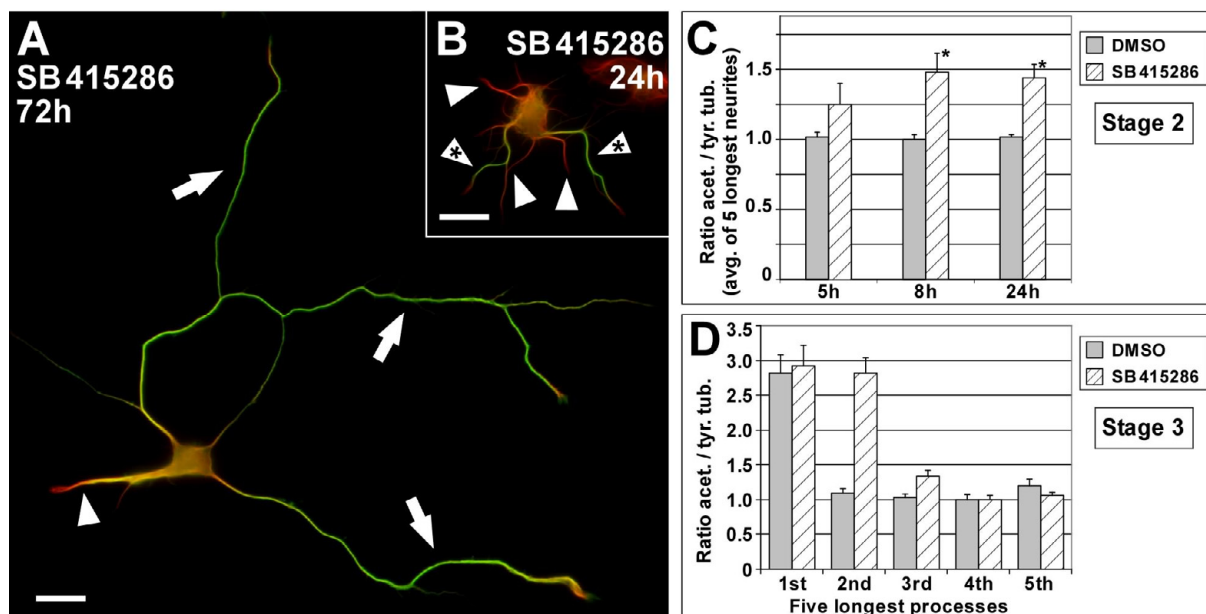


**Figure 2-6: Supernumerary axons induced by inhibition of GSK-3 $\beta$  show increased microtubule stability**

(A, B) Rat hippocampal neurons grown in the presence of GSK-3 $\beta$  inhibitor SB 415286 for 72h (A) and 24h (B) (arrow, axon; arrowheads, minor neurites; arrowheads with asterisk, neurite with increased microtubule stability). Scale bars: 20  $\mu$ m

(C) Ratio quantification of fluorescence intensities of acetylated and tyrosinated  $\alpha$ -tubulin in microtubules of unpolarized stage 2 neurons. The normalized average ratio of the 5 longest neurites is shown (mean $\pm$ SEM; n>50 neurons per condition and time point from 3 independent experiments; \*, p<0.05 by t-test).

(D) Rat hippocampal neurons (3 DIV) treated with the GSK-3 $\beta$  inhibitor SB 415286 (10-20  $\mu$ M; treatment 6-8 hours after plating) formed 2.1 $\pm$ 0.1 axons on average. These supernumerary axons show an increased ratio of acetylated to tyrosinated  $\alpha$ -tubulin, equal (p>0.35 by t-test) to that of the single axon of stage 3 control neurons (treatment 0.04% DMSO) (mean $\pm$ SEM; n>35 neurons from 3 independent experiments).

After 3 DIV, rat hippocampal neurons grown in the presence of SB415286 (10-20  $\mu$ M; applied 6-8 h after plating), had developed  $2.1 \pm 0.1$  axons, based on morphology and the presence of the axonal marker Tau-1. The stability of microtubules in the supernumerary axons was assessed by measuring the ratio of stable versus dynamic microtubules. Interestingly, additional axons induced by inhibition of GSK-3 $\beta$  showed an enrichment of acetylated microtubules similar to wild type axons (Figure 2-6 A, D; compare to Figure 2-1 D).

These data indicate that inhibition of GSK-3 $\beta$  causes an increase of microtubule stability along with the formation of multiple axons.

### **2.2.2 Inhibition of GSK-3 $\beta$ leads to microtubule stabilization before axon formation**

The next question was now whether this increase in microtubule stability occurred before or as a consequence of the axon formation induced by inhibition of GSK-3 $\beta$ . To address this issue a time-course experiment was conducted. Cells grown in the presence of SB415286 were fixed at certain time points after applying the GSK-3 $\beta$  inhibitor and their microtubule stability was assessed. An increase in microtubule acetylation in several minor neurites (Figure 2-6 B, arrowheads with asterisk) preceded the formation of multiple axons in morphologically still unpolarized stage 2 neurons treated with SB415286. To quantify this effect, the ratio of stable versus dynamic microtubules was determined for all processes; then the average of the five longest processes was formed since the analyzed neurons (stage 2) had not formed an axon yet (Figure 2-6 B). Approximately 5h after treatment with SB 415286, stage 2 neurons showed a trend towards increased microtubule acetylation ( $+23.0 \pm 10.6\%$ ), indicating a raise in microtubule stability (Figure 2-6 C). This increase was significant after  $\sim 8$ h ( $+47.4 \pm 8.7\%$ ; mean  $\pm$  SEM;  $p < 0.05$  by t-test).

Taken together, these data suggest that GSK-3 $\beta$  affects microtubule turnover in polarizing neurons. Moreover, an induction of microtubule stabilization by inhibition of GSK-3 $\beta$  seems to occur already in stage 2 neurons before axon formation.

### 2.2.3 Polarization of microtubule stability is lost in SAD A / SAD B knockout neurons

For comparison to a multi-axonal phenotype neurons from mice deficient in the PAR-1 homologs *sad-a* and *sad-b* (*sad-a*<sup>-/-</sup>; *sad-b*<sup>-/-</sup>, further on called SAD A/B<sup>-/-</sup>) were analyzed. SAD A/B knockout neurons show a polarity defect and lack a mature axons. In contrast, they generate multiple processes of similar length that are without a clear identity, containing both the dendritic marker MAP2 as well as the axonal marker Tau-1 (Kishi *et al.*, 2005).

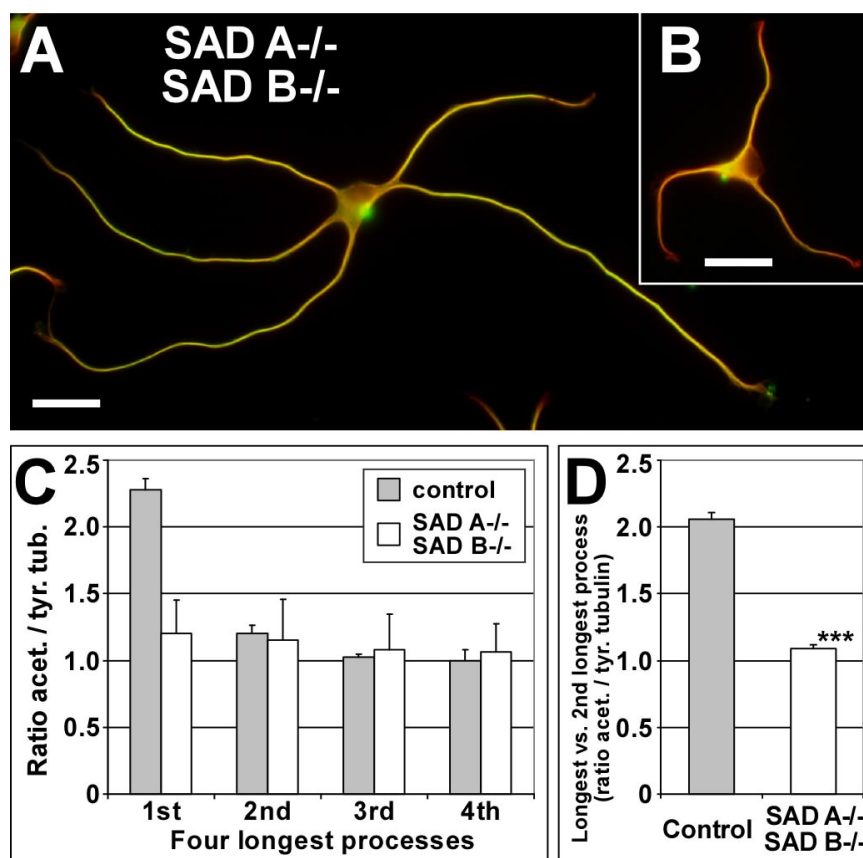


**Figure 2-7: Loss of neuronal polarity in SAD A/B knockout neurons is associated with loss of polarized microtubule stability**

(A, B) Hippocampal neurons (3 DIV) derived from mice deficient for SAD A and SAD B kinase show disturbed polarity, lacking a defined axon. Instead, SAD A/B knockout neurons form multiple processes of similar length and uniform tubulin acetylation levels (see (C)), yet a high cell-to-cell variability. Scale bars: 20  $\mu$ m

(C) Ratio quantification of fluorescence intensities of acetylated and tyrosinated  $\alpha$ -tubulin in microtubules. Processes of SAD A<sup>-/-</sup>B<sup>-/-</sup> neurons are short of the specific enrichment of acetylated microtubules in one process found in wild type neurons as well as littermate control neurons (SAD A<sup>+/+</sup>B<sup>+/+</sup>) (mean $\pm$ SEM; n=66 and 27 neurons from 3 independent experiments for SAD A<sup>-/-</sup> SAD B<sup>-/-</sup> and control, respectively). Note that the acetylation/tyrosination ratio varies slightly in control cells between species (rat vs. mouse) (C, D).

(D) Ratio of the acetylation/tyrosination ratios of the longest versus second longest process per cell for SAD A<sup>-/-</sup>B<sup>-/-</sup> and control neurons (mean $\pm$ SEM; \*\*\*, p<0.001 by t-test).

SAD A/B kinase double knockout neurons lacked the specific enrichment of stable, acetylated microtubules in a single process found in wild type neurons as well as littermate control cultures (Figure 2-7 A-C), indicating a loss of polarized microtubule stability. Some of these neurons have neurites with microtubules acetylated to a similar extent as in axons, whereas the majority has an acetylation level that resembles minor neurites. Despite this cell-to-cell variation (Figure 2-7 A, B), however, acetylation levels were mostly uniform within a given cell. The acetylation/tyrosination ratio of the longest versus the second longest neurite per cell was not significantly different in SAD A<sup>-/-</sup> B<sup>-/-</sup> neurons (1.09±0.03; p-value>0.25 by t-test) while control neurons show a clear distinction (2.06±0.05; p-value<0.01 by t-test; Figure 2-7 D). Thus, specific alterations of neuronal polarity, including the formation of supernumerary axons or a loss of polarity, correlate with characteristic changes in microtubule stability.

In summary, these results show that specific alterations of neuronal polarity correlate with characteristic changes in microtubule turnover. Moreover, they suggest that the analyzed polarity regulators act via the modulation of microtubule stability.

### **2.3 Moderate microtubule destabilization selectively reduces the formation of minor neurites**

SAD kinases and GSK-3 $\beta$  can act upstream of microtubule dynamics by controlling the affinity of microtubule-associated proteins (Jiang *et al.*, 2005; Kishi *et al.*, 2005; Yoshimura *et al.*, 2005) that are known microtubule stability modulators, yet they have various other cellular functions including the regulation of metabolism, signaling, gene transcription and endocytosis (Crump *et al.*, 2001; Grimes and Jope, 2001). This abundance of putative regulatory mechanisms raised the question whether the observed differences in microtubule turnover between axons and minor neurites play a direct role in polarization. If microtubule stability is critical in distinguishing future axonal and dendritic fate, manipulations of microtubule dynamics should affect polarization.

To test this assumption neurons were cultured in the presence of the microtubule destabilizing drug nocodazole (Hoebeke *et al.*, 1976) at low concentrations (15-75 nM) which moderately increase the catastrophe rate of microtubules (Vasquez *et al.*, 1997). Nocodazole was added to the medium after 1 DIV and cells were further cultured in the presence of the drug. After 3 DIV, cells were fixed and stained for the axonal marker Tau-1.

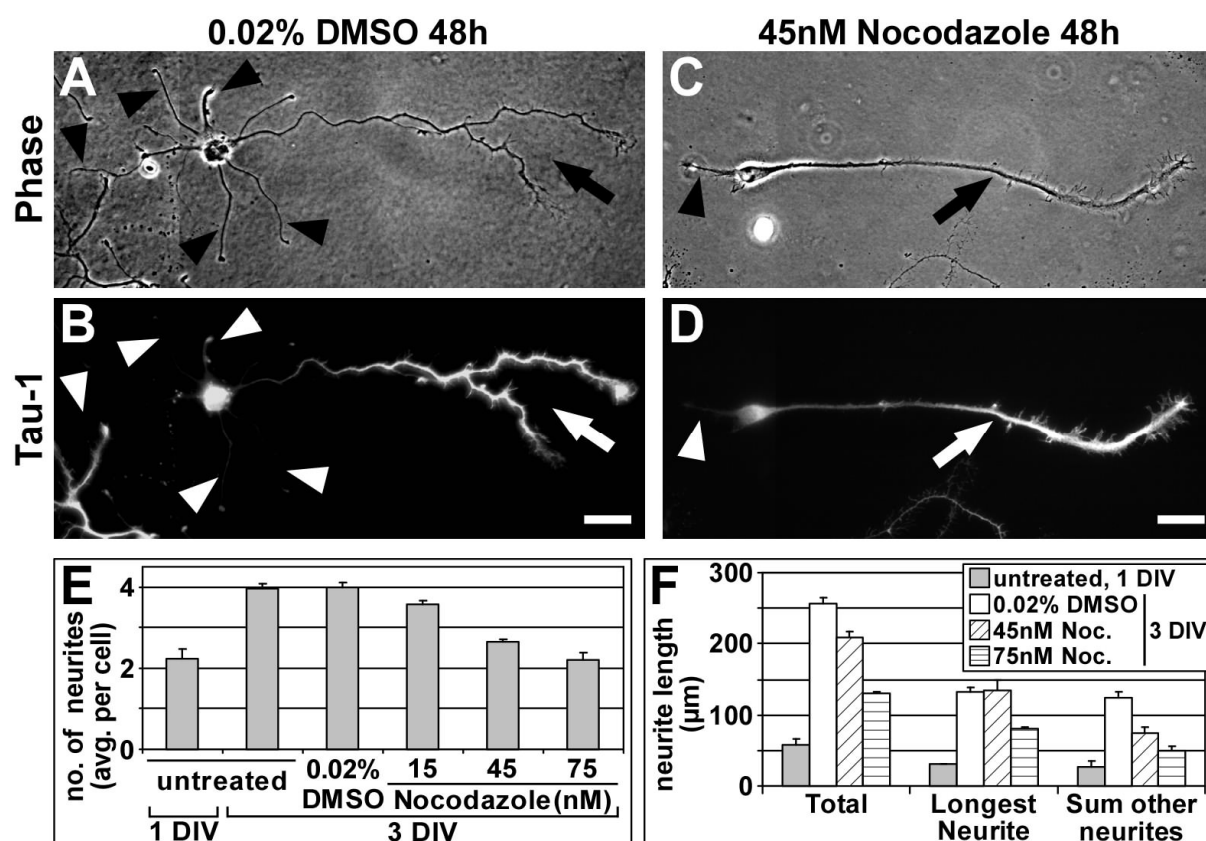


**Figure 2-8: Moderate microtubule destabilization selectively blocks the formation of minor neurites**

(A-D) Rat hippocampal neurons (3 DIV) cultured in the presence of various low concentrations of nocodazole or 0.02% DMSO (treatment after 1 DIV), stained for Tau-1 (B, D). Scale bars: 20 μm.

(A, B) Control neurons have formed one axon (A, arrow) with the typical Tau-1 gradient towards its distal part (B, arrow) and several Tau-1-negative minor neurites (arrowheads).

(C, D) The number of minor neurites (arrowheads) is reduced under growth conditions which slightly destabilize microtubules, however, neurons are still able to form an axon (arrow).

(E) Nocodazole reduces the number of minor neurites formed in a concentration-dependent manner (neurites per cell:  $4.0 \pm 0.1$ ,  $3.6 \pm 0.1$ ,  $2.6 \pm 0.1$ , and  $2.2 \pm 0.2$  for 0.02% DMSO, 15, 45 and 75 nM nocodazole, respectively;  $p$ -value < 0.001 by ANOVA;  $n > 750$  neurons from 3 independent experiments per condition).

(F) Neurite extension is not blocked by low concentrations of nocodazole. Total neurite length increased from day 1 to day 3 under all conditions ( $n > 275$  neurons per condition from 3 independent experiments;  $p$ -value < 0.001 by t-test). Data is presented as mean  $\pm$  SEM.

In control cells, the average number of processes almost doubled from day 1 ( $2.2 \pm 0.2$  processes per cell) to day 3 *in vitro* ( $4.0 \pm 0.1$  processes per cell;  $p$ -value  $< 0.001$  by ANOVA; Figure 2-8 E), reflecting the formation of an axon and several minor neurites (Figure 2-8 A, B). Cells grown in the presence of low concentrations of nocodazole were able to form and extend an axon likewise (Figure 2-8 C, D, arrow). The number of minor neurites, however, was significantly reduced in nocodazole-treated neurons (Figure 2-8 C, D, arrowhead; E). This reduction was not due to a general growth inhibition by nocodazole (Figure 2-8 F) but caused by the development of many neurons with just one or two processes (Figure 2-8 C-E). Total neurite length increased from day 1 to day 3 under all conditions ( $p$ -value  $< 0.001$  by t-test), however, to a lesser extent when treated with 45 or 75 nM nocodazole (increase from  $57.5 \pm 7.8 \mu\text{m}$  to  $255.8 \pm 9.7 \mu\text{m}$ ,  $209.3 \pm 8.6 \mu\text{m}$  and  $130.3 \pm 3.6 \mu\text{m}$  for 0.02% DMSO, 45 or 75 nM nocodazole, respectively;  $n > 275$  neurons per condition from 3 independent experiments). Interestingly, the extension of the axon was not impaired in contrast to minor neurites ( $132.1 \pm 6.1 \mu\text{m}$  and  $134.0 \pm 14.7 \mu\text{m}$  for 0.02% DMSO and 45 nM nocodazole, respectively;  $p > 0.5$  by t-test; Figure 2-8 F). Expectedly, higher concentrations of nocodazole started to inhibit axonal outgrowth as well (Figure 2-8 F). Taken together, the data suggest that the future axon is able to overcome moderate microtubule destabilizing conditions while the outgrowth of minor neurites is impaired.

## **2.4 Microtubule stabilization is sufficient to induce axon formation**

Since increased microtubule stability seemed to allow the axon to overcome microtubule destabilizing conditions it was interesting to assess whether microtubule stabilization itself is sufficient to induce axon formation. To address this question hippocampal neurons were treated after 1 DIV with the microtubule-stabilizing drug taxol (Schiff *et al.*, 1979; Schiff and Horwitz, 1980) for various durations. Previous studies (e.g. Dehmelt *et al.*, 2003; Schwamborn and Püschele, 2004) had used high concentrations of taxol ( $> 100$  nM) which render microtubules completely static and result in a block of neurite formation. In contrast, this study used low concentrations of taxol (3-10 nM) that favor microtubule polymerization (Derry *et al.*, 1995) yet do not completely block microtubule dynamics.

### 2.4.1 Microtubule stabilization promotes neurite outgrowth

Taxol-treated neurons showed a drastic increase in neurite outgrowth (Figure 2-9 A, E; Figure 2-10 A). The number of processes per cell exceeding 60  $\mu\text{m}$ , a morphological characteristic of early axons, had increased more than 2-fold in the presence of low concentrations of taxol (3-10 nM) for 2 days in comparison to control neurons (Figure 2-9 A, C, E).

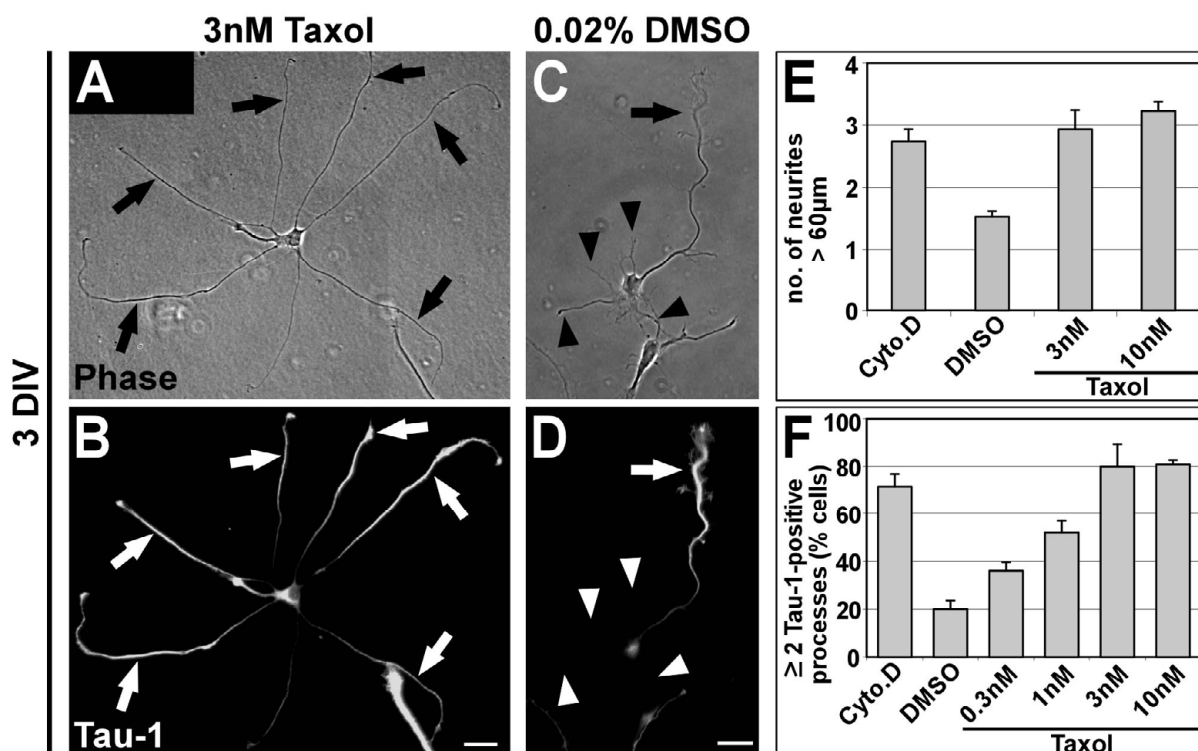


**Figure 2-9: Taxol-induced microtubule stabilization triggers the formation of multiple axons**

(A-D) Rat hippocampal neurons (3 DIV) grown in the presence of low concentrations of taxol (3 nM) or DMSO (treatment after 1 DIV), stained for the axonal marker Tau-1.

Taxol induces the formation of multiple elongated processes (A, arrows) positive for Tau-1 (B, arrows). Control neurons (C, D) have formed one axon (arrow) and several minor neurites (arrowheads). Scale bars: 20  $\mu\text{m}$ .

(E) The number of neurites longer than 60  $\mu\text{m}$  is increased after 2 days of taxol-treatment (mean $\pm$ SEM; p-value<0.001 by t-test; n>170 neurons per condition from 3 independent experiments per condition). DMSO (0.02%): vehicle; Cyto.D (1  $\mu\text{M}$  Cytochalasin D): positive control (Bradke and Dotti, 1999).

(F) The number of cells with two or more Tau-1-positive processes increases in a concentration-dependent manner in taxol-treated neurons (mean $\pm$ SEM; p-value<0.001 by ANOVA; n>800 neurons per condition from at least 3 independent experiments).

Taxol-induced processes showed a high ratio of acetylated to tyrosinated  $\alpha$ -tubulin resembling axonal characteristics (Figure 2-10 B; compare to Figure 2-1 D) and were

indistinguishable from axons in terms of their microtubule stability (Figure 2-10 C-F; compare to Figure 2-4).

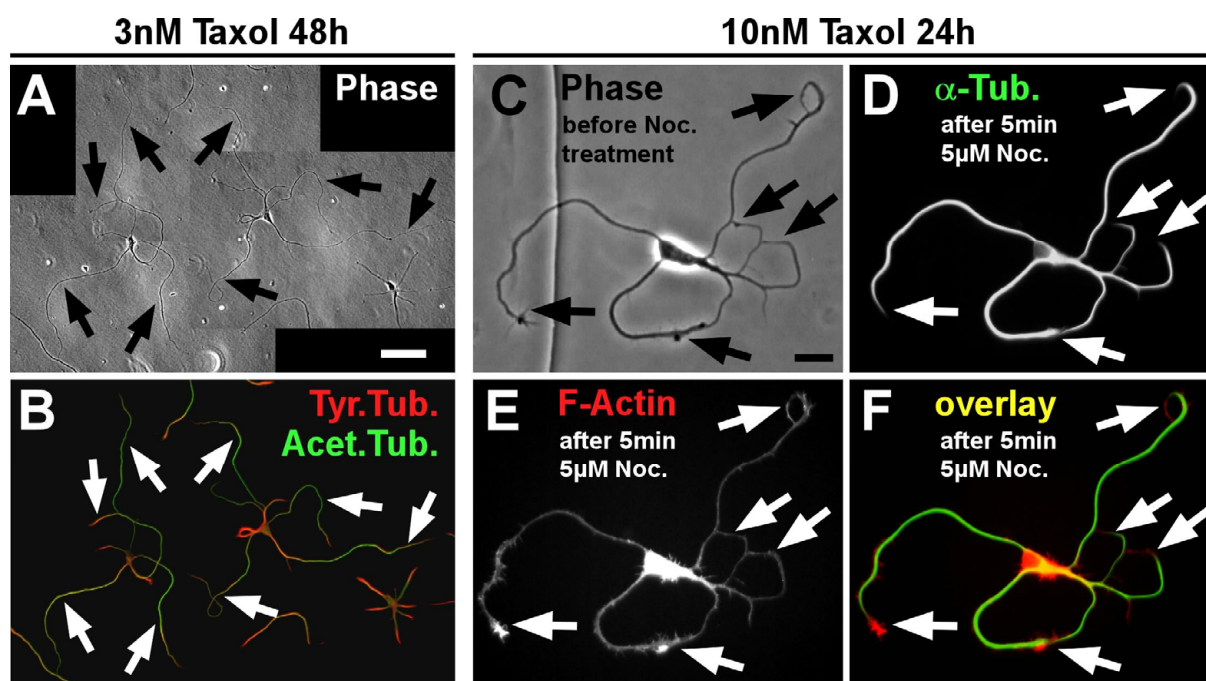


**Figure 2-10: Taxol induces the formation of axon-like processes with reduced microtubule turnover and increased stability**

(A, B) Taxol-treated rat hippocampal neurons (3 DIV, treatment with 3 nM taxol after 1 DIV). Taxol-induced processes (A, arrows) show an increased ratio of acetylated (green channel) to tyrosinated (red channel)  $\alpha$ -tubulin like axons (B, arrows; compare to Figure 2-1 D). Scale bar: 50  $\mu$ m.

(C-F) Taxol-treated rat hippocampal neurons (2 DIV, treatment with 10 nM taxol after 1 DIV). On day 2 *in vitro*, cells had formed multiple axon-like processes (A-D, arrows). Microtubule stability was assessed as before by partial depolymerization using nocodazole (see Figure 2-4 and section 5.2.1.5 in Materials and Methods). Only little retraction of microtubules (D, F, green channel) with respect to the actin cytoskeleton (E, F, red channel) occurred in the taxol-induced processes as observed in the overlay (F, arrows) ( $7.5 \pm 1.8 \mu$ m;  $n=67$  neurons from 3 independent experiments). This retraction distance did not differ significantly from the one seen for axons ( $7.6 \pm 0.9 \mu$ m;  $p$ -value  $> 0.1$  by  $t$ -test) but was significantly shorter than the distance of retraction displayed by minor neurites ( $11.9 \pm 0.9 \mu$ m;  $p$ -value  $< 0.001$  by  $t$ -test). Scale bars: 20  $\mu$ m.

Still, with the low taxol concentrations used tyrosinated microtubules prevailed in the growth cones of these processes (Figure 2-10 B), indicating that microtubule dynamics were not completely abolished. In contrast, higher taxol concentrations blocked microtubule dynamics and axonal growth completely (Dehmelt *et al.*, 2003).

### 2.4.2 Taxol-induced processes show axonal characteristics

Taxol-induced processes also showed other typical axonal features. After 3 DIV the number of cells with two or more processes positive for the axonal marker Tau-1 was increased 4-fold in taxol-treated neurons compared to control neurons (Figure 2-9 B, D, F, page 34). At later stages of development when axonal and dendritic proteins become segregated (Craig and Banker, 1994), the taxol-induced Tau-1 positive processes also showed the restriction of the dendritic marker MAP2 to the proximal part of the process as in control axons (Figure 2-11, open arrowheads). In addition to the supernumerary axons most of the cells had at least one or two dendrites.

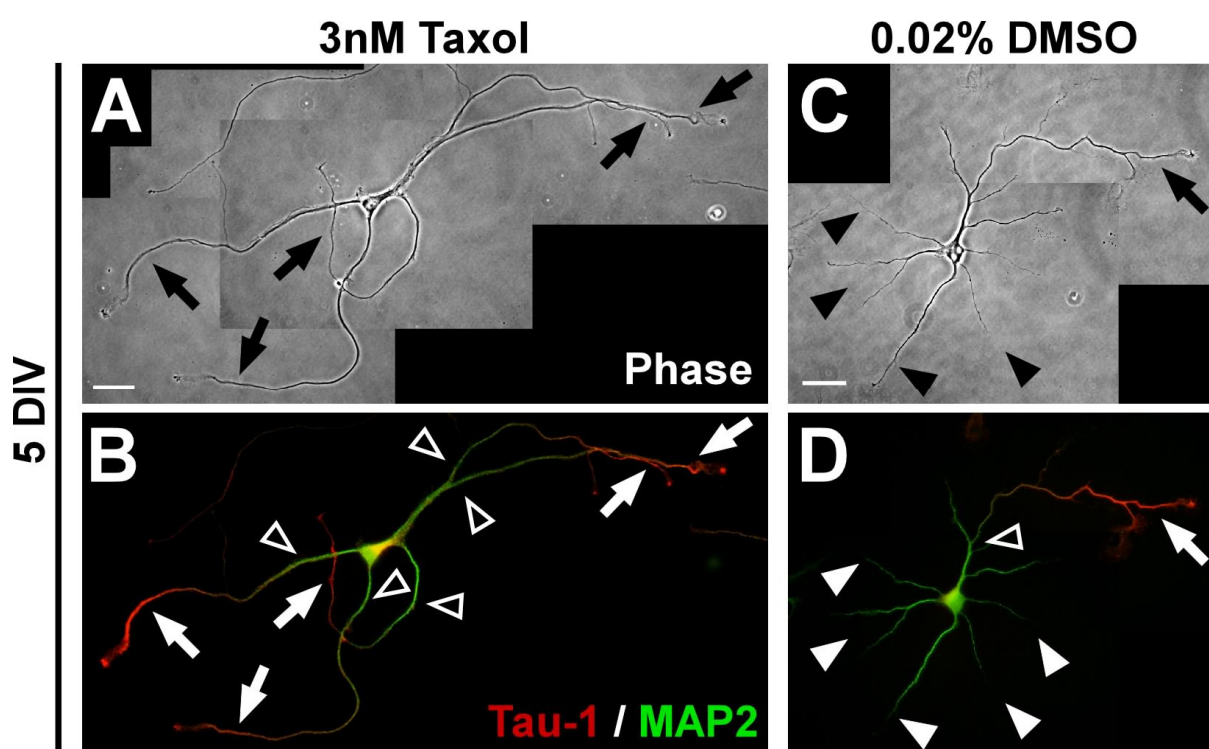


**Figure 2-11: Taxol-induced processes show axonal characteristics**

Rat hippocampal neurons (5 DIV) grown in the presence of taxol (3 nM; A, B) or DMSO (0.02%; C, D) (treatment after 1 DIV), stained for Tau-1 (B, D, red channel) and the dendritic marker MAP2 (B, D, green channel).

DMSO-treated neurons have formed one axon (arrow) and several dendrites (black arrowheads) (C). Taxol-induced processes (A, arrows) show a proximal-distal gradient of Tau-1 (B, arrows) like control axons (D, arrow). MAP2-signal is restricted to dendrites (D, white arrowheads) and the proximal part of axons and Taxol-induced processes (B, D, open arrowheads). Scale bars: 25  $\mu$ m.

The taxol-induced processes also clustered the presynaptic marker Synapsin 1 later in development (10-12 DIV; Figure 2-12) which was not observed in dendrites, further

confirming their axonal character. These results therefore indicate that microtubule stabilization causes the formation of multiple axons.

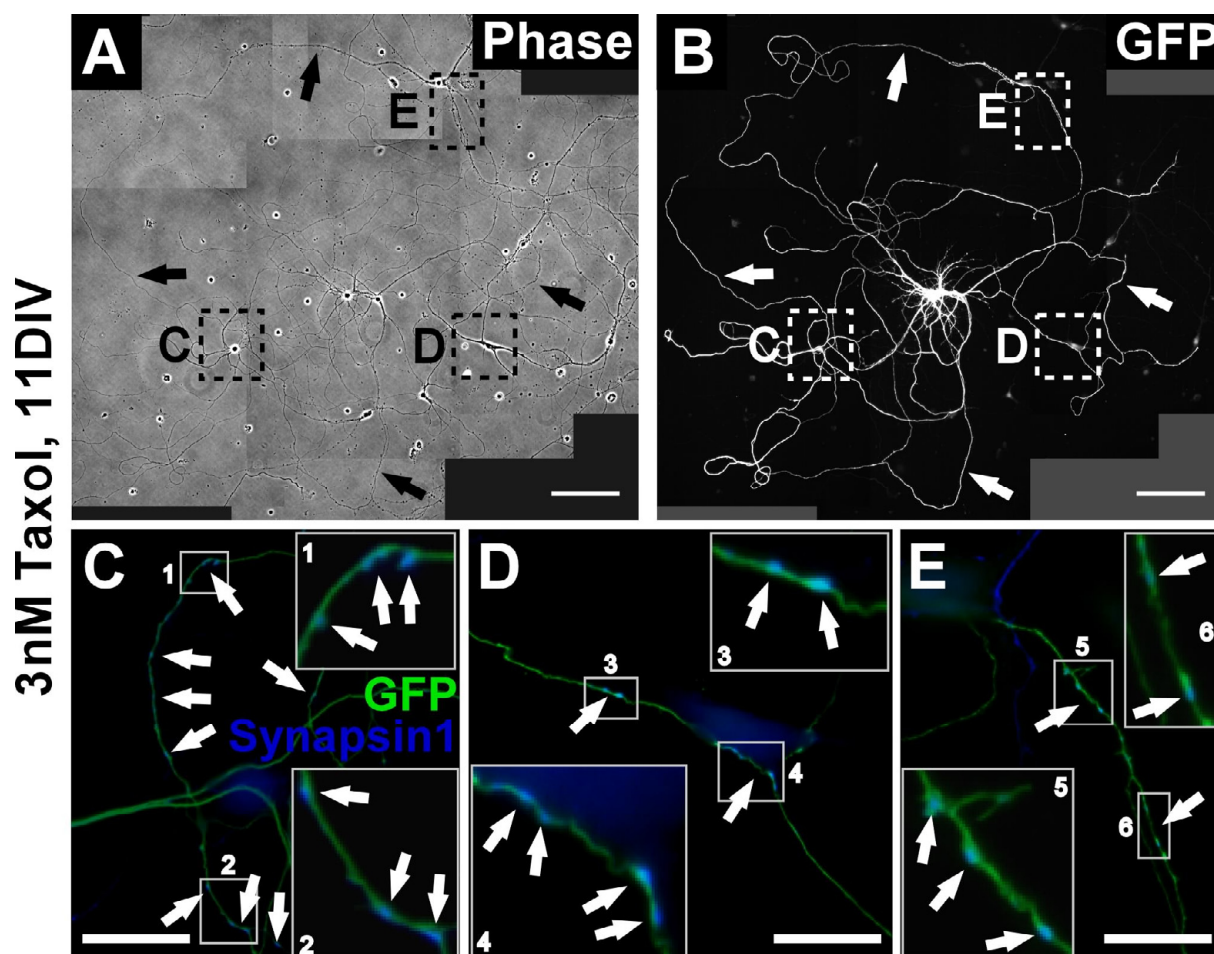


**Figure 2-12: Multiaxonal neurons mature and form neuronal networks**

Maturation of taxol-treated neurons. To unequivocally identify the origin of axons in the dense neuronal network neurons establish we used cultures of mouse hippocampal neurons in which a subset of cells expressed enhanced green fluorescent protein (eGFP) under the control of a ubiquitously active promoter (Okabe *et al.*, 1997). Mixed WT/GFP cultures containing 1-3% of neurons expressing GFP allow following individual neurons in dense networks (A, B). Taxol (3 nM) was added to the medium of the mixed culture after 1 DIV, neurons were further grown in the presence of the drug, fixed after 11 DIV and immunostained for GFP (green channel) and the presynaptic marker Synapsin 1 (blue channel).

(A, B) Taxol-treated neurons have formed multiple axons (arrows) in  $81.3 \pm 2.2\%$  of the cases ( $n > 120$  neurons).

(C-E) Higher magnifications of the regions marked in (A) and (B). The multiaxonal GFP-positive neurons cluster the presynaptic marker Synapsin 1 in their axons. Magnifications of the regions boxed in (C-E) are shown as insets to better visualize the localization of Synapsin 1 on GFP-positive axons (arrows). Scale bars: 100  $\mu\text{m}$  (A, B), 20  $\mu\text{m}$  (C-E).

### 2.4.3 Microtubule acetylation alone is not sufficient to induce axon formation

The application of taxol resulted in the stabilization of microtubules (Figure 2-10 C-D), however, it also induced acetylation of microtubules (Figure 2-10 B). Microtubule acetylation was recently reported to promote kinesin-1-mediated cargo transport to specific neurites (Reed *et al.*, 2006). Such directed transport in turn might trigger axon formation from a specific neurite. In principle, the axon-inducing effect of taxol could be related to its microtubule stabilizing function or the consecutive acetylation of microtubules. To address this point acetylation of microtubules was indirectly increased by inhibiting their deacetylation. Since posttranslational modifications themselves are a result but not the cause of altered microtubule dynamics (Khawaja *et al.*, 1988) this provided a means to assess the effect of increased microtubule acetylation independently of microtubule stabilization. Deacetylase inhibitors were added to the culture medium ~12 h after plating, cells were further cultured in the presence of the drug and fixed after 2 to 4 days.

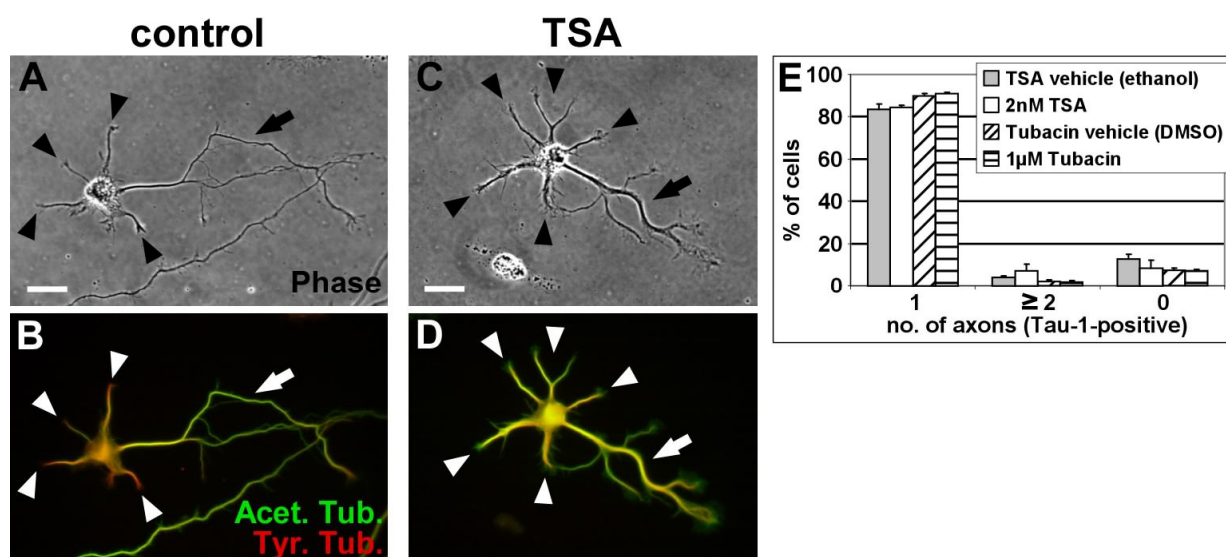


**Figure 2-13: Acetylation of microtubules alone is not sufficient to induce axon formation.**

(A–D) Hippocampal neurons grown in the presence of 0.02% ethanol (control; A, B) or deacetylase inhibitors TSA (2 nM; C, D) or tubacin (not depicted), fixed after 2 DIV (treatment ~12 h after plating). Control neurons (A, B) show a high ratio of acetylated (green channel) versus tyrosinated (red channel) microtubules in the axon (B, arrow) in comparison to minor neurites (B, arrowheads). Neurons treated with TSA (2 nM; C, D) feature an increased level of microtubule acetylation in the minor neurites (D), yet show normal polarization with one axon (arrow) and several minor neurites (arrowheads).

Scale bars: 20  $\mu$ m.

(E) Quantification of axon numbers (assessed by Tau-1 staining) in neurons treated with deacetylase inhibitors (TSA or tubacin) and control neurons (treated with ethanol or DMSO).

Posttranslational modifications of microtubules and the distribution of microtubule-associated proteins were scrutinized by immunostaining. This experiment was carried out together with Dorothee Neukirchen.

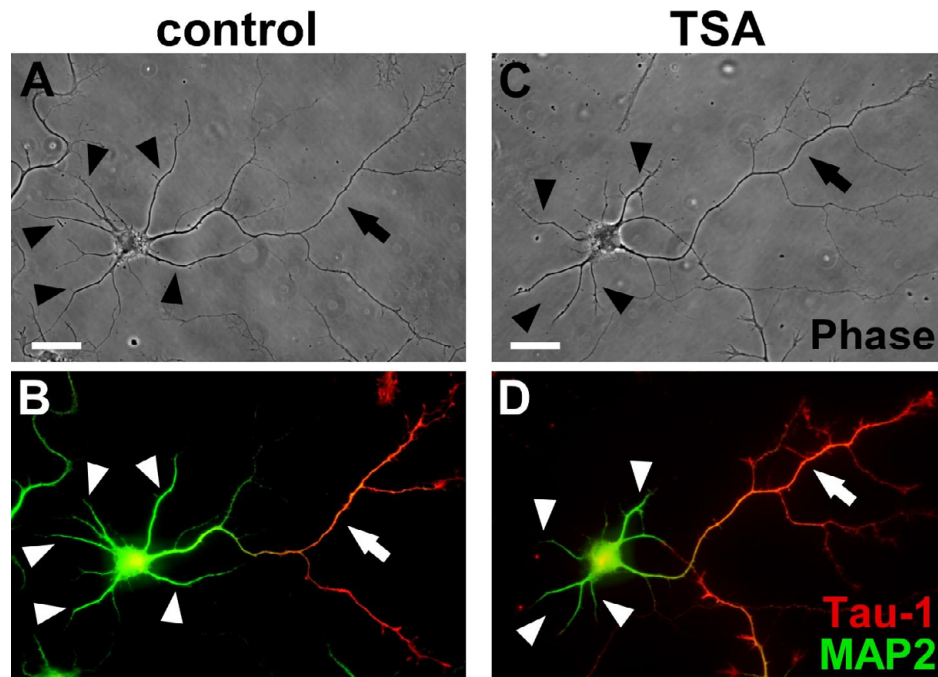


**Figure 2-14: Treatment with deacetylase inhibitors does not alter the distribution of specific microtubule associated proteins.**

Hippocampal neurons grown in the presence of 0.02% ethanol (control; A, B) or deacetylase inhibitor TSA (2 nM; C, D), fixed after 4 DIV (treatment ~12 h after plating). The distribution of Tau-1 (B, D; red channel) and MAP2 (B, D; green channel) is not altered in neurons treated with deacetylase inhibitors. Scale bars: 20  $\mu$ m.

Neurons treated with the deacetylase inhibitors tubacin (1  $\mu$ M) and trichostatin A (TSA; 2 nM) featured a clear increase of microtubule acetylation in minor neurites similar to that of axons (Figure 2-13 A-D). In spite of this elevated microtubule acetylation, polarity was not altered in these neurons and they showed no increase in supernumerary axons compared to control neurons (Figure 2-13 E). Moreover, the distribution of several microtubule-associated proteins (MAP2 and dephosphorylated Tau, recognized by Tau-1 antibody) was indistinguishable from control cells (Figure 2-14). Thus, the axon-inducing effect of taxol appears to be linked to microtubule stabilization itself. Increasing acetylation of microtubules *per se*, however, does not affect neuronal polarity.

## 2.5 Taxol application rapidly stabilizes microtubules and shifts dynamic microtubules to the tips of processes

After having established that microtubule stabilization causes the formation of multiple axons the mechanism by which taxol acts was further analyzed. To assess microtubule dynamics in living neurons during axon formation, neurons were transfected with the GFP-tagged microtubule plus end binding protein 3 (EB3; Stepanova et al., 2003). EB3 belongs to a family of proteins which specifically bind to polymerizing microtubule plus ends, the microtubule plus-end-tracking proteins (reviewed in Akhmanova and Hoogenraad, 2005). Microtubule dynamics in living neurons were monitored at different developmental stages and after addition of taxol using time lapse fluorescence microscopy.

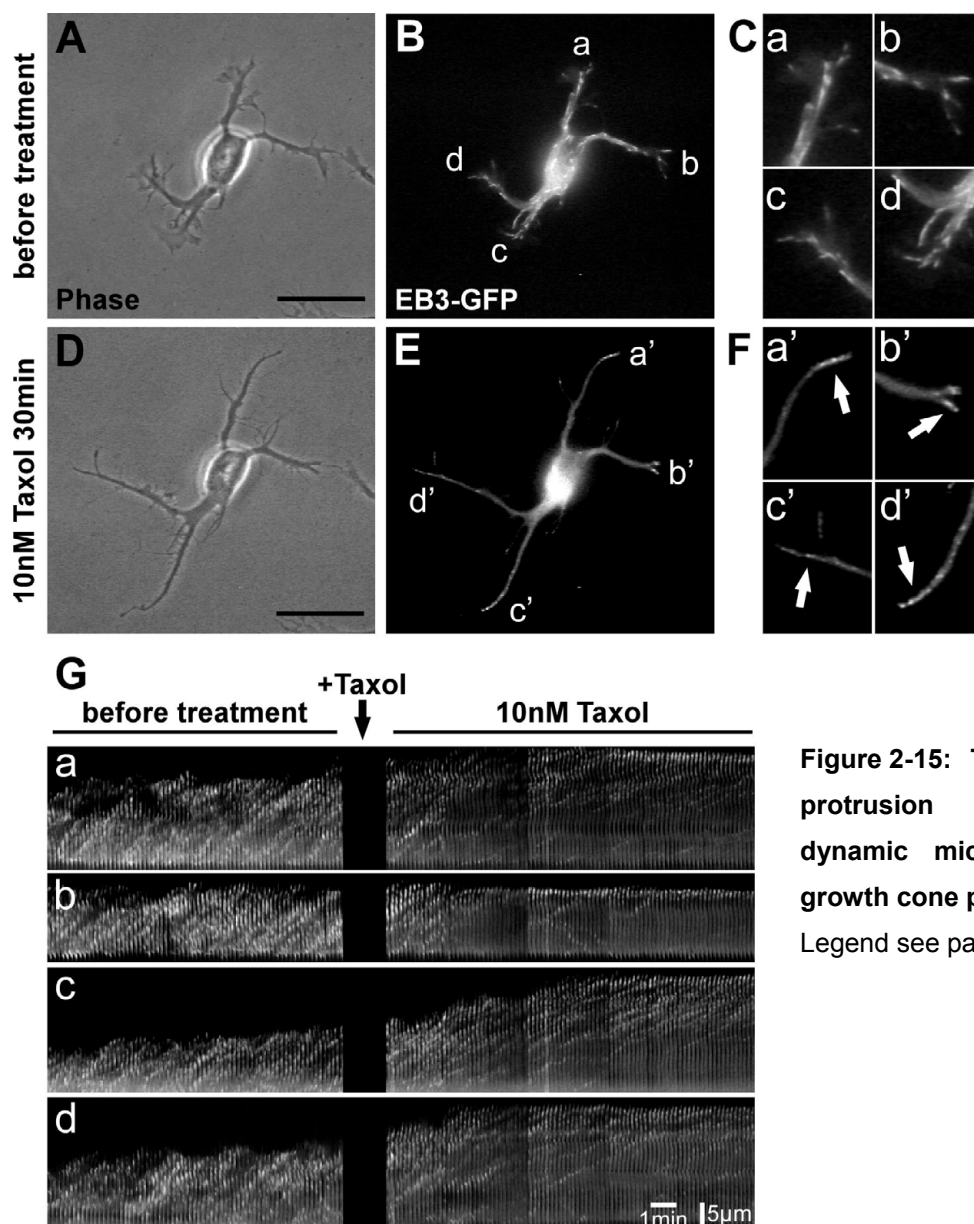


**Figure 2-15: Taxol induces the protrusion of polymerizing dynamic microtubules to the growth cone periphery**

Legend see page 41

Overall, the application of low concentrations of taxol (10 nM) reduced the dynamicity of microtubules (Figure 2-15). We observed a reduction of moving EB3-GFP particles in neurites to 51.0% of controls ( $\geq 500$  moving EB3-particles of at least 5 neurons per condition quantified). Low concentrations of taxol, however, did not completely abolish microtubule dynamics like higher taxol concentrations ( $>100$  nM) used in earlier studies (Figure 2-16, Stepanova et al., 2003).

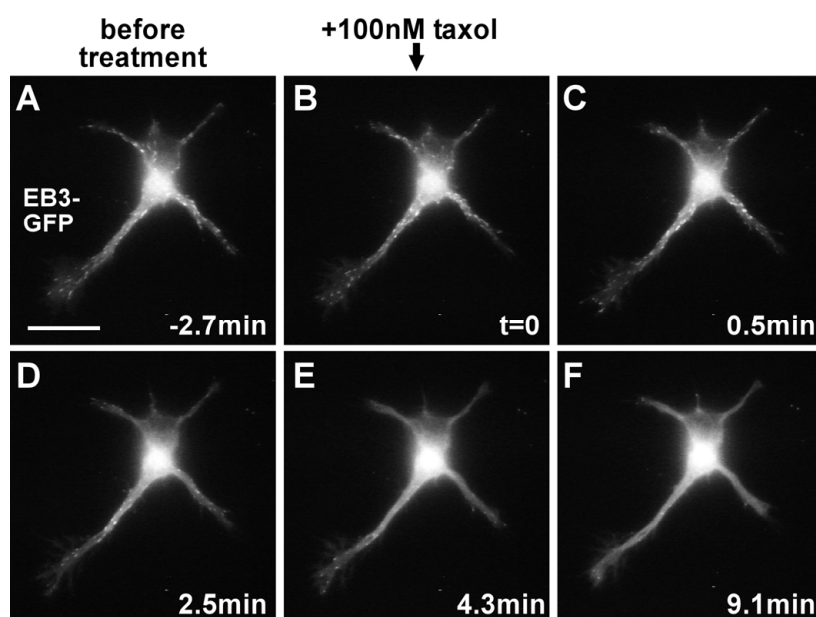


**Figure 2-16: High concentrations of taxol abolish microtubule dynamics**

Hippocampal neuron (1 DIV) expressing GFP-tagged EB3 (A). Taxol was added to a final concentration of 100 nM at  $t=0$  (after panel B). Neurons were continuously imaged before and after addition of the drug. Dynamic microtubules start to disappear several minutes after taxol addition (D) and are virtually gone in the later course of the experiment (E, F). Scale bar: 20  $\mu\text{m}$ .

**Figure 2-15: Taxol induces the protrusion of polymerizing dynamic microtubules to the growth cone periphery**

(A-F) An unpolarized neuron (1 DIV) expressing the microtubule plus end binding protein EB3 tagged with GFP. Phase and fluorescent images of the untreated neuron (A, B) were acquired every 10 seconds. Dynamic microtubules marked by EB3-GFP are present along the whole length of all processes (labeled with a-d in panel B; higher magnification in panel C). Subsequently, taxol was added to the medium to a final concentration of 10 nM (D-F) and imaging was continued. Dynamic microtubules become localized to the tips of the processes upon taxol addition (E; higher magnification in F, arrows). Scale bars: 20  $\mu\text{m}$ .

(G) Kymographs showing the movement of EB3-GFP along the process allow to follow taxol-induced changes in distribution and dynamics of GFP-tagged EB3. The horizontal axis represents time, the vertical axis distance. In all panels the top represents the distal part of the region of interest while the bottom corresponds to the proximal part. EB3-GFP diagonal streaks directed to the upper right therefore represent dynamic microtubules facing the growth cone with their plus ends, while diagonal streaks aiming at the lower right stand for dynamic microtubules facing the cell body with their plus ends. Briefly after addition of taxol, practically all dynamic microtubules face the growth cones with their plus ends (EB3-GFP streaks directed to the upper right) (panels a, c, d). Upon taxol addition, dynamic microtubules become localized to the tips of the processes (panels a-d) and rapid neurite outgrowth begins (panels a, c, d).

## 1DIV - Taxol treatment

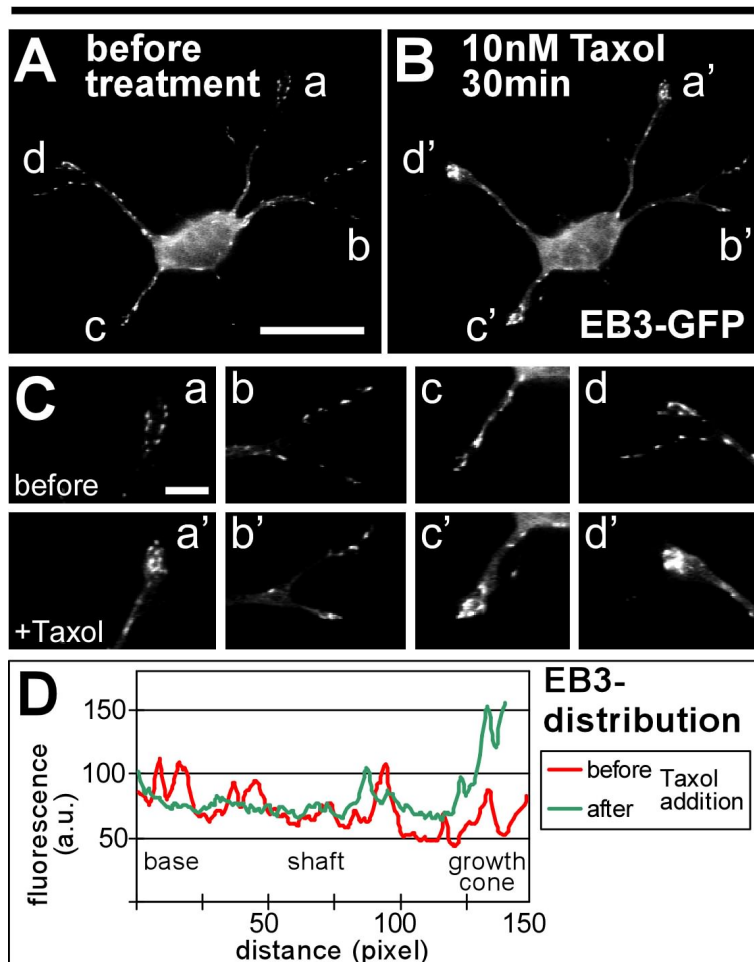


**Figure 2-17: Taxol directs growing microtubule plus ends toward the tips of processes.**

(A–D) After 1 DIV, unpolarized neurons transfected with EB3-GFP (A) were subjected to low doses of taxol. The effect on microtubule dynamics was examined 30 min after treatment by monitoring the distribution of EB3-GFP (B–D).  $n = 52$  neurons from eight independent experiments.

(C) Higher magnification of the growth cones marked in A and B. EB3-GFP is mainly localized at the tips of neurites after a 30-min treatment with 10 nM taxol (a'–d') in comparison to a more even distribution before treatment (a–d).

(D) Profiles of EB3-GFP immunofluorescence intensity (arbitrary units) of a representative neurite (neurite "c") before (red) and after (green) taxol treatment. Scale bars: (A, B) 20  $\mu\text{m}$ ; (C) 5  $\mu\text{m}$ .

Instead, low doses of taxol caused an accumulation of EB3-GFP at the tips of all minor neurites after taxol application in  $84.6 \pm 12.0\%$  of the cases (Figure 2-17; Figure 2-15). This directional shift towards the tip indicates the protrusion of polymerizing dynamic microtubules to the growth cone periphery and was accompanied by neurite outgrowth (Figure 2-15).

Interestingly, in polarizing control neurons (Figure 2-18 A, B) we observed in  $64 \pm 12\%$  of the cases an enrichment of EB3-GFP in the presumptive future axonal growth cone, which was identified by its size and dynamics (Bradke and Dotti, 1997; Bradke and Dotti, 1999; Figure 2-18 B, C, neurite I, asterisk). Such enrichment was not seen in the growth cones of other neurites (Figure 2-18 C) and indicates a shift of dynamic microtubules to the process tip by stabilization along the shaft.

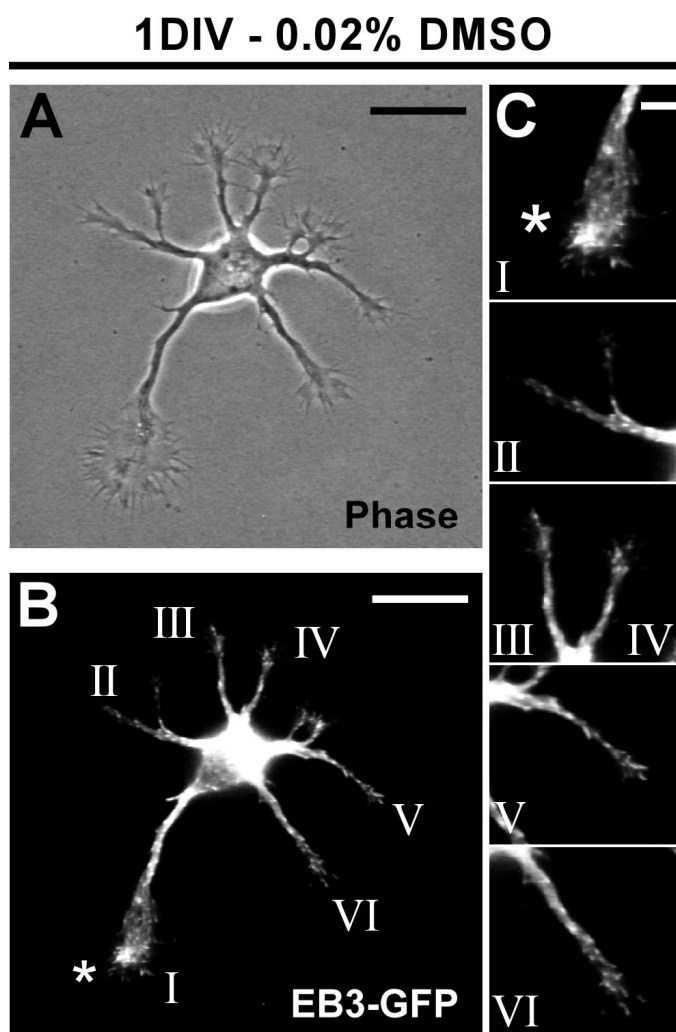


**Figure 2-18: Dynamic microtubules in polarizing neurons**

(A-C) Dynamic microtubule plus ends in polarizing neurons (1 DIV), visualized by transfection with EB3-GFP.

(C) Higher magnification of the growth cones marked in (B). The growth cone of the future axon (B, C, asterisk) harbors a high amount of dynamic microtubules in comparison to the growth cones of the remaining minor neurites in  $64 \pm 12\%$  of the cases ( $n=14$  neurons from more than five independent experiments). Scale bars: (A, B)  $20 \mu\text{m}$ ; (C)  $5 \mu\text{m}$ .

In conclusion, manipulations of microtubule stability cause drastic changes in neuronal polarity. Stabilizing microtubules using taxol promotes polymerization at their plus ends, leading to an accumulation of dynamic microtubule plus ends at the neurite tips which results in outgrowth of multiple axons.

## **2.6 Local microtubule stabilization is sufficient to bias the site of axon formation**

Initial neuronal polarization has been described as a “tug of war” (Craig and Banker, 1994) in which each neurite has the potential to become the axon, but only one neurite is singled out to acquire axonal fate. It has been postulated that a positive feedback loop triggers this selection when a critical threshold is transiently reached in one minor neurite which then allows sustained growth of the future axon (Andersen and Bi, 2000; Arimura and Kaibuchi, 2007; Bradke and Dotti, 2000b). If microtubule

stabilization is part of such a proposed feedback loop, transient microtubule stabilization in one neurite should be sufficient to trigger axon formation.

To test this hypothesis, one minor neurite of individual, unpolarized neurons (stage 2, 1 DIV) was randomly chosen and a membrane-permeant photoactivatable (caged) form of taxol (1-10 nM Paclitaxel, 2'-(4,5-dimethoxy-2-nitrobenzyl)carbonate; Buck and Zheng, 2002) was locally activated by applying UV pulses to the selected growth cone or the region directly adjacent to it (Figure 2-19 A, neurite VI, white circle) for 10 to 15 min (Figure 2-19 B). Neurons were further cultured in plain medium, reimaged two days after uncaging (Figure 2-19 E), fixed and stained for Tau-1 and MAP2 to unambiguously identify the site of axon formation (Figure 2-19 F).

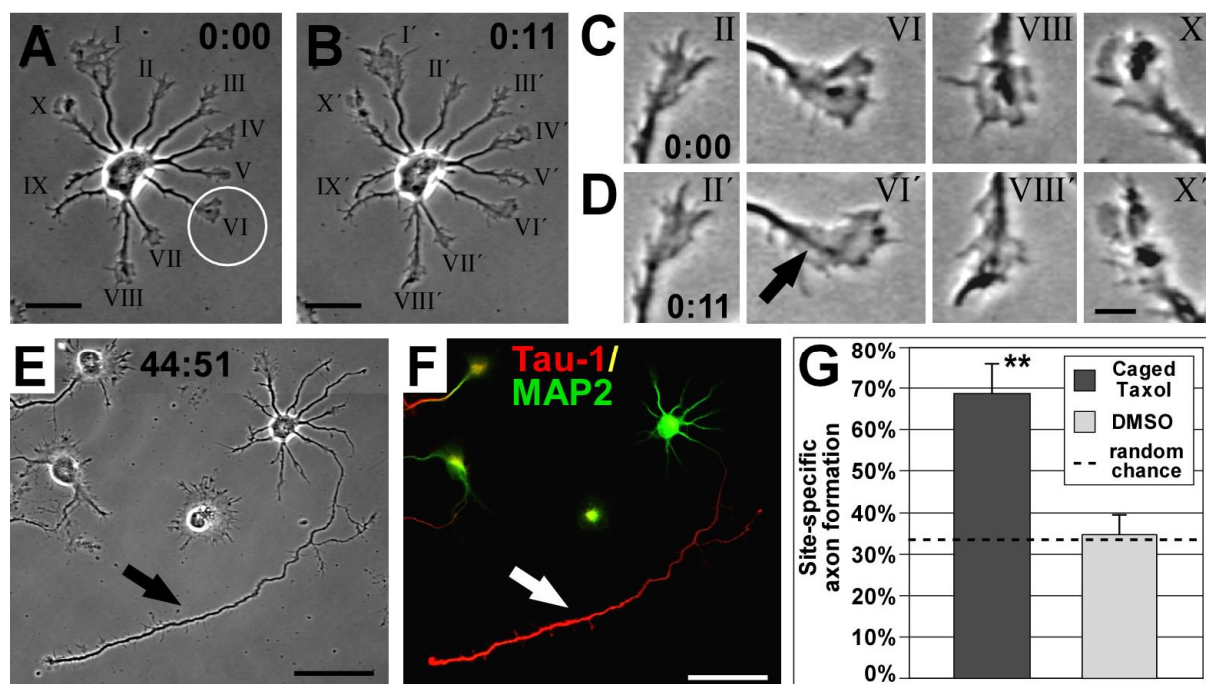


**Figure 2-19: Local microtubule stabilization promotes axon formation**

(A, B) Rat hippocampal neuron (1 DIV) before (A) and after (B) UV-mediated photoactivation (circle) of caged taxol at the tip of one randomly chosen minor neurite.

(C, D) Photoactivation did not interfere with the overall growth cone dynamics; most growth cones, including the pulsed one (arrow), are active.

(E, F) 2 days after uncaging, the pulsed process had become the axon (arrow), which is Tau-1-positive (red) and MAP2-negative (green, F).

(G) Probability of axon formation in the targeted area doubles after local activation of caged taxol compared with that expected by random chance (mean $\pm$ SEM; \*\*,  $P < 0.01$  by Chi-square test). Control treatment (DMSO and UV) does not influence randomized axon formation ( $P > 0.8$  by Chi-square test).

Scale bars: (A, B) 20  $\mu$ m; (C, D) 5  $\mu$ m; (E, F) 50  $\mu$ m.

In terms of activity, local uncaging did not interfere with growth cone dynamics (Figure 2-19 C, D). Most growth cones of the neurons including the pulsed one (arrow) remain active during the uncaging procedure. To quantify the extent of site-directed axon formation caused by local activation of caged taxol the deviation of the site of axon formation from the pulsed area was measured two days after uncaging. From 56 cells that underwent focal taxol activation 6 died and 9 did not develop further within the next 48 hours; therefore they were excluded from the analysis. From the remaining 41 cells 38 formed a single axon, only the other 3 neurons formed multiple axons.  $68.3 \pm 7.5\%$  of the developing neurons formed an axon from the pulsed neurite or close by (within a sector deviating less than  $30^\circ$  from the pulsed area), in comparison to  $32.9 \pm 1.9\%$  expected by random chance ( $p$ -value  $< 0.01$  by Chi-square test; 12 independent experiments; Figure 2-19 G). In contrast, in vehicle (DMSO)-treated cells UV-pulses did not influence randomized axon formation ( $32.1 \pm 7.8\%$  observed versus  $34.9 \pm 1.7\%$  expected;  $p$ -value  $> 0.8$  by Chi-square test;  $n=28$  neurons from 9 independent experiments). For calculation of the probability of random axon formation the number of growth cones within the sector in question was divided by the total number of the cells' growth cones.

The outcome of local uncaging in terms of site-directed axon formation was independent of the size of the growth cone and the length of the neurite receiving the UV-pulses. Pulsed neurites could become the axon even if the neuron had other longer neurites with bigger growth cones which have a higher probability to form the axon (Bradke and Dotti, 1997; Bradke and Dotti, 1999; Goslin and Banker, 1989; Figure 2-19 A), a phenomenon hardly observed in vehicle control experiments. Thus, already a short trigger (10-15 min) of microtubule stabilization is enough to bias the site of axon formation.

The immediate effects of local uncaging were visualized by performing the uncaging experiment with EB3-GFP transfected neurons. Caged taxol was activated in a restricted area at the tip of a non-growing process (Figure 2-20 A, B, white circle) with limited microtubule dynamics (visualized by the absence of EB3-GFP; Figure 2-20 E, panel 1). Photoactivation of caged taxol promoted the protrusion of polymerizing microtubules to the distal part of the process (Figure 2-20 D; E, panels 2 and 3, arrow). This effect persisted after withdrawal of the trigger, i.e. after uncaging, and

resulted in process outgrowth (Figure 2-20 A; C; E, panel 4 and 5). Local microtubule stabilization could also initiate outgrowth of a process when the cell had another rapidly growing process already (Figure 2-20 A, C, arrowhead). In conclusion, transient local stabilization of microtubules seems sufficient to induce axon formation from this site.

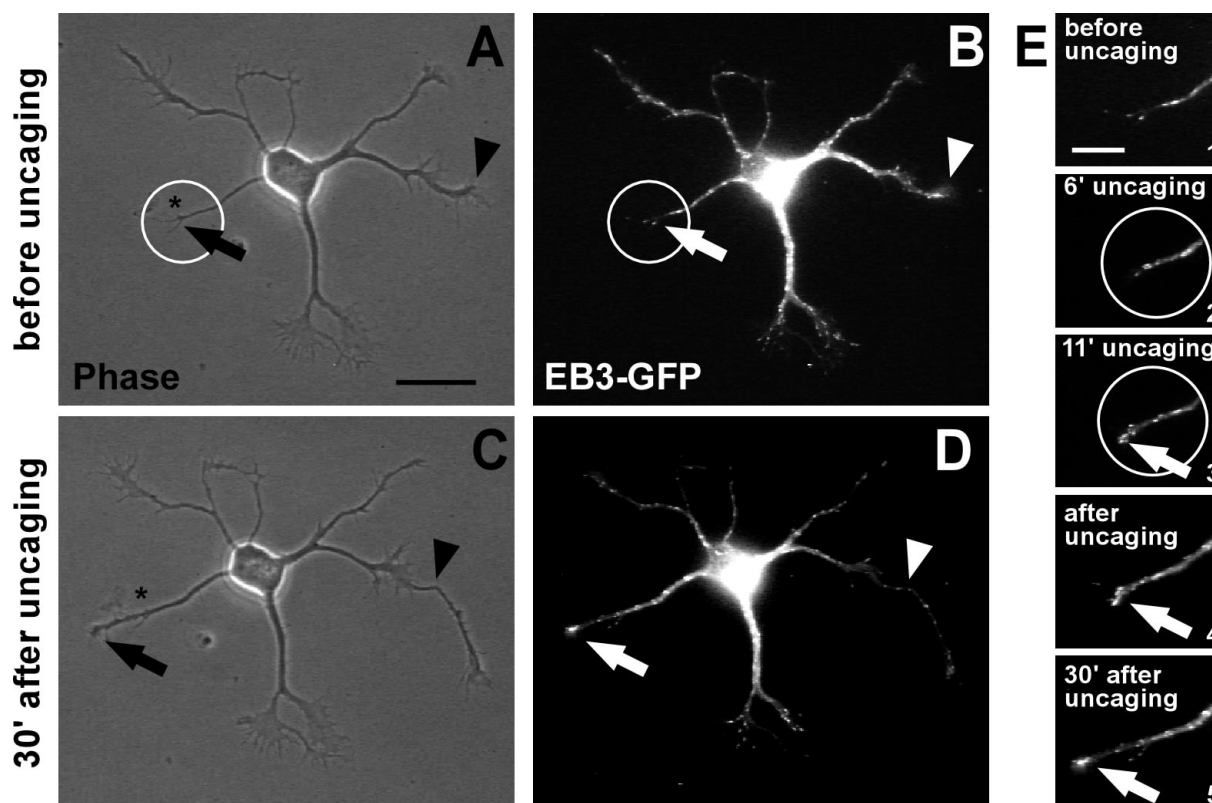


**Figure 2-20: Local microtubule stabilization shifts dynamic microtubules to the growth cone periphery**

Caged taxol was locally activated at the tip of a non-growing neurite (A and B, circle) of an EB3-GFP-transfected neuron at 1 DIV. Before uncaging, the chosen neurite does not grow and shows little microtubule dynamics (A and B, arrow; E, panel 1), whereas another neurite is rapidly growing (A and B, arrowhead; also see C and D). During uncaging (E, panels 2 and 3), the process becomes activated, visualized by enrichment of EB3-GFP at its tip (E, panel 3, arrow). After uncaging, the pulsed neurite shows increased thickness (C, D). Dynamic microtubules keep protruding to the peripheral part of the process, promoting its outgrowth (D and E, panels 4 and 5, arrow). The asterisk in A and C indicates the initial position of the neurite tip in A. Scale bars: (A-D) 20  $\mu\text{m}$ ; (E) 10  $\mu\text{m}$ .

### **3. Discussion**

In recent years, a rapidly growing number of molecules involved in neuronal polarization have been identified. Most studies have focused on polarity regulators and the control of their activity during axon formation which has led to a better understanding of the specific signaling pathways mediating neuronal polarity (reviewed in Arimura and Kaibuchi, 2007; da Silva and Dotti, 2002). In contrast, the intracellular mechanisms which actually underlie axon formation have drawn relatively little attention. Various mechanisms downstream of polarity regulators have been suggested to play a role in neuronal polarization yet have not been evaluated. In this respect the actin cytoskeleton and the regulation of its dynamics are an exception since a substantial share of research has so far concentrated on its role in axon formation. The goal of this study was to investigate which fundamental process, besides actin dynamics, could regulate neuronal polarization.

My data shows that microtubule stabilization plays an active role during the specification of axonal fate in early neuronal development. Axon formation correlates with increased microtubule stability, and interfering with the function of specific polarity regulators leads to alterations in both neuronal polarization and microtubule dynamics. Establishing a causal relation, I show that destabilizing microtubules selectively reduces the formation of future dendrites while stabilizing microtubules is sufficient to induce axon formation.

In summary, I present evidence how molecules and pathways that act independent of actin dynamics can govern neuronal polarization – by selective alteration of microtubule stability.

### **3.1 Microtubule stability correlates with the identity of neuronal processes**

#### **3.1.1 Axonal microtubules show increased stability**

Previous studies analyzing the microtubule network in developing neuronal cells have yielded conflicting results. In 1991 Arregui *et al.* had reported stable microtubules to be restricted to the axon of cerebellar macroneurons (Arregui *et al.*, 1991). Another study from the same year, however, could not confirm the confinement of stable acetylated microtubules to the axon in hippocampal neurons and concluded that microtubule stability “does not play a major role in determining which of the processes initially extended by hippocampal neurons becomes the definitive axon” (Dotti and Banker, 1991). It is conceivable that this contradiction in data within such a short period of time prevented further analysis of the role of microtubules in early neuronal polarization.

In my study I assessed the ratio of stable versus dynamic microtubules in neuronal processes, instead of individual posttranslational modifications of tubulin alone which allowed me to reevaluate microtubule stability in developing neurons. I found that stable microtubules are indeed not restricted to the axon, but nevertheless predominate in the axonal shaft in comparison to minor neurites, bringing together the results of the aforementioned studies (Arregui *et al.*, 1991; Dotti and Banker, 1991). The higher resistance of axonal microtubules to depolymerization, which I observed, confirmed an increase in microtubule stability in axons. My results therefore suggest a correlation between axonal identity and increased microtubule stability.

#### **3.1.2 Interfering with regulators of neuronal polarity results in altered microtubule stability**

Changes in the distinct morphology of neurons are often used as a readout when regulators of neuronal polarity are experimentally altered. For instance, loss of polarity or the formation of supernumerary axons are frequently the result of modified activity of specific polarity regulators, e.g. PI3K (Menager *et al.*, 2004; Shi *et al.*, 2003), Akt kinase (Jiang *et al.*, 2005) or CRMP-2 (Inagaki *et al.*, 2001) [for detailed record see Arimura and Kaibuchi, 2007]. If microtubules and their dynamics are a

final target of at least some polarity regulators it is conceivable that an analysis of neurons with altered polarity should allow to further substantiate the correlation between polarized microtubule stability and neuronal polarity.

First I examined microtubule turnover in neurons deficient in the PAR-1 homologs SAD A and SAD B which have been reported to lose polarity (Kishi *et al.*, 2005). Interestingly, I found this loss of neuronal polarity to be accompanied by a loss of polarization of microtubule stability. In contrast, when I induced multiple axons by inhibition of GSK-3 $\beta$  (Jiang *et al.*, 2005; Yoshimura *et al.*, 2005) I found that the supernumerary axons exhibit a prevalence of stable microtubules like normal axons. SAD kinases and GSK-3 $\beta$  control various processes, yet one of their common denominators is the regulation of the affinity of MAPs to microtubules (Goold *et al.*, 1999; Kishi *et al.*, 2005). MAPs, in turn, control the dynamics and stability of microtubules. Moderate inhibition of GSK-3 $\beta$ , for example, reduces phosphorylation-dependent inactivation of specific MAPs (reviewed in Doble and Woodgett, 2003; Zhou and Snider, 2005) eventually leading to increased microtubule stability and polymerization (see section 3.3.2 for further discussion). My data show that polarization of microtubule stability and neuronal polarization are parallel events. Moreover, interfering with the regulation of microtubule stability disrupts proper establishment of neuronal polarity.

## **3.2 Microtubule stabilization causes axon formation**

### **3.2.1 Global pharmacological microtubule stabilization induces the formation of multiple axons**

To investigate a potential causal relation between microtubule stability and axon formation I pharmacologically increased microtubule stability in neurons and analyzed the effect on neuronal polarity. To this end I altered microtubule dynamics using the microtubule stabilizing drug taxol (Schiff *et al.*, 1979; Schiff and Horwitz, 1980) at low concentrations which favor microtubule polymerization, yet do not block microtubule dynamics completely (Derry *et al.*, 1995). Interestingly, I found that microtubule stabilization itself is sufficient to induce axon formation. Taxol-treated neurons formed multiple axons with increased axon-like microtubule stability. In line

with previous studies (e.g. Dehmelt *et al.*, 2003; Schwamborn and Püschel, 2004), high concentrations of taxol resulted in a block of neurite formation as microtubules are hyperstabilized and thus rendered completely static. This indicates that a slight, balanced shift of microtubule dynamics towards more stable microtubules is necessary to induce axon formation.

### **3.2.2 MAPs, microtubule stabilization and axon formation**

Importantly, the pharmacological microtubule stabilization found to induce axon formation has various physiological counterparts. The regulation of assembly dynamics, organization and stability of microtubules is tightly controlled by a multitude of MAPs which are in turn the effectors of various signaling pathways (see section 3.3.2 for further discussion).

The binding of MAPs to microtubules and hence microtubule stability is regulated by several kinases, including SAD kinases (Kishi *et al.*, 2005), microtubule/MAP-affinity regulating kinases (Drewes *et al.*, 1998), GSK-3 $\beta$  (Sperber *et al.*, 1995; Trivedi *et al.*, 2005; Yoshimura *et al.*, 2005), or JNK (Chang *et al.*, 2003). The activity of most MAPs, including Tau, MAP2, APC and CRMP-2 is decreased upon phosphorylation (Murthy and Flavin, 1983; Yoshida *et al.*, 2004; Yoshimura *et al.*, 2005; Zumbrunn *et al.*, 2001), resulting in reduced microtubule stabilization or polymerization. In contrast, MAP1B is activated by phosphorylation and impedes the conversion of dynamic to stable microtubules; phosphorylation of MAP1B therefore results in increased microtubule dynamics (Goold and Gordon-Weeks, 2005; Goold *et al.*, 1999; Trivedi *et al.*, 2005).

Given the diversity of proteins regulating microtubule dynamics, it is not surprising that several different mechanisms may promote the selective alteration of microtubule dynamics in polarizing neurons. Three possibilities will be discussed in more detail: active microtubule stabilization, increased polymerization and a reduction of microtubule destabilization.

One way of actively increasing the stability of microtubules is to lower their catastrophe rate, i.e. the frequency at which microtubules switch from a growing to a

depolymerizing state. Tau (Drechsel *et al.*, 1992; Xie *et al.*, 1998) and MAP2 (Kowalski and Williams, 1993), for instance, alter microtubule dynamics via this process. Consistently, both MAPs are necessary for the formation of polar neuronal structures: Suppression of MAP2 using antisense oligonucleotides in cultured cerebellar macroneurons prevents the establishment of neurites in general (Caceres *et al.*, 1992), thereby blocking the establishment of neuronal polarity. Knockdown of Tau, instead, did not interfere with the formation of neurites on the whole but precludes axon formation (Caceres and Kosik, 1990; Caceres *et al.*, 1991), proposing different roles for Tau and MAP2 during neuronal polarization.

Interestingly, stabilization does not necessarily have to occur along the length of a microtubule. APC, for example, stabilizes microtubules by binding to their plus ends (Zumbrunn *et al.*, 2001). APC is enriched at the tip of the axon in polarized hippocampal neurons (Votin *et al.*, 2005), suggesting a role for APC in the regulation of axonal microtubule dynamics. Other localized microtubule stabilizing factors including EB1, EB3, CLASPs and mDia (Akhmanova *et al.*, 2001; Nakagawa *et al.*, 2000; Votin *et al.*, 2005; Wen *et al.*, 2004) may regulate the dynamics of microtubule plus ends the same way to accomplish local microtubule stabilization. When I assessed the dynamics of microtubules in living neurons expressing EB3-GFP I found EB3 to be enriched at the tip of the future axon. It is possible that it may function there, together with other regulators, as a localized microtubule stabilizing factor.

In addition to direct stabilization, the regulation of microtubule polymerization is also likely to play a role in axon formation. Tau, for example, is able to increase the polymerization rate of tubulin *in vitro* (Drechsel *et al.*, 1992), which may lead to a greater microtubule polymer mass in neurons. Similarly, CRMP-2 which binds to tubulin heterodimers promotes microtubule assembly and increased polymerization *in vitro* and in hippocampal neurons (Fukata *et al.*, 2002). Such increased polymerization may promote microtubule advance in growth cones and thereby stimulate axon growth. Consequently, overexpression of CRMP-2 causes the formation of multiple axons (Inagaki *et al.*, 2001). A comparable mechanism may apply to regulator of G-protein signaling 2 (RGS2) which promotes the formation of neurites in PC12 cells by stimulating microtubule polymerization (Heo *et al.*, 2006).

Like CRMP-2, RGS2 directly interacts with tubulin subunits (Heo *et al.*, 2006). Overexpression of RGS2 enhances the nerve growth factor-induced neurite outgrowth, while it is suppressed by specific knock-down of endogenous RGS2 (Heo *et al.*, 2006).

Microtubule stabilization can also be indirectly achieved by a reduction of active depolymerization. For instance, overexpression of the Rac activator dedicator of cytokinesis 7 (DOCK7), induces multiple axons which may be caused by DOCK7-mediated downregulation of the microtubule depolymerizing activity of stathmin (Watabe-Uchida *et al.*, 2006). Like APC, stathmin acts on the plus-ends of microtubules, and its inactivation has the same outcome as active microtubule stabilization, a reduced catastrophe rate. Inactivation of MAP1B –which increases microtubule dynamics in its active state (Trivedi *et al.*, 2005)– likewise leads to enhanced microtubule stability in axons (Goold and Gordon-Weeks, 2005; Goold *et al.*, 1999). Comparably, increased activity of the neuron-specific microtubule destabilizing factor SCG10 (Riederer *et al.*, 1997; Stein *et al.*, 1988) which is controlled by JNK during neuronal polarization leads to reduced process outgrowth (Tararuk *et al.*, 2006). Knockdown of SCG10, however, also suppresses neurite outgrowth indicating that dynamic microtubules are to some extent necessary for neurite formation (Morii *et al.*, 2006), consistent with the results of my taxol experiments and earlier studies (Tanaka *et al.*, 1995). Consequently, a moderate increase of SCG10 levels increases neurite growth (Morii *et al.*, 2006), possibly by increasing the amount of free tubulin at growth cones. My hypothesis that a well-balanced control of microtubule dynamics is necessary to induce axon formation (see section 3.2.1) is consistent with these results.

In summary, neurons possess a broad repertoire of mechanisms to achieve microtubule stabilization during polarization. Pharmacologically induced microtubule stabilization, e.g. by taxol application, mimics these mechanisms to induce axon formation. I propose that the fundamental process the different signaling pathways converge on is increased microtubule stability in the axon, no matter whether it is accomplished by active microtubule stabilization, increased polymerization or a reduction of microtubule destabilization. The increased stability and polymerization

allows microtubules to protrude with their dynamic ends more distally, thereby promoting axon formation.

### **3.3 Microtubule stabilization precedes axon formation**

#### **3.3.1 Microtubule stabilization and axon formation - Sequential events**

During initial neuronal development one out of several seemingly equal neurites is singled out to become the axon. My data suggest that microtubule stabilization in this neurite precedes morphological polarization, based on the following observations: 1) Microtubule stability is increased in one neurite of a subpopulation of morphologically unpolarized neurons, as shown using markers for microtubule turnover and assessing microtubule stability by partial depolymerization. 2) Neurons grown under mild microtubule destabilizing conditions are able to form an axon, while formation of minor neurites is impaired, suggesting that only one minor neurite is able to overcome the destabilizing environment. 3) Local microtubule stabilization in one minor neurite by focal activation of a caged form of taxol strongly biases the site of axon formation. Consistent with my findings, the overexpressed kinesin-1 motor domain, which preferably binds to microtubules containing markers of lower turnover (Reed *et al.*, 2006), accumulates in the future axon before morphological polarization occurs (Jacobson *et al.*, 2006; see section 3.3.3 for further discussion). Taken together, my data argue that changes in microtubule dynamics govern neuronal polarization and that microtubule stabilization precedes axon formation.

#### **3.3.2 Regulation of microtubule stabilization during neuronal polarization**

How could local microtubule stabilization be achieved during axon formation? Presumably, both an environmental cue (Adler *et al.*, 2006) or an internal signal like centrosome localization (de Anda *et al.*, 2005; Zmuda and Rivas, 1998) could initiate a local imbalance inside the microtubule network. In the following sections I will discuss putative external signals including guidance cues, neurotrophins and other signaling pathways involved in axon specification with respect to their ability to regulate microtubule dynamics.

In the nematode *C. elegans*, directional netrin cues define the site of axon initiation of a subtype of motor neurons by promoting a PI3K signaling-dependent asymmetric distribution of the actin-regulator MIG-10/lamellipodin (Adler *et al.*, 2006). Interestingly, asymmetric PI3K-signaling itself plays an important role in neuronal polarization (Menager *et al.*, 2004) and promotes microtubule stabilization in migrating fibroblasts via Akt and GSK-3 $\beta$  (Onishi *et al.*, 2007). Similarly, netrin-induced activation of Rac (Li *et al.*, 2002) may promote microtubule stabilization via reducing the microtubule depolymerizing activity of stathmin (Watabe-Uchida *et al.*, 2006; see section 3.2.2 above). Thus, netrin-induced axon formation may function, at least in part, via regulation of microtubule dynamics, in line with the netrin turning response depending on microtubules (Buck and Zheng, 2002) and the GSK-3 $\beta$  target MAP1B (Del Rio *et al.*, 2004).

Interestingly, semaphorin 3A, another repulsive guidance cue, is also involved in the specification of neuronal polarity (reviewed in Whitford *et al.*, 2002). In cortical neurons, semaphorin 3A regulates the oriented growth of axons toward the white matter (Polleux *et al.*, 1998). This function may be mediated to some extent by the modulation of microtubule dynamics since semaphorin 3A signaling was reported to influence the activity of GSK-3 $\beta$  (Eickholt *et al.*, 2002) and CRMP-2 (Mitsui *et al.*, 2002). It seems therefore conceivable that axon guidance cues do not only direct the growing axon but also stimulate and orient the asymmetrical growth of neurites before axon specification.

Similarly, WNT-signaling has been reported to determine the polarity of a subset of mechanosensory neurons along the anterior–posterior body axis in *C. elegans* (Hilliard and Bargmann, 2006; Prasad and Clark, 2006). WNT-signaling is known to control various polarity-related developmental processes, including asymmetric cell division, cell fate determination and tissue polarity (reviewed in Logan and Nusse, 2004). Downstream of the WNT-receptor Frizzled, the scaffold protein Dishevelled mediates the inhibition of GSK-3 $\beta$  together with JNK (Ciani *et al.*, 2004; Ciani and Salinas, 2007). Given the fact that WNT-signaling is able to induce microtubule stabilization (Ciani *et al.*, 2004; Krylova *et al.*, 2000), the regulation of microtubule

dynamics is likely to be involved in WNT-mediated axon specification. The modulation of MAP1B-activity, for instance, seems to be part of such WNT-induced microtubule stabilization during axon formation (Lucas *et al.*, 1998). In summary, the regulation of microtubule dynamics by WNT-signaling likely plays a role during axon formation.

Neurotrophic factors, including nerve growth factor (NGF), brain-derived neurotrophic factor (BDNF) and neurotrophin 3 (NT3) are putative extracellular cues to determine neuronal polarity as well. NT3, for instance, has been reported to accelerate neuronal polarization by enhancing axon growth (Morfini *et al.*, 1994). The receptors of neurotrophins are tyrosine receptor kinases (Trks; reviewed in Huang and Reichardt, 2003) which allow them to access a broad variety of downstream effectors. PI3K, for example, signals downstream of Trks and regulates neuronal polarization (Menager *et al.*, 2004) and microtubule stabilization (Onishi *et al.*, 2007), presumably by inactivation of GSK-3 $\beta$  via PI3K and Akt-kinase (Jiang *et al.*, 2005; Zhou *et al.*, 2004; compare section 1.3.1). Taking into account the central role of GSK-3 $\beta$  in several pathways governing neuronal polarization and my findings that microtubule stabilization precedes axon formation, local inactivation of GSK-3 $\beta$  is probably of special interest in initial neuronal polarization. It may induce axon outgrowth, for instance by MAP-mediated microtubule stabilization (Kim *et al.*, 2006; Zhou *et al.*, 2004) or enhanced polymerization via CRMP-2 (Yoshimura *et al.*, 2006). Interestingly, the small GTPase R-Ras which is selectively localized to a single neurite of unpolarized hippocampal neurons (Oinuma *et al.*, 2007) is activated by Trks upon neurotrophin stimulation (reviewed in Reichardt, 2006). Since R-Ras can inhibit GSK-3 $\beta$  via PI3K and Akt-kinase it might account for local GSK-3 $\beta$  inactivation in response to neurotrophic factors. Similarly, the ganglioside-converting enzyme plasma membrane ganglioside sialidase (PMGS) which promotes the activation of TrkA at the tips of neurites, accumulates in a single immature neurite during stage 2 (Da Silva *et al.*, 2005). This local TrkA-activation by PMGS leads to activation of PI3K which in turn provides a link to a localized regulation of microtubule dynamics. In hippocampal neurons, BDNF has been reported to promote axon differentiation (Shelly *et al.*, 2007). It has also been shown to induce an increase in cellular cAMP levels by inhibition of phosphodiesterase-4 in cerebellar neurons (Gao *et al.*, 2003)

that leads to activation of LKB1 via cAMP-dependent protein kinase (PKA; Shelly et al., 2007). Active LKB1 in turn phosphorylates and thereby activates SAD A and SAD B kinases (Barnes *et al.*, 2007), providing a link to the regulation of microtubule dynamics. Interestingly, LKB1 is also linked to WNT-signaling (Ossipova *et al.*, 2003), suggesting that different extracellular cues like WNT and neurotrophins cooperate to control neuronal polarization.

In addition to diffusible factors, the extracellular matrix and cell adhesion molecules are possible initiators of neuronal polarization. When hippocampal neurons are plated on substrates patterned with stripes of poly-L-lysine and either laminin or neuron–glia cell adhesion molecule (NgCAM), axons formed preferentially from undifferentiated neurites that have contact with laminin or NgCAM (Esch *et al.*, 1999). Similarly, the contact of individual neurites with laminin-coated beads caused a rapid elongation, suggesting this neurite to become the axon (Menager *et al.*, 2004). The increased outgrowth was marked by an accumulation of PIP<sub>3</sub>, the lipid product of PI3K, at the tip of the growing neurite (Menager *et al.*, 2004). Elevated PIP<sub>3</sub>-levels indicate a high PI3K-activity which links microtubule stabilization (e.g. via the PI3K/Akt/GSK-3 $\beta$  pathway) and axon specification. Extracellular signals may therefore trigger both neurite outgrowth and the specification of a process to acquire axonal fate by regulation of microtubule dynamics.

Intracellular signals pose an alternative explanation to extracellular signals specifying axon formation. During early developmental stages, the centrosome and the Golgi apparatus cluster close to the area where neurons form their first neurite, which will later become the axon (de Anda *et al.*, 2005; Zmuda and Rivas, 1998). The localization of the centrosome may therefore be responsible for an early bias of microtubule stability between different neurites which could account for axon specification. In a study from 2001, Palazzo *et al.* show that the orientation of the centrosome and microtubule stabilization are independent events in migrating fibroblasts (Palazzo *et al.*, 2001b). In the light of these results, an instructive role for the centrosome in local microtubule stabilization during neuronal polarization seems unlikely. Moreover, the centrosome position itself is controlled by PI3K and Cdc42 (reviewed in Etienne-Manneville and Hall, 2003), it may therefore not be the cause for local microtubule stabilization but rather a result of axon-inducing signaling

(Arimura and Kaibuchi, 2007; Siegrist and Doe, 2006). An alternative explanation for an early bias of microtubule stabilization comes from CLIP-associated protein (CLASP)-mediated nucleation of non-centrosomal microtubules at the Golgi network (Efimov *et al.*, 2007). Since Golgi network and centrosome are often in close proximity, microtubules emanating from the Golgi apparatus might be one explanation for the supposed correlation between centrosome position and the site of axon formation.

Currently, it seems most likely that extracellular signals determine the site of axon formation. The signaling pathways I have discussed are all connected to the regulation of microtubule dynamics and may thus trigger neuronal polarization by inducing a local stabilization of microtubules.

### **3.3.3 Microtubule stability, posttranslational modifications and axonal transport**

Local microtubule stabilization as a promoter for axon formation in morphologically unpolarized neurons offers an explanation for the increased membrane traffic which precedes axon formation (Bradke and Dotti, 1997). Microtubule-dependent motor proteins show a higher affinity towards stabilized microtubules (Liao and Gundersen, 1998; Reed *et al.*, 2006), which is in line with enhanced vesicle transport on stable microtubules (Lin *et al.*, 2002; Nakata and Hirokawa, 2003). Increased microtubule stability in the future axon may therefore lead to polarized membrane flow, contributing to determining the site of axon formation. The inhibition of membrane trafficking, in contrast, prevents the development of polarity and axonal growth (Jareb and Banker, 1997). Interestingly, a recent study from Horiguchi *et al.* has shown that guanylate kinase-associated kinesin (GAKIN) mediates the transport of PIP<sub>3</sub> itself or factors that stimulate the production of PIP<sub>3</sub> (Horiguchi *et al.*, 2006). The accumulation of PIP<sub>3</sub> at the tip of one neurite precedes axon specification in hippocampal neurons (Shi *et al.*, 2003); such enrichment might be mediated by increased GAKIN-binding to locally stabilized microtubules. Whether GAKIN actually prefers binding to stable microtubules, however, remains to be shown.

A recent study from Reed *et al.* proposes microtubule acetylation to be key to control motor-protein trafficking. Kinesin-1 shows reduced binding to microtubules isolated from the ciliate *Tetrahymena* when microtubule acetylation is abolished (Reed *et al.*, 2006). Similarly, in stage 2 hippocampal neurons with pharmacologically increased microtubule acetylation the selective localization of the kinesin-1 cargo JNK-interacting protein 1 (JIP1) to only a subset of neurites is lost, JIP1 rather accumulates at the tips of nearly all neurites under such conditions (Reed *et al.*, 2006), suggesting that microtubule acetylation controls directed transport to neurites during axon formation. My data, in contrast, argue that the acetylation of microtubules alone is not sufficient to induce initial axon formation. Neurons treated with the same deacetylase inhibitors as used in the study from Reed *et al.* did not show altered polarity, suggesting normal axonal transport. It has to be considered, however, that in my study low concentrations of the deacetylase inhibitor TSA were used. These low concentrations were necessary to avoid cell death during the extended incubation time which is required to assess neuronal polarization but were nevertheless sufficient to induce hyperacetylation of microtubules (compare Figure 2-13 D). Reed *et al.*, on the other hand, assessed only the first few hours after addition of the deacetylase inhibitors, using ~60-fold more TSA than in my study which may have additional side effects. My data argue that changes in microtubule dynamics but not acetylation of microtubules alone are the primary cause of axon formation. This is in line with recent results from Zhang *et al.* which show that mice deficient for histone deacetylase 6 (HDAC 6) are viable and fertile (Zhang *et al.*, 2008). Importantly, the development of most tissues including the nervous system is normal in these mice although microtubules show increased acetylation levels (Zhang *et al.*, 2008).

Possibly, other posttranslational modifications of tubulin, including polyglycylation or polyglutamylated tubulin, might play a role in neuronal polarization. For instance, tubulin polyglutamylated tubulin seems to influence MAP/microtubule interactions. *In vitro*, Tau, MAP1B, and MAP2 preferentially bind to moderately polyglutamylated tubulins (~3 glutamyl units; Bonnet *et al.*, 2001; Boucher *et al.*, 1994) whereas MAP1A shows optimal affinity for tubulins with a high level of modification (~6 glutamyl units; Bonnet *et al.*, 2001). Since glutamylated tubulin levels change during neuronal development (Audebert *et al.*, 1994) they might control developmental transitions in

binding of different MAPs (Bonnet *et al.*, 2001). A loss of polyglutamylation also affects binding of microtubule-dependent motor proteins (Ikegami *et al.*, 2007; Reed *et al.*, 2006), leading to abnormal trafficking. Hippocampal neurons derived from mice deficient in tubulin-tyrosine-ligase, the enzyme retyrosinating  $\alpha$ -tubulin, showed high levels of  $\Delta 2$ -tubulin in microtubules with increased stability (Erck *et al.*, 2005). Interestingly, these neurons showed accelerated neurite outgrowth and a premature axonal differentiation. Moreover, they had a tendency to form multiple axons, similar to the phenotype observed in my experiments with pharmacological microtubule stabilization. The results from Erck *et al.* are in line with a putative instructive role for microtubule stability during neuronal polarization proposed by my work. Future studies may address in more detail which role in neuronal polarization the enzymes play that mediate posttranslational modifications of microtubules. It will be interesting to see whether posttranslational modifications other than acetylation are the cause for or the consequence of axon formation.

### **3.3.4 Local microtubule stabilization and feedback loops**

In the context of initial neuronal polarization a system of intracellular feedback loops has been proposed to determine the site of axon formation (Andersen and Bi, 2000; Bradke and Dotti, 2000b). Initially, all neurites are assumed to be equal, competing to become the axon. It was postulated that on the one hand a positive feedback loop promotes outgrowth of one neurite to acquire axonal fate while on the other hand negative feedback loops inhibit outgrowth of the remaining neurites (Andersen and Bi, 2000; Bradke and Dotti, 2000b). Increased microtubule stability in one neurite would allow to induce intracellular events such as increased microtubule-dependent transport (Liao and Gundersen, 1998; Lin *et al.*, 2002) that, again, could reinforce microtubule stability, thereby creating a positive feedback loop. A recent study on the selective enrichment of the Kif5 kinesin motor domain in the growing axon postulated that microtubules in the axon should biochemically differ from the minor neurites' microtubules (Jacobson *et al.*, 2006). My work directly shows such distinct characteristics between the microtubules of axons and minor neurites –their different stability– that could specifically enhance membrane traffic in the growing axon. Polarized transport may lead to a selective enrichment of microtubule-stabilizing

factors during neuronal polarization. These factors may stabilize microtubules at their target, thereby further driving the aforementioned positive feedback loop.

My results support the idea that microtubule stabilization plays a role in a putative positive feedback loop triggering axon specification. When I locally stabilized microtubules at the tip of one process of an unpolarized neuron by photoactivation of caged taxol I observed increased microtubule polymerization, visualized by EB3-GFP, and neurite outgrowth (see section 2.6, page 46). Although the trigger was short (~15 min), local microtubule stabilization was sufficient to strongly bias the site of axon formation (see section 2.6, page 44). Likely, a short pulse of microtubule stabilization activates a cascade of events leading to a positive feedback loop which is able to promote sustained axonal outgrowth. For instance, CRMP-2, which promotes microtubule polymerization, is a cargo of kinesin-1 (Kimura *et al.*, 2005). Local microtubule stabilization might enhance kinesin-dependent transport (Lin *et al.*, 2002; Nakata and Hirokawa, 2003) and therefore lead to an enrichment of CRMP-2 at the growth cone of one neurite. This could then promote further microtubule stabilization and sustained axonal outgrowth. Since CRMP-2 additionally mediates the interaction of kinesin-1 with the Sra-1/WAVE1 complex (Kawano *et al.*, 2005) which is involved in actin reorganization (Steffen *et al.*, 2004) it provides a link between actin and microtubule dynamics. The enrichment of PIP<sub>3</sub> at the tip of the future axon (Shi *et al.*, 2003) might trigger a positive feedback loop as well. PIP<sub>3</sub> could on the one hand set off microtubule stabilization via the Akt/GSK-3 $\beta$  pathway and increased MAP binding to microtubules (see sections 1.3.1 and 3.2.2). This in turn might contribute to further transport of PIP<sub>3</sub> to the tip of the future axon via the kinesin-like motor protein GAKIN (Horiguchi *et al.*, 2006). Moreover, additional PIP<sub>3</sub> would be generated by the feedback loop of PI3K, Rho GTPases and the Par-3 / Par-6 / aPKC polarity complex (see section 1.3.1 and Arimura and Kaibuchi, 2007; Weiner *et al.*, 2002) which would again cause more microtubule stabilization.

More experimental evidence for a role of feedback loops controlling axon specification comes from the observation that an individual neurite accumulates PIP<sub>3</sub> at its tip and commences rapid outgrowth when touched with a laminin-coated bead (Menager *et al.*, 2004), in line with the proposed positive feedback loop. When a second neurite contacts a laminin-coated bead, however, the first neurite stops

growing, suggesting a suppression of its outgrowth by a negative feedback loop induced by the second neurite (Menager *et al.*, 2004). Although the exact nature of these feedback signals remains to be determined, local microtubule stabilization evoked by PIP<sub>3</sub>-signaling may be involved and offers an explanation how to drive sustained axon outgrowth.

Interestingly, microtubule-dependent transport also provides a link between the dynamics of microtubules and the actin cytoskeleton. For instance, the RhoA activator p190RhoGEF (van Horck *et al.*, 2001) presumably interacts with kinesin via the JIP1 scaffold protein (Meyer *et al.*, 1999; Verhey *et al.*, 2001). RhoA regulates actin dynamics via ROCK (Leung *et al.*, 1996; reviewed in Riento and Ridley, 2003) but was more recently also discovered to control microtubule stabilization via mDia (Palazzo *et al.*, 2001a) and its downstream effectors. Transport of p190RhoGEF to specific neurites mediated by increased microtubule stability might therefore on the one hand forward additional microtubule stabilization. On the other hand, RhoA may modulate retrograde actin flow (Amano *et al.*, 1996; Delorme *et al.*, 2007; Kimura *et al.*, 1996; Sumi *et al.*, 2001) which can promote neurite outgrowth (Rösner *et al.*, 2007). The Cdc42-specific GEFs Asef1 and 2 (Hamann *et al.*, 2007) use a similar means as p190RhoGEF to reach microtubule ends. Asef is activated by binding to APC (Hamann *et al.*, 2007) which concentrates at growing microtubule plus ends (Mimori-Kiyosue *et al.*, 2000), presumably via an indirect interaction with the plus-end-directed motor proteins KIF3A and KIF3B (Jimbo *et al.*, 2002). Thus, APC might deliver Asef to neurite tips where it could specifically activate Cdc42. The localization of TrioGEF1, a specific activator of RhoG, also depends on an intact microtubule cytoskeleton (Blangy *et al.*, 2000; Gauthier-Rouviere *et al.*, 1998) and probably kinesin (Gauthier-Rouviere *et al.*, 1998; Vignal *et al.*, 2001). RhoG itself can activate both Rac1 and Cdc42 (Blangy *et al.*, 2000; Gauthier-Rouviere *et al.*, 1998). Increased Rac1 activity may lead to further microtubule stabilization via inactivation of stathmin (Watabe-Uchida *et al.*, 2006; see section 3.2.2 above) and could drive a positive feedback loop in the future axon for the kinesin-dependent delivery of TrioGEF1. In such a scenario the RhoG-activated Cdc42 could render the actin cytoskeleton more dynamic, e.g. via cofilin (Garvalov *et al.*, 2007), which would release restraint to microtubule-driven axon outgrowth. Interestingly, both active Cdc42 and Rac1 activate p21-activated kinase 5 (PAK5; Cau *et al.*, 2001; Dan *et al.*,

2002), thereby providing another link to cytoskeletal dynamics. PAK5 has recently been reported to suppress the activity of MARK2 (Matenia *et al.*, 2005), a regulator of MAP/microtubule interaction (Biernat *et al.*, 2002). MARK2 phosphorylation causes the detachment of MAPs like Tau from microtubules, hence its inactivation leads to microtubule stabilization. Additionally, PAK5 causes a destabilization of the actin cytoskeleton via as yet unknown effectors (Matenia *et al.*, 2005), and might thus further link TrioGEF1, RhoG, Cdc24 and Rac1 to cytoskeletal dynamics. To review, the microtubule-dependent intracellular distribution of Rho-GEFs likely contributes to orchestrate the regulation of both actin and microtubule dynamics during initial neuronal polarization.

## 4. Outlook

In summary, I present here for the first time direct evidence that microtubule stability is an active determinant of neuronal polarization. Recent work has shown that actin and microtubules mutually influence each other (Basu and Chang, 2007). Taking into account my findings about the instructive role of microtubules in neuronal polarization, I hypothesize that the initial trigger for axon formation could derive from both actin and microtubules. Their reciprocal regulation in turn may drive a positive feedback loop which sustains axonal growth. The next challenge beyond the scope of this study will be to characterize this molecular interplay of microtubules and the actin cytoskeleton during neuronal polarization. Moreover, molecules involved in the regulation of microtubule dynamics in processes like cell migration or axon guidance should be reassessed for a potential role in neuronal polarization. Interestingly, it was recently shown that microtubule organization is a crucial factor for the formation of the two distinct structures following axonal lesion – actively protruding growth cones and non-growing retraction bulbs (Ertürk *et al.*, 2007). It might therefore also be worth to explore the ability of taxol to convert a non-growing minor neurite into a growing axon in situations where process growth is restrained, e.g. in the context of central nervous system lesions.



# 5. Materials and Methods

## 5.1 Materials

### 5.1.1 Chemicals

High-purity chemicals were purchased from Biomol, Invitrogen, Merck, Roth, and Sigma-Aldrich. Water used to prepare solutions was filtered with the “Milli-Q-Synthesis A-10” system from Millipore.

**Table 1:** Chemicals used in this study

<b>Chemical</b>	<b>Supplier</b>	<b>Product number</b>
Agarose	Biomol	01280
Apo-transferrin, human	Sigma	T-2252
Borax	Sigma	B-9876
Boric acid	Merck	1.00165
Bovine serum albumin, powder	Sigma	A-7906
Copper (II) sulfate pentahydrate (CuSO <sub>4</sub> *5H <sub>2</sub> O)	Merck	1.02790
Dimethyl sulfoxide (DMSO)	Roth	A994
EDTA (Ethylenediamine-tetraacetic acid)	Sigma	E-5134
EGTA (Ethylene glycol-bis(2-aminoethylether)-N,N,N',N'-tetraacetic acid)	Sigma	E-3889
Ethanol absolute (≥99.8%)	Sigma	32205
Fetal bovine serum	Invitrogen	10500-064
Fish gelatin	Sigma	G-7765
Gelmount mounting medium	Sigma	G-0918
D(+)-Glucose monohydrate	Merck	1.08342
L-Glutamine 200mM (100x)	Invitrogen	25030
Hank's balanced salt solution (HBSS) with Calcium and Magnesium	Invitrogen	14025
HEPES (N-2-Hydroxyethylpiperazine-N'-2- ethane sulfonic acid)	Biomol	05288
Horse Serum	Sigma	H-1270
Hydrochloric acid (HCl; 1 M)	Merck	1.09057
Hydrochloric acid, fuming (HCl; 37%)	Merck	1.00317
Insulin	Sigma	I-5500
Magnesium chloride hexahydrate (MgCl <sub>2</sub> *6H <sub>2</sub> O)	Merck	1.05833
MEM 10x	Invitrogen	21430
MEM essential amino acids 50x	Invitrogen	11130
MEM non-essential amino acids 100x	Invitrogen	11140
Nitric acid (HNO <sub>3</sub> ; ≥65%)	Roth	4989
Ovalbumin (albumin from chicken egg white)	Sigma	A-5503

**Table 1:** Chemicals (continued)

Chemical	Supplier	Product number
Paraffin (non-caking, solidification point 57-60°C)	Merck	1.07158
Paraformaldehyde	Merck	1.04005
PIPES (1,4-Piperazinediethanesulfonic acid)	Sigma	P-1851
Poly-L-lysine	Sigma	P-2636
Progesteron	Sigma	P-8783
Putrescine-dihydrochloride	Sigma	P-5780
Pyruvate (piruvic acid)	Sigma	P-2256
Selenium-dioxide	Sigma	325473
Sodiumhydrogencarbonate (NaHCO <sub>3</sub> )	Merck	1.06329
Sodium hydroxide (NaOH)	Merck	1.06482
Sucrose	Merck	1.07651
Tris(hydroxymethyl)-aminomethane	Merck	1.08382
Triton X (TX)-100	Roth	6683
Trypsin-EDTA (1x; 0.05% Trypsin, 0.53 mM EDTA•4Na)	Invitrogen	25300

### 5.1.2 Drugs

**Table 2:** Drugs used in this study

Drug	Stock [mM]	Solvent	Supplier	Function
taxol	5	DMSO	Sigma or LC laboratories	microtubule stabilization
cytochalasin D	10	DMSO	Sigma	destabilization of F-actin
nocodazole	6.67	DMSO	Sigma	microtubule destabilization
SB 415286	25	DMSO	Tocris Bioscience	GSK-3 $\beta$ inhibitor
tubacin	20	DMSO	gift from Ralph Mazitschek and Stuart Schreiber	deacetylase inhibitor
trichostatin A	4	ethanol	Cell Signaling Technology	deacetylase inhibitor

Single-use aliquots of the drug stock solutions were kept at -20°C.

### 5.1.3 Commercial kits

**Table 3:** Commercial kits

Name	Supplier & Product number
EndoFree Plasmid Maxi Kit	Qiagen, #12326
Rat Neuron Nucleofector Kit	Amaxa, #VPG-1003

### 5.1.4 Enzymes and DNA markers

**Table 4:** Enzymes and DNA markers

Name	Supplier & Product number
Taq DNA Polymerase (5 U/μl)	Invitrogen, #18038-026
100 bp ladder (500 ng/μl)	New England Biolabs, # N3231
1 kb ladder (500 ng/μl)	New England Biolabs, # N3232

**Fragments of the 100bp ladder [bp]:** 1.517, 1.200, 1.000, 900, 800, 700, 600, 517/500, 400, 300, 200, 100

The 100 bp-ladder has bands with increased intensity at 1000 bp and 500/517 bp.

**Fragments of the 1 kb ladder [bp]:** 10.002, 8.001, 6.001, 5.001, 4.001, 3.001, 2.000, 1.500, 1.000, 517, 500

The 1 kb-ladder has a band with increased intensity at 3.000 bp.

### 5.1.5 Equipment

**Table 5:** Equipment

Equipment	Model	Supplier
<i>Lab equipment</i>		
Bunsen burner, mobile	Fireboy eco / Fireboy plus	Integra Biosciences
Centrifuges	Universal 30F	Hettich
	5810	Eppendorf
	Table centrifuges: 5415 C and 5415 R	Eppendorf
	Mini centrifuge GMC-060	Laboratory & Medical Supplies Co.
Electroporator	Nucleofector™ II	Amaxa
Hemocytometer	Neubauer improved (depth 0.100 mm, 0.0025 mm <sup>2</sup> )	Optik Labor
Ice machine	AF 100	Scotsman
Incubator (for bacteria)	B 6200	Heraeus
Incubator (with CO <sub>2</sub> )	HERAcell® 240	Kendro
Incubator shaker	innova 4000	New Brunswick Scientific
Magnetic hot plate stirrer	IKAMAG RET or RCT	IKA Labortechnik
Microwave	NN-T251W	Panasonic
Mixing rotor	Mixing rotor variospeed	Renner GmbH
Mood enhancer, CD-based	Micro Component High Fidelity System UX-S1	JVC
Multi pipette	Multipette® plus	Eppendorf
PCR machines	T3000 Thermocycler	Biometra / Whatman
	T Gradient	Biometra / Whatman
	Mastercycler Gradient	Eppendorf
pH meter	inoLab pH Level 1	WTW GmbH & Co. KG

**Table 5:** Equipment (continued)

<b>Equipment</b>	<b>Model</b>	<b>Supplier</b>
Pipettes	P2 / P20 / P200 / P1000	Gilson
Pipetting aid	pipetus®	Hirschmann Laborgeräte
Power supplies (electrophoresis)	Standard Power Pack P25	Biometra / Whatman
	LKB GPS 200/400	Pharmacia
Racks for glass coverslips	porcelain staining racks, no. 8542-E40	Thomas Scientific
Scales	PC 2000	Mettler
	Scout™ Pro SPU 2001	Ohaus Corp.
	AT261 DeltaRange® (precision scale)	Mettler
Spectrophotometer	Ultrospec 3000	Amersham Biosciences
Sterilizing oven	T 5050 E	Heraeus
Thermo mixer	Thermomixer comfort	Eppendorf
Vacuum aspiration system	PC 2004 vario	Vacuubrand, Inc.
Vortexer	K-550-GE / Vortex Genie 2	Scientific Industries
Water baths	Lauda Ecoline E-100 / bath 025	Brinkmann Instruments
	C-58 / 3	Julabo Labortechnik
<b><i>Gel documentation system</i></b>		
Gel documentation system	IP-CF01.SD incl. digital camera	Peqlab
UV transilluminator	ECX-20.M incl. CN-08 setup	Peqlab
Hoods	SterilGARD Hood, Class II Type A/B3	The Baker Company, Inc
	LaminAir HA 2448 GS	Heraeus
Laminar air flow hoods (for dissection)	HERAGuard® HPH15	Kendro
	EdgeGARD Hood EG-3252	The Baker Company, Inc.
Thermo printer	P93	Mitsubishi
<b><i>Dissection</i></b>		
<b>Dissection lamp</b>	<b>KL 1500 LCD / KL 200</b>	<b>Schott</b>
Dissection stereomicroscope	Stemi SV 6	Zeiss
Forceps	Straight forceps Dumont #5, 11 cm, Biologie tips (#11252-20)	Fine Science Tools
	Curved forceps Dumont #7, 11.5 cm, Biologie tips (#11297-10)	Fine Science Tools
Scissors	Vannas-Tübingen spring scissors, 8.5 cm, straight tips (#15003-08)	Fine Science Tools
	Hardened fine iris scissor, 11 cm, straight tips (#14090-11)	Fine Science Tools
	Extra fine scissors, model “Bonn”, 8.5 cm, straight tips (#14084-08)	Fine Science Tools

**Table 5:** Equipment (continued)

Equipment	Model	Supplier
<i>Microscopy and time lapse imaging</i>		
CCD camera	4912-5000 or 4912-5100	Cohu
Camera control panel	C 2741	Hamamatsu
Image acquisition hardware for PC	LG3 image grabber	Scion Corp.
Inverted epifluorescence microscopes	Axiovert 135TV	Zeiss
	AxioObserver.D1	Zeiss
Inverted bright field microscope	Wilovert®	Will
Mechanical microscope shutters	Uniblitz-Shutter for phase light (incl. adapter) VS25S 2 ZM 0 – 21	Vincent Associates
	Uniblitz-Shutter for fluorescence light (incl. adapter) VS25S 2 ZM 0 R1 – 21 (with high temperature modification)	Vincent Associates
Shutter driver	VMM-D1 or VCM-D1	Vincent Associates

### 5.1.6 Consumables

**Table 6:** Consumables

Material	Type	Supplier
<i>Disinfection, cleaning and sterilization</i>		
Cleaning concentrate for glassware and instruments	Deconex® 11 Universal	Borer Chemie AG
Disinfectant for hands	Sterillium®	Bode Chemie
Sterilizing bags	MELAfol 1502 (for instruments)	MELAG
	Polypropylene 200x300 mm	Roth
Wipes	TORK® facial tissues, extra soft	SCA
	Precision wipes KIMTECH Science	Kimberly-Clark
<i>Filtration systems</i>		
Bottle top filters	Steritop™ bottle top filter 250 ml / 500 ml (0.22 µm)	Millipore
Filtration systems	Stericup™ filter unit 250 ml / 500 ml (0.22 µm)	Millipore
	Filter system 250 ml / 500 ml (0.22 µm)	Corning Inc.
Syringe driven filter units	Millex®-GV, 0.22 µm (sterilization) or Millex®-HA, 0.45 µm (clarification)	Millipore
<i>Microscopy and immunohistochemistry</i>		
Cover glasses for microscopy	No. 1, Ø 15 mm	Marienfeld

**Table 6:** Consumables (continued)

<b>Material</b>	<b>Type</b>	<b>Supplier</b>
Cover glasses with relocation grid	CELLocate® glass coverslips, square size 55 µm	Eppendorf
	Custom-made glass coverslips with 4 x 4 mm relocation grid	Laserzentrum Hannover
Glass bottom dishes (for live-cell imaging)	3 cm (#P35G-1.5-14-C; 14mm hole size) 3 cm (#P35G-1.5-20-C; 20 mm hole size)	MatTek
High pressure metal halide arc lamp (for AxioObserver)	X-CITE 120, 120 Watt	EXFO Photonic Solutions
Mercury short arc bulb (for Axiovert)	103W/2	Osram
Microscope slides	76 x 26 mm, with frosted end	Menzel
<b><i>Pipettes and accessories</i></b>		
Combitips for multi pipette	0.1 ml / 0.2 ml / 0.5 ml / 1 ml / 2.5 ml / 50 ml	Eppendorf
Pasteur pipettes, glass	150 mm or 230 mm, unplugged	Poulsen & Graf
	150 mm or 230 mm with cotton plugs	VWR International
Pipette tips	2 µl / 20 µl / 200 µl / 1000 µl	Peske
Plastic pipettes	5 ml or 25 ml Costar® Stripette®	Corning Inc.
	Falcon® serological pipette 10 ml	Becton Dickinson
<b><i>Reaction tubes</i></b>		
PCR reaction tubes	PCR softstrips 0.2 ml, with attached cap strip (#711690)	Biozym
Reaction tubes	Safelock 1.5 ml or 2 ml	Eppendorf
Tubes (conical bottom, screw-top)	15 ml or 50 ml tubes	Becton Dickinson (Falcon®) or Corning
<b><i>Tissue culture</i></b>		
Tissue culture flasks	Nunclon™ Delta surface, 75 cm <sup>2</sup> (#153732)	Nunc
Tissue culture plastic dishes	Nunclon™ Ø 3 cm or 6 cm	Nunc
	Falcon® Ø 10 cm	Becton Dickinson
<b><i>Miscellaneous</i></b>		
Ear tags for mice	Four digit ear tags (#73850)	Hauptner & Herberholz
Gloves, powder-free, disposable	Semperguard, latex or nitrile	Semperit Technische Produkte GmbH
Injection needles, disposable	20G / 22G / 23G / 26G / 27G	Braun, Terumo or Becton Dickinson
Plastic laboratory film	Parafilm “M” 38 m x 10 cm (#PM-996)	Pechiney Plastic Packaging
Syringes	1 ml / 5 ml / 10 ml / 50 ml	Becton Dickinson
Thermal recording paper	KP61B-CE	Mitsubishi

All other consumable materials are mentioned in the methods section.

## 5.1.7 Media and standard solutions

### 5.1.7.1 Buffers and standard solutions

Table 7: Buffers and standard solutions

Solution	Ingredients and preparation		
<b>10× Agarose gel-loading buffer</b>	50% (v/v) 1x	glycerol TBE buffer	Mix 5.75 ml of 87% glycerol, 1 ml of 10x TBE buffer and distilled water to final volume of 10 ml and add saturated Bromphenol blue solution for dark blue color (approximately 50 µl). Store in aliquots at 4°C.
<b>Borate buffer, pH 8.5</b>	1.24 g 1.90 g	Boric acid Borax	Dissolve in 390 ml of distilled water. pH should be 8.5, adjust with 1 M HCl or NaOH if necessary. Adjust volume to 400 ml and filter-sterilize. Store at RT.
<b>0.5 M EDTA, pH 8.0</b>	186.1 g	EDTA	Add EDTA (disodium salt dihydrate) to 800 ml of distilled water. Adjust to pH 8.0: Add about 15 g of NaOH pellets while stirring, then carefully add 5 N NaOH to bring the pH to 8.0. The EDTA won't dissolve completely until pH≈8.0. Adjust volume to 1 l with distilled water. Clear solution with 0.45 µm filter and sterilize by autoclaving. Store at RT.
<b>1 M MgCl<sub>2</sub></b>	Dissolve 20.33 g MgCl <sub>2</sub> *6 H <sub>2</sub> O in 100 ml of distilled water and filter-sterilize. Store in small aliquots at RT since MgCl <sub>2</sub> is hygroscopic.		
<b>5M NaCl</b>	Dissolve 292.2 g of NaCl in 1 l of distilled water. Autoclave and store at RT.		
<b>5 N NaOH</b>	Dissolve 200 g NaOH in 1 l distilled water.		
<b>16% PFA / Sucrose</b>	16% (w/v) 16% (w/v)	PFA Sucrose	PFA should be handled under fume hood. Heat 650 ml water to approximately 60°C, add ~3 pellets of NaOH and 160 g PFA powder. Close the beaker well to prevent evaporation of PFA. The solution should start clearing up within ~30 min. Continue heating and stirring until the PFA is fully dissolved. Add 160 g sucrose, keep stirring until fully dissolved. Add 100 ml 10x PBS. Adjust pH to 7.4 with 37% HCl if necessary and adjust volume to 1 l with 1x PBS. Filter solution through paper filter. Store as aliquots of 50 ml at -20°C.
<b>5x PHEM buffer, pH 6,9</b>	300 mM 125 mM 50 mM 10mM	PIPES HEPES EGTA MgCl <sub>2</sub>	<u>for 250 ml</u> 4,54 g PIPES powder 1,49 g HEPES powder 5 ml EGTA (500mM) 0,5 ml MgCl <sub>2</sub> (1M)  Dissolve all ingredients in 200 ml of distilled water. Adjust the pH to 6,9 with ~1/10 of the final volume of 5 N NaOH. The PIPES will not dissolve until the pH is adjusted. Adjust volume to 250 ml with distilled water and check pH again. Filter solution through 0.45 µm filter and store at RT.

Table 7: Buffers and standard solutions (continued)

Solution	Ingredients and preparation		
<b>Phosphate-buffered saline (PBS)</b>	137 mM	NaCl	for 1 l 8 g NaCl
	2.7 mM	KCl	0.2 g KCl
	8 mM	Na <sub>2</sub> HPO <sub>4</sub>	1.15 g Na <sub>2</sub> HPO <sub>4</sub>
	1.5 mM	KH <sub>2</sub> PO <sub>4</sub>	0.24 g KH <sub>2</sub> PO <sub>4</sub>
	Dissolve all ingredients in 800 ml of distilled water. Adjust to pH 7.4 with HCl and adjust volume to 1 l with distilled water. Sterilize by autoclaving and store at RT.		
	For 10x PBS use the 10-fold amount of salts in 1 l of distilled water.		
<b>1M Tris-HCl, pH 7.4 or 8.0</b>	Dissolve 121.1 g Tris base in 800 ml of distilled water. Adjust pH to the desired value by adding 37% HCl (~70 ml for pH 7.4; ~42 ml for pH 8.0). Adjust volume to 1 l. Sterilize by autoclaving and store at RT.		
<b>Tris-EDTA (TE) buffer, pH 8.0</b>	10 mM	Tris-HCl	Mix 1 ml 1 M Tris-HCl pH 8.0 and 200 µl 0.5 M EDTA pH 8.0 in 90 ml distilled water, check pH and adjust to 8.0 by adding 37% HCl if necessary. Add distilled water to final volume of 100 ml. Sterilize by autoclaving and store at RT.
	1 mM	EDTA	
<b>50× Tris-acetate-EDTA (TAE) electrophoresis buffer</b>	242 g	Tris base	Add distilled water to 1 l. May be autoclaved. Store at RT.
	57.1 ml	glacial acetic acid	
	100 ml	0.5 M EDTA (pH 8.0)	Dilute the concentrated stock buffer to 1x prior to use and prepare both gel solution and electrophoresis buffer from the diluted buffer.
<b>10× Tris-borate-EDTA (TBE) electrophoresis buffer</b>	108 g	Tris base	Add distilled water to 1 l. May be autoclaved. Store at RT.
	55 g	boric acid	
	40 ml	0.5 M EDTA (pH 8.0)	
	Dilute the concentrated stock buffer to 0.5-1x prior to use and prepare both gel solution and electrophoresis buffer from the diluted buffer.		

### 5.1.7.2 Media and supplements for primary cell culture

Table 8: Stock solutions

Solution	Ingredients		Preparation
<b>5.5% (w/v) NaHCO<sub>3</sub></b>	27.5 g	NaHCO <sub>3</sub>	Dissolve NaHCO <sub>3</sub> in distilled water and filter-sterilize. Store at 4°C.
<b>20% (w/v) Glucose</b>	20% (w/v)	D(+)-glucose	Warm up distilled water and add glucose stepwise under constant stirring. <i>Do not autoclave</i> but rather filter-sterilize. Store at 4°C.
<b>L-glutamine (100x)</b>	200 mM	glutamine	Dissolve glutamine in warm distilled water. Store 5 ml aliquots at -20°C.
<b>Pyruvate (100x)</b>	1.1 g	pyruvate	Dissolve pyruvate in 100 ml distilled water. Filter-sterilize and store at 4°C for up to ~3 months.

**Table 9:** N2 supplements

Supplement	Preparation
<b>Insulin (1.000x)</b>	Dissolve 50mg insulin in 10ml 0.01N HCl, store aliquots at -20°C.
<b>Progesteron (1.000x)</b>	Dissolve 63 mg Progesteron in 100 ml ethanol, add 1 ml of this solution to 99 ml distilled water. Store aliquots at -20°C.
<b>Putrescine-dihydrochloride (1.000x)</b>	Dissolve 161 mg putrescine-dihydrochloride in 10 ml distilled water, store aliquots at -20°C.
<b>Selenium-dioxide (1.000x)</b>	Dissolve 33 mg selenium-dioxide in 100 ml distilled water, add 1 ml of this solution to 99 ml distilled water. Store aliquots at -20°C.
<b>N2 supplement stock (10x)</b>	Mix 5 ml of each insulin, progesteron, putrescine-dihydrochloride and selenium-dioxide 1.000x-stocks with 500 mg human apo-transferrin in a total volume of 500 ml N-MEM. Store aliquots for up to ~6 months at -20°C.

**Table 10:** Cell culture media

<b>MEM-HS</b> (Minimal essential medium supplemented with 10% (v/v) horse serum)	300 ml distilled water 50 ml 10x MEM 20 ml 5,5% NaHCO <sub>3</sub> 15 ml 20% (w/v) glucose 5 ml L-glutamine (100x) 10 ml 50x MEM essential aminoacids 10 ml 100x MEM non-essential aminoacids 50 ml horse-serum
	Adjust pH to 7.3 with 1M NaOH, add distilled water to 500 ml. Filter-sterilize and store at 4°C for up to ~2 weeks.
<b>N-MEM</b>	50ml 10xMEM 20 ml 5.5% NaHCO <sub>3</sub> 15 ml 20% (w/v) glucose 5 ml L-Glutamine (100x) 5 ml Pyruvate (100x)
	Mix all ingredients in a total volume of 500 ml distilled water. Filter-sterilize and store at 4°C for up to ~2 weeks.
<b>N2 medium</b>	450 ml N-MEM 50 ml N2 supplement stock (10x) 100 mg Ovalbumin
	Check pH, adjust to 7.3 if necessary. Filter-sterilize and store at 4°C for up to ~2 weeks.

### 5.1.7.3 Media and antibiotics for bacterial culture

**Table 11:** Bacterial media

<b>LB (Luria-Bertani-) media</b>	1% (w/v) Bacto-Trypton 0.5% (w/v) Yeast extract 0.5% (w/v) NaCl Add distilled water to final volume, adjust pH to 7.5 if necessary. Sterilize by autoclaving and store at RT.
<b>LB-plates</b>	Like LB media, but supplemented with 1.5% Bacto-Agar before autoclaving. Store at 4°C.

LB-Agar was cooled to 55°C, LB-media to RT before the addition of antibiotics. After addition of antibiotics selection media and plates were stored at 4°C.

**Table 12:** Antibiotic stocks

1.000x stock solutions

<b>Ampicillin</b>	100 mg/ml
<b>Kanamycin</b>	50 mg/ml

Dissolve antibiotics in distilled water, filter-sterilize and store aliquots at -20°C.

### 5.1.8 Antibodies

Antibodies were stored in aliquots at -20°C, thawed aliquots were kept at 4°C.

#### 5.1.8.1 Primary antibodies

**Table 13:** Primary antibodies used for immunohistochemistry

<b>Antibody</b>	<b>Dilution</b>	<b>Type</b>	<b>Supplier &amp; Product number</b>
<b>anti-acetylated tubulin</b> (clone 6-11B-1)	1:50.000	mouse monoclonal, ascites fluid	Sigma, #T-6793
<b>anti-GFP</b> (goat)	1:5.000	goat polyclonal	USBiological, #G8965-05
<b>anti-GFP</b> (rabbit)	1:2.000	rabbit polyclonal	RDI Research Diagnostics Inc., #RDI-GRNFP4abr
<b>anti-MAP2</b> (goat)	1:2.000	goat polyclonal	Santa Cruz, #sc-5357
<b>anti-MAP2</b> (mouse)	1:5.000	mouse monoclonal	Sigma, #M-4403
<b>anti-MAP2</b> (rabbit)	1:6.000	rabbit polyclonal	Chemicon, #AB5622
<b>anti-PSD95</b> (clone 6G6-1C9)	1:1.000	mouse monoclonal	ABR Affinity BioReagents, #MA1-045
<b>anti-Synapsin 1</b>	1:200 (blue channel)	rabbit polyclonal	Chemicon, #AB1543
<b>anti-<math>\alpha</math>-tubulin</b> (clone B-5-1-2)	1:20.000	mouse monoclonal	Sigma, #T-5168

**Table 13:** Primary antibodies (continued)

Antibody	Dilution	Type	Supplier & Product number
<b>anti-tubulin</b>	1:200	rabbit polyclonal	Sigma, #T-3526
<b>anti-tyrosinated tubulin (YL1/2)</b>	1:40.000	rat monoclonal	Abcam, #ab6160 (purified)
	1:200 to 1:3.000		gift from M. Schleicher (supernatant of hybridoma cells)
<b>Tau-1</b>	1:5.000	mouse monoclonal	Chemicon, #MAB 3420
<b>anti-neuronal Class III <math>\beta</math>-Tubulin (Tuj-1)</b>	1:5.000 to 1:20.000	mouse monoclonal	Covance, # MMS-435P
<b>anti-neuron specific beta III tubulin (Tuj-1)</b>	1:50-1:100 (blue channel)	rabbit polyclonal	Abcam, ab18207

### 5.1.8.2 Secondary antibodies

All secondary antibodies were purchased from Invitrogen (formerly Molecular Probes).

The dilution for all secondary antibodies was **1:500**.

**Table 14:** Secondary antibodies

Specificity	Host	Fluorochrome	Order number (Invitrogen)
<b>anti-goat</b>	<b>donkey</b>	Alexa Fluor 350	A21081
		Alexa Fluor 488	A11055
		Alexa Fluor 568	A11057
<b>anti-mouse</b>	<b>donkey</b>	Alexa Fluor 555	A31570
	<b>goat</b>	Alexa Fluor 350	A31045
		Alexa Fluor 488	A11029
		Alexa Fluor 555	A21429
		Alexa Fluor 568	A11004
<b>anti-rabbit</b>	<b>donkey</b>	Alexa Fluor 488	A21206
	<b>goat</b>	Alexa Fluor 350	A21068
		Alexa Fluor 488	A11034
		Alexa Fluor 555	A21429
		Alexa Fluor 568	A11036
<b>anti-rat</b>	<b>goat</b>	Alexa Fluor 568	A11077
		Alexa Fluor 488	A11006

### 5.1.9 Other dyes

**Table 15:** Other dyes

Dye	Fluorochrome	Concentration	Supplier & Product number	Function
Rhodamine-Phalloidin	TRITC (red)	2 to 4 U/ml	Invitrogen, #R415	visualization of F-actin
Cell Tracker Blue CMAC®	CMAC (blue)	5-20 µM	Invitrogen, #C2110	cytoplasmic dye

Rhodamine-Phalloidin was applied together with secondary antibodies during immunostaining.

Cell Tracker Blue was added to the media of living cells, excess dye was washed out after 30 minutes incubation.

### 5.1.10 Bacteria

For plasmid propagation the *E. coli* strain DH5α (Hanahan, 1983) was used.

The relevant genotype of DH5α is: F' / *endA1 hsdR17*(r<sub>K</sub><sup>-</sup>m<sub>K</sub><sup>+</sup>) *glnV44 thi-1 recA1 gyrA* (Na<sup>f</sup>) *relA1 Δ(lacZYA-argF)U169 deoR* (Φ80*dlacΔ(lacZ)M15*)

### 5.1.11 Plasmids

**Table 16:** Plasmids

Plasmid name	Selection marker	Description	Reference
pEGFP-N1-EB3	Kan <sup>R</sup> (confers resistance to 30 µg/ml Kanamycin to <i>E. coli</i> hosts)	Contains the full length cDNA of human end binding protein 3 (EB3) cloned into the Sall- / BamHI-restriction sites of pEGFP-N1	Stepanova et al., 2003
pEGFP-T7/C1-α-Tubulin		Contains alpha-tubulin-cDNA cloned into the XhoI- / BamHI-restriction sites of pEGFP-T7/C1	

pEGFP-N1-EB3 was a gift from Vic Small (IMBA, Vienna, Austria) and Anna Akhmanova (Erasmus Medical Center, Rotterdam, Netherlands). pEGFP-T7/C1-α-Tubulin was a gift from Susanna Nagel and Erich Nigg (MPI of Biochemistry, Martinsried, Germany).

### 5.1.12 Oligonucleotides

All oligonucleotides were synthesized by Metabion. Desalted Oligonucleotides were used as primers for PCR genotyping or sequencing. Primer sequences are shown from their 5' to their 3' end.

**pEYFP-N1 for** and **EGFP N-term rev** primers were used as sequencing primers for pEGFP-N vectors.

**pEGFP-C1 for** and **pEGFP-C1 rev** primers were used as sequencing primers for pEGFP-C vectors.

**Table 17:** Oligonucleotides

Primer name	Sequence (5' → 3')
<b>pEYFP-N1 for</b>	GGG CGG TAG GCG TGT ACG GTG G
<b>EGFP N-term rev</b>	CGT CGC CGT CCA GCT CGA CCA G
<b>pEGFP-C1 for</b>	GAT CAC TCT CGG CAT GGA C
<b>pEGFP-C1 rev</b>	CAT TTT ATG TTT CAG GTT CAG GG
<b>SAD A common</b>	TGG GAA GGT AAG CAG GGA GGC CAG GTA ACC
<b>SAD A WT</b>	TGC CCC TGC TCA CCT TAG GTG TCA CCA TG
<b>SAD B common</b>	AAT GAA GAT GGC TTG ATA GGC TTA CCA C
<b>SAD B common 4</b>	GGA GGA ATT TTG TAG ATT TAG CAC CCT GCC
<b>SAD B WT</b>	TGT CTC CTA TAC CTT GAT AGG TAG GCA G
<b>J25</b>	TGC CAA GTT CTA ATT CCA TCA GAA GCT G
<b>Fabpi-200 control primer 3'</b>	TAG AGC TTT GCC ACA TCA CAG GTC ATT CAG
<b>Fabpi-200 control primer 5'</b>	TGG ACA GGA CTG GAC CTC TGC TTT CCT AGA

Sequences for Fabpi-200 control primers were designed by the *Mouse Genetics Core* facility, Washington University in St. Louis, School of Medicine (publicly available on [http://mgc.wustl.edu/protocols/pcr\\_primer\\_set.html](http://mgc.wustl.edu/protocols/pcr_primer_set.html)).

## 5.2 Methods

### 5.2.1 Cell Culture

#### 5.2.1.1 Primary culture of hippocampal neurons

Glass coverslips for hippocampal neurons were bathed overnight in nitric acid ( $\geq 65\%$ ), rinsed 5x in distilled water, sterilized at 220°C for 6 h and distributed to 6 cm petri dishes (5-6 coverslips per dish) under sterile conditions. Coverslips were then provided with paraffin dots and coated with poly-L-lysine (1 mg/ml in borate buffer, pH 8.5) overnight at RT. Coverslips were washed 3x with distilled water to remove excess poly-L-lysine and subsequently incubated with MEM-HS overnight.

Primary hippocampal neurons derived from rat embryos were cultured as described (de Hoop *et al.*, 1997; Goslin and Banker, 1991). In brief, the hippocampi of E17 or E18 rats or mice were dissected, trypsinized for 10 min with 0.05% Trypsin-EDTA at 36°C and washed 3x in HBSS. Cells were then triturated approximately 10-20x in ~2 ml HBSS with both a regular and a fire-polished glass pasteur pipette until the suspension was homogeneous. The volume of the suspension was then increased to 5 ml with HBSS and cell density was determined using a

hemocytometer (Neubauer Improved).  $1.0\text{--}1.3 \times 10^5$  cells were plated onto poly-lysine-coated glass coverslips in 6 cm petri dishes containing minimal essential medium (MEM) and 10% heat-inactivated horse serum. The cells were kept in 5% CO<sub>2</sub> at 36.5°C. After 6-12 hours, the coverslips were transferred to a 6 cm dish containing astrocytes in MEM and N2 supplements. Hippocampal neurons from E18 SAD A SAD B knockout mice were cultured as described above, using mouse wild type astrocytes. For mixed wild type/GFP neuronal cultures wild type mouse hippocampal neurons were combined with 1-3% of hippocampal neurons isolated from mice expressing enhanced green fluorescent protein (eGFP) under control of the ubiquitously active CAG promoter (Ikawa *et al.*, 1998; Okabe *et al.*, 1997), a hybrid promoter composed of the cytomegalovirus (CMV) enhancer, a fragment of the chicken  $\beta$ -actin promoter and rabbit  $\beta$ -globin exons (Niwa *et al.*, 1991).

### **5.2.1.2 Primary culture of glia cells**

Cerebral hemispheres were collected after removing the meninges during dissection of hippocampi from E17 or E18 rats or mice (~4-5 hemispheres for one culture flask or ~4 hemispheres for ~15 dishes for use during the next days). The hemispheres could be kept in HBSS at RT during the preparation of the hippocampal neurons. Hemispheres were washed 1-2x with HBSS to remove debris and then trypsinized for ~10 min at 36°C (8-10 brains in 5 ml 0.05% Trypsin-EDTA containing 10mM HEPES pH 7,25). Subsequently, Trypsin was removed and the hemispheres were carefully washed 2-3x with 5 ml HBSS. Hemispheres were then triturated approximately 20 times with the help of a regular and a fire-polished glass pasteur pipette, first in 4 ml, then in 10 ml total volume until the suspension was homogeneous. To pellet big pieces of debris the suspension was centrifuged for 5-10 sec at 80 g after titration. A volume corresponding to 4-5 hemispheres was then added to untreated tissue culture flasks containing 15-20 ml pre-warmed MEM-HS. The next day the medium was changed completely to remove cell debris. When the cells reached about 70-80% confluency (7-10 days), they were trypsinized for 3-4 min with ~2 ml 0.05% Trypsin-EDTA containing 10 mM HEPES pH 7,25 and afterwards split to new flasks (at a ratio of 1:3) or 6 cm-dishes (1 confluent flask for ~40 dishes). The astrocyte cultures could be passaged up to three times.

### **5.2.1.3 Transfection of hippocampal neurons**

Neurons were transfected before plating with the Amaxa Nucleofector system using highly purified DNA (EndoFree Maxi Prep; Qiagen). Directly after isolation of hippocampal neurons up to 3-7.5 $\mu$ g of plasmid DNA was used for electroporation of 500.000 cells according to the manufacturers' instructions. In brief, cells were centrifuged with 80 g for 5 min at RT, subsequently all the supernatant but 50-100  $\mu$ l was removed. 100  $\mu$ l transfection buffer and the plasmid DNA were then added, the cells were resuspended by gently pipetting up and down approximately 10 times with a 200  $\mu$ l pipette and transferred to an electroporation cuvette. Next, cells were electroporated using the Amaxa Nucleofector program O-003 for rat hippocampal neurons. Directly after electroporation, 500  $\mu$ l of pre-warmed MEM-HS was added to the neurons to increase cell survival. Subsequently, neurons were plated in one to three 6 cm dishes containing MEM-HS and further cultured as described above.

#### **5.2.1.4 Drug treatment**

When necessary, drugs were pre-diluted in their solvent to achieve the desired final concentration with the last dilution step in media or HBSS.

Depending on the experiment, 0.3 to 100 nM taxol, 1  $\mu$ M cytochalasin D, 15 to 225 nM nocodazole, 10-20  $\mu$ M SB415286, 2 nM trichostatin A and 1  $\mu$ M tubacin were added to culture medium after 6 to 18 hours after plating, and cells were further incubated at 36.5°C in the presence of the drug.

For short term incubation, 10 to 100 nm taxol or 3.3 to 5  $\mu$ M nocodazole were added to cells in HBSS. Cells were then incubated at 36.5°C in the incubator or on the microscope stage in the presence of the drug.

Nocodazole and SB415286 precipitate in aqueous solutions. To ensure homogenous distribution of these drugs, 1 ml of the medium or HBSS of the cells to be treated was transferred to a 2 ml Eppendorf tube, the drugs were added to the tube and vortexed immediately after addition. After a short spin (~1 sec ) in a table centrifuge to collect the liquid, medium or HBSS were transferred back to the dish and mixed by swirling.

#### **5.2.1.5 Microtubule stability assay**

Directly before the experiment, solutions of 3.3 to 5  $\mu$ M nocodazole in HBSS were prepared: Nocodazole was added from the stock to the required amount of HBSS in a 50 ml tube which was then vortexed immediately after drug addition. The solution was then distributed to 3 cm dishes and warmed up to 36.5°C in the incubator. Neurons grown on glass coverslips with a relocation grid were transferred to plain Hepes-buffered HBSS in glass bottom dishes, imaged and then transferred (cells facing up) to one of the dishes containing 3.3-5  $\mu$ M nocodazole for 5 min. Subsequently, neurons were simultaneously fixed and permeabilized to remove  $\alpha$ -tubulin not incorporated in microtubules (PHEM-fixation, see 5.2.3.1 on page 82) and immunostained with rhodamine-coupled phalloidin and an anti- $\alpha$ -tubulin antibody (Sigma, #T 5168). F-actin outlining the neuron was used as a reference point for measuring microtubule retraction.

### **5.2.2 Microscopy**

#### **5.2.2.1 Image acquisition**

Images were captured using a Zeiss Axiovert 135TV or a Zeiss Axio Observer D1 microscope equipped with a CCD camera from the 4912 series (Cohu) at room temperature (fixed samples) or 36°C (living neurons). The camera was connected to a Hamamatsu CCD camera C 2741 control panel. Pictures were recorded on a hard disc using an LG3 image grabber and Scion Image, version Beta 4.0.2 (both from Scion Corp.). To acquire both phase and fluorescence images from the same time point I constructed a dual-control cable which allows the simultaneous control of both phase and fluorescence shutters of the microscope setup (Figure 5-1).

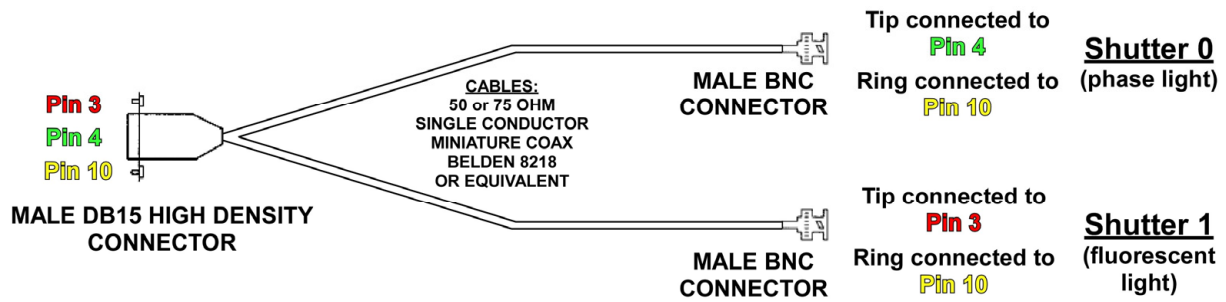


Figure 5-1: Wiring diagram for dual-control shutter cable

### 5.2.2.2 Time lapse imaging (Video microscopy)

Living neurons were kept at 36°C on the stage of a Zeiss Axiovert 135TV microscope. Glass bottom dishes (MatTek Corporation, Ashland, MA) filled with HEPES-buffered HBSS were used for observation with Zeiss LD A-Plan 32x (NA 0.4) or Zeiss Plan-Apochromat 40x (NA 1.0) objectives. Alternatively, custom-made cell chambers served for live observation of neurons with a Zeiss Plan-Apochromat 63x (NA 1.4) objective. When necessary, drugs were diluted to 4x concentration in HBSS and added on stage during the observation. Cells were illuminated with 100 W, 12 V halogen light (Osram) or fluorescence light from a 103W/2 mercury short arc bulb (Osram). Halogen light was set to minimal intensity to avoid phototoxicity, fluorescence radiation was reduced to 5% or 25% with transmission filters to avoid phototoxicity and reduce bleaching.

### 5.2.2.3 Image Analysis and Quantification

Length and intensity measurements were taken using Scion Image, version Beta 4.0.2 (Scion Corp.) for Windows (Microsoft) or ImageJ analysis software (NIH). Plot profiles of fluorescence intensity were created with ImageJ. Average neurite length in experiments with long term nocodazole treatment was determined taking into account neurons without processes. To analyze movement of fluorescent particles in EB3-GFP-transfected neurons, both phase and fluorescent images were acquired in 5-10 sec-intervals during the experiment. Subsequently, kymographs from the regions of interest were made from the individual images using Scion Image and a purpose-written macro. EB3-particles were only considered for analysis if they could be followed clearly for 3 or more frames in the kymographs. The ratio of acetylated versus tyrosinated  $\alpha$ -tubulin was determined from the average fluorescence intensity of both channels in a square of 3x3 to 5x5 pixels in the medial part of each process, after background subtraction with Adobe Photoshop.

### 5.2.2.4 Scion image macros for image acquisition and analysis

Several macros were written as plug-ins for Scion Image, version Beta 4.0.2 (Scion Corp.) for Windows (Microsoft) to facilitate or allow the acquisition and annotation of phase and fluorescence images of multiple

channels, time lapse imaging, measurement of fluorescence intensities and ratios, control of irradiation during photoactivation of caged substances, and building and analysis of kymographs of moving particles.

The source codes of the macros are given in the appendix (p. 103).

#### **5.2.2.5 Focal photoactivation of caged taxol**

Near-UV-light ( $\lambda=365$  nm) was focused on a spot of 20-30  $\mu\text{m}$  in diameter using the fluorescence iris of a Zeiss Axiovert 135 equipped with a Zeiss Plan-Apochromat 40x (NA 1.0) oil immersion objective. A sample stained with Cell Tracker Blue CMAC (Molecular Probes) was used to determine the exact position of the spot before the experiment. For the uncaging experiment with EB3-GFP transfected neurons, a Zeiss Plan-Apochromat 63x (NA 1.4) oil immersion objective was used instead and the cells were handled as described above. Under phase light, one dynamic growth cone of an unpolarized stage 2 neuron grown on a relocation coverslip was randomly chosen. Subsequently, caged taxol or DMSO was added to the neurons on the microscope stage to a final concentration of 1-10 nM or 0.02%, respectively. After equilibration, the tip of the selected growth cone or the region directly adjacent to it was pulsed for 10-15 min with near-UV-light (pulse duration 50-100 msec; frequency 0.2-0.33 Hz). After uncaging, the neurons were incubated in 5% CO<sub>2</sub> at 36.5°C for another 2 days.

Neurons were then fixed, stained for Tau-1 and MAP2, relocated and the site of axon formation determined. Only neurons which had formed an axon during the 48 hours after uncaging were taken into account. For analysis the angle between the edge of the uncaged area, the center of the cell body and the site of axon formation was measured.

For calculation of the probability of random axon formation the number of growth cones within the sector in question was divided by the total number of the cells' growth cones.

#### **5.2.2.6 Fluorescence recovery after photo-bleaching (FRAP)**

FRAP experiments were performed with a life cell imaging setup (Deltavision RT; Applied Precision) based on an inverted fluorescence microscope (IX71; Olympus) with a UPlanApo 100x (NA 1.35) oil immersion objective (Olympus). The setup included a quantifiable laser module (488nm diode laser) for bleaching GFP and an incubation chamber (Solent Scientific). Living neurons were imaged in Hepes-buffered HBSS at 36°C. Complete bleaching of the signal of GFP-tubulin was achieved by a 1-3 s laser pulse with 50-100% power intensity. Images were acquired using a Photometrics CoolSnap HQ camera (Roper Scientific). SoftWoRx 3.5.0 (Applied Precision) was used for control of bleaching (one spot; alternatively, two spots simultaneously), image recording, deconvolution (based on measured point spread function, iteration method: additive) and analysis of the FRAP experiments.

## **5.2.3 Immunocytochemistry**

### **5.2.3.1 Fixation methods**

#### **PFA-fixation**

For staining of Tau-1, MAP2, GFP or Synapsin 1, cells were fixed with pre-warmed 4% paraformaldehyde / 4% sucrose in phosphate-buffered saline (PBS) for 15-20 min at RT, washed 3x with PBS and quenched in 50 mM ammonium chloride in PBS at RT for 15 min to inactivate residual formaldehyde. After quenching cells were permeabilized with 0.1% Triton X-100 in PBS for 3-5 min at RT and washed again 3x with PBS.

#### **PHEM-fixation**

Alternatively, to assess acetylated, tyrosinated and total tubulin without unpolymerized tubulin subunits, i.e. to analyze only microtubules, cells were simultaneously fixed and permeabilized for 15 min in pre-warmed PHEM buffer (60 mM Pipes, 25 mM Hepes, 5 mM EGTA and 1 mM MgCl) containing 0.25% glutaraldehyde, 3.7% paraformaldehyde, 3.7% sucrose, and 0.1% Triton X-100 (modified from Smith, 1994), washed 3x with PBS, quenched in 50 mM ammonium chloride in PBS at RT for 15 min and washed again 3x with PBS.

### **5.2.3.2 Immunostaining**

For immunostaining quenched coverslips were transferred to a dark moist chamber, cells facing up. Samples were blocked for 1 hr at RT with a solution containing 2% fetal bovine serum, 2% bovine serum albumin, and 0.2% fish gelatin dissolved in PBS. Subsequently, cells were incubated with primary antibodies diluted in 10% blocking solution in PBS for at least 1 h at RT or overnight at 4°C. Cells were then washed 4x with PBS and incubated with secondary antibodies diluted in 10% blocking solution in PBS for at least 30 min at RT. When necessary, rhodamine-phalloidin was applied together with secondary antibodies. If secondary antibodies were incompatible in double or triple stainings, they were applied sequentially with 4 wash steps with PBS in-between. After incubation with secondary antibodies, cells were washed 3x with PBS and 2x with distilled water. Wax dots of the coverslips were then removed manually, coverslips were mounted using Mowiol or Gelmount and slides were dried for ~1h in the dark at RT.

## **5.2.4 Molecular Biology**

### **5.2.4.1 Culturing of *E. coli***

*E. coli* was cultivated at 37°C under aerobic conditions either in liquid LB-media with vigorous shaking (220 rpm) or on LB-plates. Cultures were inoculated from single colonies. For plasmid selection, media or plates containing appropriate antibiotics were used.

The density of a bacterial culture was determined photometrically. An optical density (OD) of 1 at  $\lambda=600$  nm in relation to the blank value (pure medium) corresponds to approximately  $1 \times 10^9$  cells/ml.

### **5.2.4.2 Transformation of *E. coli***

#### **Preparation of competent *E. coli* cells**

To set up an overnight culture, 6 ml of plain LB medium were inoculated with *E. coli* (strain DH5 $\alpha$ ) and grown overnight with vigorous shaking. The next day, ~5 ml of the dense overnight culture were used to inoculate 500 ml of plain LB medium. Cells were then grown at 37°C with vigorous shaking until the culture reached an OD<sub>600</sub> of 0.5 (within the range of OD<sub>600</sub> 0.4-0.6). Subsequently, cells were pelleted in 50 ml conical tubes at 1600 g for 5 min at 4°C, the supernatant was discarded and the pellets resuspended and pooled in 250 ml of cold sterile 0.1M CaCl<sub>2</sub>. Cells were incubated on ice for at least 15-30 minutes (longer incubations do not pose a problem). Then cells were pelleted again at 1600 g for 5 min at 4°C, the pellet resuspended in 10 ml of cold sterile 0.1M CaCl<sub>2</sub> and sterile glycerol was added to a final concentration of 20%. Aliquots of 100  $\mu$ l were snap-frozen in liquid nitrogen and stored at -80°C.

#### **Transformation of competent *E. coli* cells**

10 to 100 $\mu$ l of chemical competent bacteria were gently thawed on ice and mixed with the plasmid to be transformed in an 1.5 ml Eppendorf tube. The tube was incubated on ice for 10 min. Bacteria were heat-shocked by incubation at 42°C for 1 min and then chilled on ice for 2 min. 1 ml of plain LB medium (pre-warmed to 37°C) was added to the cells, incubated at 37°C for 60 min with shaking at 225-250 rpm. 50 to 100  $\mu$ l of the transformation were plated on LB agar plates containing the appropriate antibiotic for plasmid selection and incubated at 37°C overnight. Alternatively, when few transformants were expected, the transformation was spun down at maximum speed for 10 sec in a table top centrifuge and 900  $\mu$ l of the supernatant discarded. The bacterial pellet was resuspended in the remaining liquid, plated and cultured as described above.

### **5.2.4.3 Preparation of plasmid DNA**

Plasmid DNA was purified from small-scale (3 ml, minipreparation) or from large-scale (100 ml, maxipreparation) bacterial cultures. LB medium containing 100  $\mu$ g/ml ampicillin or 50  $\mu$ g/ml kanamycin was inoculated from single colonies of transformed bacteria, starter cultures or bacterial glycerol stocks and incubated overnight at 37°C with vigorous shaking. The bacterial suspension was pelleted by centrifugation at 6.000 g for 5 min at RT and then resuspended in buffer P1 (Qiagen; 50 mM Tris-Cl, pH 8.0; 10mM EDTA; 100  $\mu$ g/ml RNase A). Mini- and EndoFree® Maxipreparation of plasmid DNA were carried out according to the Qiagen protocol employing alkaline lysis of the cells and binding of the plasmid DNA to an anion exchange resin. After washing, elution and precipitation the plasmid DNA was redissolved in a suitable volume of TE buffer (alternatively 10 mM Tris-Cl, pH 8.0), usually 30  $\mu$ l for minipreparations and 150  $\mu$ l for maxipreparations. After determining the DNA concentration, plasmid DNA was stored at 4°C to avoid strand breaks induced by repeated freeze-thaw cycles.

#### **5.2.4.4 Handling of nucleic acids**

##### **Measurement of DNA concentration**

DNA concentration was measured in duplicates in a UV photometer at 260 nm. Samples were diluted in distilled water.

At a wavelength of 260 nm and a sample thickness of 1 cm an OD of 1 corresponds to a concentration of 50 µg/ml for double stranded DNA, 33 µg/ml for single stranded DNA and 40 µg/ml for RNA. The concentration of the sample was therefore  $OD_{260} \times T \times \text{dilution factor} = X \text{ µg/ml}$ , with T being 50 µg/ml for double stranded DNA, 33 µg/ml for single stranded DNA and 40 µg/ml for RNA.

##### **Separation of DNA on agarose gels**

Agarose gels (0.8-2% w/v) for non-denaturing gel electrophoresis were prepared by boiling agarose in 0.5x TBE or 1x TAE buffer in a microwave oven. After the agarose had cooled to 55°C, ethidium bromide was added to a final concentration between 100 to 200 ng/ml and the gel was poured into a gel casting system. The DNA sample and 6× DNA loading buffer (one fifth of the sample volume) were mixed, loaded onto the agarose gel in 0.5x TBE or 1x TAE buffer and run for approximate 30 to 35 min at 100 to 180 V. After electrophoresis the gel was analyzed using an ECX-20.M UV-transilluminator and an IP-CF01.SD gel documentation system (both from Peqlab).

#### **5.2.4.5 Genotyping**

##### **Preparation of genomic DNA from tissue**

Genomic DNA was prepared from mouse tails by alkaline lysis of the tissue. 150 µl of 50 mM NaOH was added to a mouse tail of approximately 2 mm length and heated to 95°C for 1 h until the tissue is lysed. During the incubation the samples are vortexed approximately every 15 min for ~10 sec at medium intensity to support tissue lysis. After lysis, samples are then chilled on ice for 1 to 2 min, neutralized by addition of 50 µl 1 M Tris-HCl (pH 7.5) containing 4 mM EDTA, vortexed at medium intensity and centrifuged at 4°C with maximum speed in a table top centrifuge for 5 min. Samples were stored at 4°C and could be used as PCR templates for more than one year after preparation.

##### **Genotyping using PCR**

For genotyping, 1 µl of the preparation of genomic DNA was used in a 20 µl-hot start reaction for PCR amplification (see Table 18 on page 85). Primers specific for the gene encoding the fatty acid binding protein (Fabpi primers) were included in each reaction as an internal control since they yield a PCR product independent of the SAD A/B genotype of the animal. For primer sequences see section 5.1.12 Oligonucleotides, page 77.

Final concentrations in the reactions were: 3.5 mM MgCl<sub>2</sub>; 0.5 mM dNTPs; 1 U Taq Polymerase; 0.5 µM of all SAD primers included in the reaction; 0.2 µM of both Fabpi-200 primers.

**Table 18:** PCR mix for SAD A/B genotyping:

all amounts in [µl]	SAD A combined	SAD-B Wild type	SAD-B Knockout
DNA		1	
Water	10.60	11.60	11.60
10xPuffer		2	
MgCl <sub>2</sub> (50mM)		1.4	
dNTPs (10mM)		1	
Polymerase (Invitrogen; 5U/µl)		0.2	
J25 (10µM)	1	-	1
SAD A common (10µM)	1	-	-
SAD A wild type (10µM)	1	-	-
SAD B common (10µM)	-	1	-
SAD B wild type (10µM)	-	1	-
SAD B common 4 (10µM)	-	-	1
Fabpi-200--3' (10µM)		0.4	
Fabpi-200--5' (10µM)		0.4	
<b>Total</b>		<b>20</b>	

19 µl of the mastermix was transferred to PCR strip tubes on ice using an Eppendorf Multipette. 1 µl of the genomic DNA was then added to each tube, mixed thoroughly by vortexing and briefly centrifuged to collect the liquid. Samples were then placed into the preheated PCR machine and a program using the following PCR cycling parameters was started:

**95°C hot start**

**95°C 3min**

**95°C 30sec**

**72°C 45sec**

**72°C 1min**

10 cycles, annealing temperature -0.5°C per cycle (Touchdown-PCR)

**95°C 30sec**

**68°C 45sec**

**72°C 1min**

25 cycles

**72°C 10min**

**4°C hold**

PCRs were subsequently mixed with 10× loading buffer and analyzed by gel electrophoresis in a 1.5% agarose gel (0.5x TBE). After electrophoresis, gels were analyzed using a UV-transilluminator and a gel documentation system (see section 5.2.4.4).

**Expected band sizes for SAD A/B genotyping:**

**SAD A wild type** ~480bp

**SAD A knockout** ~320 bp (+faint band at ~550bp)

**SAB B wild type** ~380bp

**SAB B knockout** ~330bp

**Fabpi 200** 194 bp (for all reactions regardless of the SAD A/B genotype)

### 5.2.5 Transgenic mice

SAD A/B knockout mice were kept in a C57/Black6 genetic background (C57BL/6NCrIMpi, animal house, Max-Planck-Institute of Neurobiology). Mice were separated from their parents at the age of about three weeks, males and females were housed separately. Tail biopsies were taken from mice at the age of approximately 4 weeks when mice were ear tagged using four-digit number ear tags from Hauptner & Herberholz. For all experiments, males heterozygous for both SAD A and SAD B were crossed with females heterozygous for SAD A and homo- or heterozygous for SAD B. For analysis, mice of one litter were compared. Breedings were usually set up with a male to female ratio of 1:2, 2:2 or 3:3, depending on the availability of litter mate males. Because of the reduced fertility of SAD A/B knockout mice it was necessary to keep males and females together for two days. Embryos were taken 18 days after setting up the breeding, i.e. at E16.5 or E17.5.

### 5.2.6 Data analysis

For all data sets, the arithmetic average  $\bar{x}$ , the standard deviation  $s$  and the standard error of the mean SEM were calculated. Computations were performed using Microsoft Excel.

$$\text{arithmetic average: } \bar{x} = \frac{1}{n} \sum_{i=1}^n x_i; \quad \text{standard deviation: } s = \sqrt{\frac{\sum_{i=1}^n (x_i - \bar{x})^2}{n-1}}; \quad \text{standard error of the mean: } SEM = \frac{s}{\sqrt{n}}$$

Error bars depict the SEM. The significance of the data was analyzed using suitable statistical tests: Student's T-tests (paired or unpaired), analysis of variance (ANOVA), Hampel outlier test or Chi-square test. Data were considered significant with  $p < 0.05$  and highly significant with  $p < 0.01$ .

## 6. References

- Adler, C.E., R.D. Fetter, and C.I. Bargmann. 2006. UNC-6/Netrin induces neuronal asymmetry and defines the site of axon formation. *Nat Neurosci.* 9:511-8.
- Akhmanova, A., and C.C. Hoogenraad. 2005. Microtubule plus-end-tracking proteins: mechanisms and functions. *Curr Opin Cell Biol.* 17:47-54.
- Akhmanova, A., C.C. Hoogenraad, K. Drabek, T. Stepanova, B. Dortland, T. Verkerk, W. Vermeulen, B.M. Burgering, C.I. De Zeeuw, F. Grosveld, and N. Galjart. 2001. Clasps are CLIP-115 and -170 associating proteins involved in the regional regulation of microtubule dynamics in motile fibroblasts. *Cell.* 104:923-35.
- Akhmanova, A., and M.O. Steinmetz. 2008. Tracking the ends: a dynamic protein network controls the fate of microtubule tips. *Nat Rev Mol Cell Biol.* 9:309-22.
- Alessi, D.R., S.R. James, C.P. Downes, A.B. Holmes, P.R. Gaffney, C.B. Reese, and P. Cohen. 1997. Characterization of a 3-phosphoinositide-dependent protein kinase which phosphorylates and activates protein kinase Balpha. *Curr Biol.* 7:261-9.
- Allen, C., and G.G. Borisy. 1974. Structural polarity and directional growth of microtubules of *Chlamydomonas* flagella. *J Mol Biol.* 90:381-402.
- Amano, M., M. Ito, K. Kimura, Y. Fukata, K. Chihara, T. Nakano, Y. Matsuura, and K. Kaibuchi. 1996. Phosphorylation and activation of myosin by Rho-associated kinase (Rho-kinase). *J Biol Chem.* 271:20246-9.
- Amos, L., and A. Klug. 1974. Arrangement of subunits in flagellar microtubules. *J Cell Sci.* 14:523-49.
- Andersen, S.S., and G.Q. Bi. 2000. Axon formation: a molecular model for the generation of neuronal polarity. *Bioessays.* 22:172-9.
- Arimura, N., and K. Kaibuchi. 2007. Neuronal polarity: from extracellular signals to intracellular mechanisms. *Nat Rev Neurosci.* 8:194-205.
- Arregui, C., J. Busciglio, A. Caceres, and H.S. Barra. 1991. Tyrosinated and detyrosinated microtubules in axonal processes of cerebellar macroneurons grown in culture. *J Neurosci Res.* 28:171-81.
- Audebert, S., A. Koulakoff, Y. Berwald-Netter, F. Gros, P. Denoulet, and B. Edde. 1994. Developmental regulation of polyglutamylated alpha- and beta-tubulin in mouse brain neurons. *J Cell Sci.* 107 ( Pt 8):2313-22.
- Baas, P.W., and M.M. Black. 1990. Individual microtubules in the axon consist of domains that differ in both composition and stability. *J Cell Biol.* 111:495-509.
- Baas, P.W., M.M. Black, and G.A. Banker. 1989. Changes in microtubule polarity orientation during the development of hippocampal neurons in culture. *J Cell Biol.* 109:3085-94.
- Baas, P.W., J.S. Deitch, M.M. Black, and G.A. Banker. 1988. Polarity orientation of microtubules in hippocampal neurons: uniformity in the axon and nonuniformity in the dendrite. *Proc Natl Acad Sci U S A.* 85:8335-9.
- Banker, G.A., and W.M. Cowan. 1977. Rat hippocampal neurons in dispersed cell culture. *Brain Res.* 126:397-42.

- Barnes, A.P., B.N. Lilley, Y.A. Pan, L.J. Plummer, A.W. Powell, A.N. Raines, J.R. Sanes, and F. Polleux. 2007. LKB1 and SAD kinases define a pathway required for the polarization of cortical neurons. *Cell*. 129:549-63.
- Bartlett, W.P., and G.A. Banker. 1984a. An electron microscopic study of the development of axons and dendrites by hippocampal neurons in culture. I. Cells which develop without intercellular contacts. *J Neurosci*. 4:1944-53.
- Bartlett, W.P., and G.A. Banker. 1984b. An electron microscopic study of the development of axons and dendrites by hippocampal neurons in culture. II. Synaptic relationships. *J Neurosci*. 4:1954-65.
- Basu, R., and F. Chang. 2007. Shaping the actin cytoskeleton using microtubule tips. *Curr Opin Cell Biol*. 19:88-94.
- Bear, M.F., B.W. Connors, and M.A. Paradiso. 2007. Neuroscience - Exploring the Brain. Lippincott Williams & Wilkins, Baltimore / Philadelphia.
- Bennett, M.V., and R.S. Zukin. 2004. Electrical coupling and neuronal synchronization in the Mammalian brain. *Neuron*. 41:495-511.
- Benson, D.L., F.H. Watkins, O. Steward, and G. Banker. 1994. Characterization of GABAergic neurons in hippocampal cell cultures. *J Neurocytol*. 23:279-95.
- Biernat, J., Y.Z. Wu, T. Timm, Q. Zheng-Fischhofer, E. Mandelkow, L. Meijer, and E.M. Mandelkow. 2002. Protein kinase MARK/PAR-1 is required for neurite outgrowth and establishment of neuronal polarity. *Mol Biol Cell*. 13:4013-28.
- Bjorkblom, B., N. Ostman, V. Hongisto, V. Komarovski, J.J. Filen, T.A. Nyman, T. Kallunki, M.J. Courtney, and E.T. Coffey. 2005. Constitutively active cytoplasmic c-Jun N-terminal kinase 1 is a dominant regulator of dendritic architecture: role of microtubule-associated protein 2 as an effector. *J Neurosci*. 25:6350-61.
- Blangy, A., E. Vignal, S. Schmidt, A. Debant, C. Gauthier-Rouviere, and P. Fort. 2000. TrioGEF1 controls Rac- and Cdc42-dependent cell structures through the direct activation of rhoG. *J Cell Sci*. 113 ( Pt 4):729-39.
- Bogoyevitch, M.A., and B. Kobe. 2006. Uses for JNK: the many and varied substrates of the c-Jun N-terminal kinases. *Microbiol Mol Biol Rev*. 70:1061-95.
- Bonnet, C., D. Boucher, S. Lazereg, B. Pedrotti, K. Islam, P. Denoulet, and J.C. Larcher. 2001. Differential binding regulation of microtubule-associated proteins MAP1A, MAP1B, and MAP2 by tubulin polyglutamylation. *J Biol Chem*. 276:12839-48.
- Bornshein, M.B., and P.G. Model. 1972. Development of synapses and myelin in cultures of dissociated embryonic mouse spinal cord, medulla and cerebrum. *Brain Res*. 37:287-93.
- Boucher, D., J.C. Larcher, F. Gros, and P. Denoulet. 1994. Polyglutamylation of tubulin as a progressive regulator of in vitro interactions between the microtubule-associated protein Tau and tubulin. *Biochemistry*. 33:12471-7.
- Bradke, F., and C.G. Dotti. 1997. Neuronal polarity: vectorial cytoplasmic flow precedes axon formation. *Neuron*. 19:1175-86.
- Bradke, F., and C.G. Dotti. 1999. The role of local actin instability in axon formation. *Science*. 283:1931-4.
- Bradke, F., and C.G. Dotti. 2000a. Differentiated neurons retain the capacity to generate axons from dendrites. *Curr Biol*. 10:1467-70.

- Bradke, F., and C.G. Dotti. 2000b. Establishment of neuronal polarity: lessons from cultured hippocampal neurons. *Curr Opin Neurobiol.* 10:574-81.
- Buck, K.B., and J.Q. Zheng. 2002. Growth cone turning induced by direct local modification of microtubule dynamics. *J Neurosci.* 22:9358-67.
- Caceres, A., and K.S. Kosik. 1990. Inhibition of neurite polarity by tau antisense oligonucleotides in primary cerebellar neurons. *Nature.* 343:461-3.
- Caceres, A., J. Mautino, and K.S. Kosik. 1992. Suppression of MAP2 in cultured cerebellar macroneurons inhibits minor neurite formation. *Neuron.* 9:607-18.
- Caceres, A., S. Potrebic, and K.S. Kosik. 1991. The effect of tau antisense oligonucleotides on neurite formation of cultured cerebellar macroneurons. *J Neurosci.* 11:1515-23.
- Cantley, L.C. 2002. The phosphoinositide 3-kinase pathway. *Science.* 296:1655-7.
- Cassimeris, L., and C. Spittle. 2001. Regulation of microtubule-associated proteins. *Int Rev Cytol.* 210:163-226.
- Catterall, W.A. 2000. From ionic currents to molecular mechanisms: the structure and function of voltage-gated sodium channels. *Neuron.* 26:13-25.
- Cau, J., S. Faure, M. Comps, C. Delsert, and N. Morin. 2001. A novel p21-activated kinase binds the actin and microtubule networks and induces microtubule stabilization. *J Cell Biol.* 155:1029-42.
- Chang, L., Y. Jones, M.H. Ellisman, L.S. Goldstein, and M. Karin. 2003. JNK1 is required for maintenance of neuronal microtubules and controls phosphorylation of microtubule-associated proteins. *Dev Cell.* 4:521-33.
- Chapin, S.J., and J.C. Bulinski. 1992. Microtubule stabilization by assembly-promoting microtubule-associated proteins: a repeat performance. *Cell Motil Cytoskeleton.* 23:236-43.
- Ciani, L., O. Krylova, M.J. Smalley, T.C. Dale, and P.C. Salinas. 2004. A divergent canonical WNT-signaling pathway regulates microtubule dynamics: dishevelled signals locally to stabilize microtubules. *J Cell Biol.* 164:243-53.
- Ciani, L., and P.C. Salinas. 2007. c-Jun N-terminal kinase (JNK) cooperates with Gsk3beta to regulate Dishevelled-mediated microtubule stability. *BMC Cell Biol.* 8:27.
- Craig, A.M., and G. Banker. 1994. Neuronal polarity. *Annu Rev Neurosci.* 17:267-310.
- Cross, D.A., D.R. Alessi, P. Cohen, M. Andjelkovich, and B.A. Hemmings. 1995. Inhibition of glycogen synthase kinase-3 by insulin mediated by protein kinase B. *Nature.* 378:785-9.
- Crump, J.G., M. Zhen, Y. Jin, and C.I. Bargmann. 2001. The SAD-1 kinase regulates presynaptic vesicle clustering and axon termination. *Neuron.* 29:115-29.
- da Silva, J.S., and C.G. Dotti. 2002. Breaking the neuronal sphere: regulation of the actin cytoskeleton in neuritogenesis. *Nat Rev Neurosci.* 3:694-704.
- Da Silva, J.S., T. Hasegawa, T. Miyagi, C.G. Dotti, and J. Abad-Rodriguez. 2005. Asymmetric membrane ganglioside sialidase activity specifies axonal fate. *Nat Neurosci.* 8:606-15.
- Da Silva, J.S., M. Medina, C. Zuliani, A. Di Nardo, W. Witke, and C.G. Dotti. 2003. RhoA/ROCK regulation of neuritogenesis via profilin Ila-mediated control of actin stability. *J Cell Biol.* 162:1267-79.

- Dan, C., N. Nath, M. Liberto, and A. Minden. 2002. PAK5, a new brain-specific kinase, promotes neurite outgrowth in N1E-115 cells. *Mol Cell Biol.* 22:567-77.
- Daniels, M.P. 1972. Colchicine inhibition of nerve fiber formation in vitro. *J Cell Biol.* 53:164-76.
- de Anda, F.C., G. Pollarolo, J.S. Da Silva, P.G. Camoletto, F. Feiguin, and C.G. Dotti. 2005. Centrosome localization determines neuronal polarity. *Nature.* 436:704-8.
- de Hoop, M.J., L. Meyn, and C.G. Dotti. 1997. Culturing hippocampal neurons and astrocytes from fetal rodent brain. *In Cell Biology: A Laboratory Handbook.* J.E. Celis, editor. Academic Press, San Diego, CA. 154-163.
- Dehmelt, L., F.M. Smart, R.S. Ozer, and S. Halpain. 2003. The role of microtubule-associated protein 2c in the reorganization of microtubules and lamellipodia during neurite initiation. *J Neurosci.* 23:9479-90.
- Del Rio, J.A., C. Gonzalez-Billault, J.M. Urena, E.M. Jimenez, M.J. Barallobre, M. Pascual, L. Pujadas, S. Simo, A. La Torre, F. Wandosell, J. Avila, and E. Soriano. 2004. MAP1B is required for Netrin 1 signaling in neuronal migration and axonal guidance. *Curr Biol.* 14:840-50.
- Delorme, V., M. Machacek, C. DerMardirossian, K.L. Anderson, T. Wittmann, D. Hanein, C. Waterman-Storer, G. Danuser, and G.M. Bokoch. 2007. Cofilin activity downstream of Pak1 regulates cell protrusion efficiency by organizing lamellipodium and lamella actin networks. *Dev Cell.* 13:646-62.
- Derry, W.B., L. Wilson, and M.A. Jordan. 1995. Substoichiometric binding of taxol suppresses microtubule dynamics. *Biochemistry.* 34:2203-11.
- Desai, A., and T.J. Mitchison. 1997. Microtubule polymerization dynamics. *Annu Rev Cell Dev Biol.* 13:83-117.
- Doble, B.W., and J.R. Woodgett. 2003. GSK-3: tricks of the trade for a multi-tasking kinase. *J Cell Sci.* 116:1175-86.
- Dotti, C.G., and G. Banker. 1991. Intracellular organization of hippocampal neurons during the development of neuronal polarity. *J Cell Sci Suppl.* 15:75-84.
- Dotti, C.G., C.A. Sullivan, and G.A. Banker. 1988. The establishment of polarity by hippocampal neurons in culture. *J Neurosci.* 8:1454-68.
- Drechsel, D.N., A.A. Hyman, M.H. Cobb, and M.W. Kirschner. 1992. Modulation of the dynamic instability of tubulin assembly by the microtubule-associated protein tau. *Mol Biol Cell.* 3:1141-54.
- Drewes, G., A. Ebner, and E.M. Mandelkow. 1998. MAPs, MARKs and microtubule dynamics. *Trends Biochem Sci.* 23:307-11.
- Edson, K., B. Weisshaar, and A. Matus. 1993. Actin depolymerisation induces process formation on MAP2-transfected non-neuronal cells. *Development.* 117:689-700.
- Efimov, A., A. Kharitonov, N. Efimova, J. Loncarek, P.M. Miller, N. Andreyeva, P. Gleeson, N. Galjart, A.R. Maia, I.X. McLeod, J.R. Yates, 3rd, H. Maiato, A. Khodjakov, A. Akhmanova, and I. Kaverina. 2007. Asymmetric CLASP-Dependent Nucleation of Noncentrosomal Microtubules at the trans-Golgi Network. *Dev Cell.* 12:917-30.
- Eickholt, B.J., F.S. Walsh, and P. Doherty. 2002. An inactive pool of GSK-3 at the leading edge of growth cones is implicated in Semaphorin 3A signaling. *J Cell Biol.* 157:211-7.

- Erck, C., L. Peris, A. Andrieux, C. Meissirel, A.D. Gruber, M. Vernet, A. Schweitzer, Y. Saoudi, H. Pointu, C. Bosc, P.A. Salin, D. Job, and J. Wehland. 2005. A vital role of tubulin-tyrosinase for neuronal organization. *Proc Natl Acad Sci U S A*. 102:7853-8.
- Ertürk, A., F. Hellal, J. Enes, and F. Bradke. 2007. Disorganized microtubules underlie the formation of retraction bulbs and the failure of axonal regeneration. *J Neurosci*. 27:9169-80.
- Esch, T., V. Lemmon, and G. Banker. 1999. Local presentation of substrate molecules directs axon specification by cultured hippocampal neurons. *J Neurosci*. 19:6417-26.
- Etienne-Manneville, S., and A. Hall. 2002. Rho GTPases in cell biology. *Nature*. 420:629-35.
- Etienne-Manneville, S., and A. Hall. 2003. Cdc42 regulates GSK-3beta and adenomatous polyposis coli to control cell polarity. *Nature*. 421:753-6.
- Evans, L., T. Mitchison, and M. Kirschner. 1985. Influence of the centrosome on the structure of nucleated microtubules. *J Cell Biol*. 100:1185-91.
- Fiol, C.J., A.M. Mahrenholz, Y. Wang, R.W. Roeske, and P.J. Roach. 1987. Formation of protein kinase recognition sites by covalent modification of the substrate. Molecular mechanism for the synergistic action of casein kinase II and glycogen synthase kinase 3. *J Biol Chem*. 262:14042-8.
- Forscher, P., and S.J. Smith. 1988. Actions of cytochalasins on the organization of actin filaments and microtubules in a neuronal growth cone. *J Cell Biol*. 107:1505-16.
- Fukata, Y., T.J. Itoh, T. Kimura, C. Menager, T. Nishimura, T. Shiromizu, H. Watanabe, N. Inagaki, A. Iwamatsu, H. Hotani, and K. Kaibuchi. 2002. CRMP-2 binds to tubulin heterodimers to promote microtubule assembly. *Nat Cell Biol*. 4:583-91.
- Gao, Y., E. Nikulina, W. Mellado, and M.T. Filbin. 2003. Neurotrophins elevate cAMP to reach a threshold required to overcome inhibition by MAG through extracellular signal-regulated kinase-dependent inhibition of phosphodiesterase. *J Neurosci*. 23:11770-7.
- Garvalov, B.K., K.C. Flynn, D. Neukirchen, L. Meyn, N. Teusch, X. Wu, C. Brakebusch, J.R. Bamberg, and F. Bradke. 2007. Cdc42 regulates cofilin during the establishment of neuronal polarity. *J Neurosci*. 27:13117-29.
- Gauthier-Rouviere, C., E. Vignal, M. Meriane, P. Roux, P. Montcourier, and P. Fort. 1998. RhoG GTPase controls a pathway that independently activates Rac1 and Cdc42Hs. *Mol Biol Cell*. 9:1379-94.
- Goldschmidt-Clermont, P.J., M.I. Furman, D. Wachsstock, D. Safer, V.T. Nachmias, and T.D. Pollard. 1992. The control of actin nucleotide exchange by thymosin beta 4 and profilin. A potential regulatory mechanism for actin polymerization in cells. *Mol Biol Cell*. 3:1015-24.
- Goldstein, L.S., and Z. Yang. 2000. Microtubule-based transport systems in neurons: the roles of kinesins and dyneins. *Annu Rev Neurosci*. 23:39-71.
- Goold, R.G., and P.R. Gordon-Weeks. 2005. The MAP kinase pathway is upstream of the activation of GSK3beta that enables it to phosphorylate MAP1B and contributes to the stimulation of axon growth. *Mol Cell Neurosci*. 28:524-34.
- Goold, R.G., R. Owen, and P.R. Gordon-Weeks. 1999. Glycogen synthase kinase 3beta phosphorylation of microtubule-associated protein 1B regulates the stability of microtubules in growth cones. *J Cell Sci*. 112 ( Pt 19):3373-84.
- Goslin, K., and G. Banker. 1989. Experimental observations on the development of polarity by hippocampal neurons in culture. *J Cell Biol*. 108:1507-16.

- Goslin, K., and G. Banker. 1991. Rat hippocampal neurons in low-density culture. *In* *Culturing Nerve Cells*. G. Banker and K. Goslin, editors. MA: MIT Press, Cambridge. 251-281.
- Govek, E.E., S.E. Newey, and L. Van Aelst. 2005. The role of the Rho GTPases in neuronal development. *Genes Dev.* 19:1-49.
- Grimes, C.A., and R.S. Jope. 2001. The multifaceted roles of glycogen synthase kinase 3beta in cellular signaling. *Prog Neurobiol.* 65:391-426.
- Gu, C., Y.N. Jan, and L.Y. Jan. 2003. A conserved domain in axonal targeting of Kv1 (Shaker) voltage-gated potassium channels. *Science.* 301:646-9.
- Gustke, N., B. Trinczek, J. Biernat, E.M. Mandelkow, and E. Mandelkow. 1994. Domains of tau protein and interactions with microtubules. *Biochemistry.* 33:9511-22.
- Hamann, M.J., C.M. Lubking, D.N. Luchini, and D.D. Billadeau. 2007. Asef2 functions as a Cdc42 exchange factor and is stimulated by the release of an autoinhibitory module from a concealed C-terminal activation element. *Mol Cell Biol.* 27:1380-93.
- Hanahan, D. 1983. Studies on transformation of *Escherichia coli* with plasmids. *J Mol Biol.* 166:557-80.
- Harry, G.J., M. Billingsley, A. Bruinink, I.L. Campbell, W. Classen, D.C. Dorman, C. Galli, D. Ray, R.A. Smith, and H.A. Tilson. 1998. In vitro techniques for the assessment of neurotoxicity. *Environ Health Perspect.* 106 Suppl 1:131-58.
- Heim, N., O. Garaschuk, M.W. Friedrich, M. Mank, R.I. Milos, Y. Kovalchuk, A. Konnerth, and O. Griesbeck. 2007. Improved calcium imaging in transgenic mice expressing a troponin C-based biosensor. *Nat Methods.* 4:127-9.
- Heo, K., S.H. Ha, Y.C. Chae, S. Lee, Y.S. Oh, Y.H. Kim, S.H. Kim, J.H. Kim, A. Mizoguchi, T.J. Itoh, H.M. Kwon, S.H. Ryu, and P.G. Suh. 2006. RGS2 promotes formation of neurites by stimulating microtubule polymerization. *Cell Signal.* 18:2182-92.
- Hilliard, M.A., and C.I. Bargmann. 2006. Wnt signals and frizzled activity orient anterior-posterior axon outgrowth in *C. elegans*. *Dev Cell.* 10:379-90.
- Hoebeke, J., G. Van Nijen, and M. De Brabander. 1976. Interaction of oncodazole (R 17934), a new antitumoral drug, with rat brain tubulin. *Biochem Biophys Res Commun.* 69:319-24.
- Horiguchi, K., T. Hanada, Y. Fukui, and A.H. Chishti. 2006. Transport of PIP3 by GAKIN, a kinesin-3 family protein, regulates neuronal cell polarity. *J Cell Biol.* 174:425-36.
- Huang, E.J., and L.F. Reichardt. 2003. Trk receptors: roles in neuronal signal transduction. *Annu Rev Biochem.* 72:609-42.
- Hüttelmaier, S., D. Zenklusen, M. Lederer, J. Dichtenberg, M. Lorenz, X. Meng, G.J. Bassell, J. Condeelis, and R.H. Singer. 2005. Spatial regulation of beta-actin translation by Src-dependent phosphorylation of ZBP1. *Nature.* 438:512-5.
- Hyman, A.A., S. Salsler, D.N. Drechsel, N. Unwin, and T.J. Mitchison. 1992. Role of GTP hydrolysis in microtubule dynamics: information from a slowly hydrolyzable analogue, GMPCPP. *Mol Biol Cell.* 3:1155-67.
- Ikawa, M., S. Yamada, T. Nakanishi, and M. Okabe. 1998. 'Green mice' and their potential usage in biological research. *FEBS Lett.* 430:83-7.
- Ikegami, K., R.L. Heier, M. Taruishi, H. Takagi, M. Mukai, S. Shimma, S. Taira, K. Hatanaka, N. Morone, I. Yao, P.K. Campbell, S. Yuasa, C. Janke, G.R. Macgregor, and M. Setou. 2007.

- Loss of alpha-tubulin polyglutamylation in ROSA22 mice is associated with abnormal targeting of KIF1A and modulated synaptic function. *Proc Natl Acad Sci U S A*. 104:3213-8.
- Inagaki, N., K. Chihara, N. Arimura, C. Menager, Y. Kawano, N. Matsuo, T. Nishimura, M. Amano, and K. Kaibuchi. 2001. CRMP-2 induces axons in cultured hippocampal neurons. *Nat Neurosci*. 4:781-2.
- Jacobson, C., B. Schnapp, and G.A. Banker. 2006. A change in the selective translocation of the Kinesin-1 motor domain marks the initial specification of the axon. *Neuron*. 49:797-804.
- Jareb, M., and G. Banker. 1997. Inhibition of axonal growth by brefeldin A in hippocampal neurons in culture. *J Neurosci*. 17:8955-63.
- Jiang, H., W. Guo, X. Liang, and Y. Rao. 2005. Both the establishment and the maintenance of neuronal polarity require active mechanisms: critical roles of GSK-3beta and its upstream regulators. *Cell*. 120:123-35.
- Jimbo, T., Y. Kawasaki, R. Koyama, R. Sato, S. Takada, K. Haraguchi, and T. Akiyama. 2002. Identification of a link between the tumour suppressor APC and the kinesin superfamily. *Nat Cell Biol*. 4:323-7.
- Joshi, H.C., D. Chu, R.E. Buxbaum, and S.R. Heidemann. 1985. Tension and compression in the cytoskeleton of PC 12 neurites. *J Cell Biol*. 101:697-705.
- Just, I., J. Selzer, M. Wilm, C. von Eichel-Streiber, M. Mann, and K. Aktories. 1995. Glucosylation of Rho proteins by *Clostridium difficile* toxin B. *Nature*. 375:500-3.
- Kaech, S., and G. Banker. 2006. Culturing hippocampal neurons. *Nat Protoc*. 1:2406-15.
- Kanai, Y., J. Chen, and N. Hirokawa. 1992. Microtubule bundling by tau proteins in vivo: analysis of functional domains. *Embo J*. 11:3953-61.
- Kang, F., D.L. Purich, and F.S. Southwick. 1999. Profilin promotes barbed-end actin filament assembly without lowering the critical concentration. *J Biol Chem*. 274:36963-72.
- Kawano, Y., T. Yoshimura, D. Tsuboi, S. Kawabata, T. Kaneko-Kawano, H. Shirataki, T. Takenawa, and K. Kaibuchi. 2005. CRMP-2 is involved in kinesin-1-dependent transport of the Sra-1/WAVE1 complex and axon formation. *Mol Cell Biol*. 25:9920-35.
- Keely, P.J., J.K. Westwick, I.P. Whitehead, C.J. Der, and L.V. Parise. 1997. Cdc42 and Rac1 induce integrin-mediated cell motility and invasiveness through PI(3)K. *Nature*. 390:632-6.
- Khawaja, S., G.G. Gundersen, and J.C. Bulinski. 1988. Enhanced stability of microtubules enriched in deetyrosinated tubulin is not a direct function of deetyrosination level. *J Cell Biol*. 106:141-9.
- Kim, W.Y., F.Q. Zhou, J. Zhou, Y. Yokota, Y.M. Wang, T. Yoshimura, K. Kaibuchi, J.R. Woodgett, E.S. Anton, and W.D. Snider. 2006. Essential roles for GSK-3s and GSK-3-primed substrates in neurotrophin-induced and hippocampal axon growth. *Neuron*. 52:981-96.
- Kimura, K., M. Ito, M. Amano, K. Chihara, Y. Fukata, M. Nakafuku, B. Yamamori, J. Feng, T. Nakano, K. Okawa, A. Iwamatsu, and K. Kaibuchi. 1996. Regulation of myosin phosphatase by Rho and Rho-associated kinase (Rho-kinase). *Science*. 273:245-8.
- Kimura, T., H. Watanabe, A. Iwamatsu, and K. Kaibuchi. 2005. Tubulin and CRMP-2 complex is transported via Kinesin-1. *J Neurochem*. 93:1371-82.
- Kishi, M., Y.A. Pan, J.G. Crump, and J.R. Sanes. 2005. Mammalian SAD kinases are required for neuronal polarization. *Science*. 307:929-32.

- Kole, T.P., Y. Tseng, I. Jiang, J.L. Katz, and D. Wirtz. 2005. Intracellular mechanics of migrating fibroblasts. *Mol Biol Cell*. 16:328-38.
- Kowalski, R.J., and R.C. Williams, Jr. 1993. Microtubule-associated protein 2 alters the dynamic properties of microtubule assembly and disassembly. *J Biol Chem*. 268:9847-55.
- Kozak, L.P. 1977. The transition from embryonic to adult isozyme expression in reaggregating cell cultures of mouse brain. *Dev Biol*. 55:160-9.
- Kozma, R., S. Sarnar, S. Ahmed, and L. Lim. 1997. Rho family GTPases and neuronal growth cone remodelling: relationship between increased complexity induced by Cdc42Hs, Rac1, and acetylcholine and collapse induced by RhoA and lysophosphatidic acid. *Mol Cell Biol*. 17:1201-11.
- Krendel, M., and M.S. Mooseker. 2005. Myosins: tails (and heads) of functional diversity. *Physiology (Bethesda)*. 20:239-51.
- Krens, S.F., H.P. Spaank, and B.E. Snaar-Jagalska. 2006. Functions of the MAPK family in vertebrate development. *FEBS Lett*. 580:4984-90.
- Krylova, O., M.J. Messenger, and P.C. Salinas. 2000. Dishevelled-1 regulates microtubule stability: a new function mediated by glycogen synthase kinase-3beta. *J Cell Biol*. 151:83-94.
- Kunda, P., G. Paglini, S. Quiroga, K. Kosik, and A. Caceres. 2001. Evidence for the Involvement of Tiam1 in Axon Formation. *J. Neurosci*. 21:2361-2372.
- Lawlor, M.A., and D.R. Alessi. 2001. PKB/Akt: a key mediator of cell proliferation, survival and insulin responses? *J Cell Sci*. 114:2903-10.
- Leung, T., X.Q. Chen, E. Manser, and L. Lim. 1996. The p160 RhoA-binding kinase ROK alpha is a member of a kinase family and is involved in the reorganization of the cytoskeleton. *Mol Cell Biol*. 16:5313-27.
- Li, X., E. Saint-Cyr-Proulx, K. Aktories, and N. Lamarche-Vane. 2002. Rac1 and Cdc42 but not RhoA or Rho kinase activities are required for neurite outgrowth induced by the Netrin-1 receptor DCC (deleted in colorectal cancer) in N1E-115 neuroblastoma cells. *J Biol Chem*. 277:15207-14.
- Liao, G., and G.G. Gundersen. 1998. Kinesin is a candidate for cross-bridging microtubules and intermediate filaments. Selective binding of kinesin to detyrosinated tubulin and vimentin. *J Biol Chem*. 273:9797-803.
- Liao, G., T. Nagasaki, and G.G. Gundersen. 1995. Low concentrations of nocodazole interfere with fibroblast locomotion without significantly affecting microtubule level: implications for the role of dynamic microtubules in cell locomotion. *J Cell Sci*. 108 ( Pt 11):3473-83.
- Lin, C.H., E.M. Espreafico, M.S. Mooseker, and P. Forscher. 1996. Myosin drives retrograde F-actin flow in neuronal growth cones. *Neuron*. 16:769-82.
- Lin, S.X., G.G. Gundersen, and F.R. Maxfield. 2002. Export from pericentriolar endocytic recycling compartment to cell surface depends on stable, detyrosinated (glu) microtubules and kinesin. *Mol Biol Cell*. 13:96-109.
- Logan, C.Y., and R. Nusse. 2004. The Wnt signaling pathway in development and disease. *Annu Rev Cell Dev Biol*. 20:781-810.
- Lucas, F.R., R.G. Goold, P.R. Gordon-Weeks, and P.C. Salinas. 1998. Inhibition of GSK-3beta leading to the loss of phosphorylated MAP-1B is an early event in axonal remodelling induced by WNT-7a or lithium. *J Cell Sci*. 111 ( Pt 10):1351-61.

- Mains, R.E., and P.H. Patterson. 1973. Primary cultures of dissociated sympathetic neurons. III. Changes in metabolism with age in culture. *J Cell Biol.* 59:361-6.
- Mandelkow, E.M., R. Schultheiss, R. Rapp, M. Muller, and E. Mandelkow. 1986. On the surface lattice of microtubules: helix starts, protofilament number, seam, and handedness. *J Cell Biol.* 102:1067-73.
- Masson, D., and T.E. Kreis. 1993. Identification and molecular characterization of E-MAP-115, a novel microtubule-associated protein predominantly expressed in epithelial cells. *J Cell Biol.* 123:357-71.
- Matenia, D., B. Grieshaber, X.Y. Li, A. Thiessen, C. Johne, J. Jiao, E. Mandelkow, and E.M. Mandelkow. 2005. PAK5 kinase is an inhibitor of MARK/Par-1, which leads to stable microtubules and dynamic actin. *Mol Biol Cell.* 16:4410-22.
- Meijer, L., M. Flajolet, and P. Greengard. 2004. Pharmacological inhibitors of glycogen synthase kinase 3. *Trends Pharmacol Sci.* 25:471-80.
- Menager, C., N. Arimura, Y. Fukata, and K. Kaibuchi. 2004. PIP3 is involved in neuronal polarization and axon formation. *J Neurochem.* 89:109-18.
- Meyer, D., A. Liu, and B. Margolis. 1999. Interaction of c-Jun amino-terminal kinase interacting protein-1 with p190 rhoGEF and its localization in differentiated neurons. *J Biol Chem.* 274:35113-8.
- Mimori-Kiyosue, Y., N. Shiina, and S. Tsukita. 2000. Adenomatous polyposis coli (APC) protein moves along microtubules and concentrates at their growing ends in epithelial cells. *J Cell Biol.* 148:505-18.
- Mitchison, T., and M. Kirschner. 1984. Dynamic instability of microtubule growth. *Nature.* 312:237-42.
- Mitsui, N., R. Inatome, S. Takahashi, Y. Goshima, H. Yamamura, and S. Yanagi. 2002. Involvement of Fes/Fps tyrosine kinase in semaphorin3A signaling. *Embo J.* 21:3274-85.
- Morfini, G., M.C. DiTella, F. Feiguin, N. Carri, and A. Caceres. 1994. Neurotrophin-3 enhances neurite outgrowth in cultured hippocampal pyramidal neurons. *J Neurosci Res.* 39:219-32.
- Morii, H., Y. Shiraishi-Yamaguchi, and N. Mori. 2006. SCG10, a microtubule destabilizing factor, stimulates the neurite outgrowth by modulating microtubule dynamics in rat hippocampal primary cultured neurons. *J Neurobiol.* 66:1101-14.
- Murthy, A.S., and M. Flavin. 1983. Microtubule assembly using the microtubule-associated protein MAP-2 prepared in defined states of phosphorylation with protein kinase and phosphatase. *Eur J Biochem.* 137:37-46.
- Nakada, C., K. Ritchie, Y. Oba, M. Nakamura, Y. Hotta, R. Iino, R.S. Kasai, K. Yamaguchi, T. Fujiwara, and A. Kusumi. 2003. Accumulation of anchored proteins forms membrane diffusion barriers during neuronal polarization. *Nat Cell Biol.* 5:626-32.
- Nakagawa, H., K. Koyama, Y. Murata, M. Morito, T. Akiyama, and Y. Nakamura. 2000. EB3, a novel member of the EB1 family preferentially expressed in the central nervous system, binds to a CNS-specific APC homologue. *Oncogene.* 19:210-6.
- Nakata, T., and N. Hirokawa. 2003. Microtubules provide directional cues for polarized axonal transport through interaction with kinesin motor head. *J Cell Biol.* 162:1045-55.
- Nishimura, T., T. Yamaguchi, K. Kato, M. Yoshizawa, Y. Nabeshima, S. Ohno, M. Hoshino, and K. Kaibuchi. 2005. PAR-6-PAR-3 mediates Cdc42-induced Rac activation through the Rac GEFs STEF/Tiam1. *Nat Cell Biol.* 7:270-7.

- Niwa, H., K. Yamamura, and J. Miyazaki. 1991. Efficient selection for high-expression transfectants with a novel eukaryotic vector. *Gene*. 108:193-9.
- Nobes, C.D., and A. Hall. 1995. Rho, rac, and cdc42 GTPases regulate the assembly of multimolecular focal complexes associated with actin stress fibers, lamellipodia, and filopodia. *Cell*. 81:53-62.
- Oinuma, I., H. Katoh, and M. Negishi. 2007. R-Ras controls axon specification upstream of glycogen synthase kinase-3beta through integrin-linked kinase. *J Biol Chem*. 282:303-18.
- Okabe, M., M. Ikawa, K. Kominami, T. Nakanishi, and Y. Nishimune. 1997. 'Green mice' as a source of ubiquitous green cells. *FEBS Lett*. 407:313-9.
- Oliva, A.A., Jr., C.M. Atkins, L. Copenagle, and G.A. Banker. 2006. Activated c-Jun N-terminal kinase is required for axon formation. *J Neurosci*. 26:9462-70.
- Onishi, K., M. Higuchi, T. Asakura, N. Masuyama, and Y. Gotoh. 2007. The PI3K-Akt pathway promotes microtubule stabilization in migrating fibroblasts. *Genes Cells*. 12:535-46.
- Ossipova, O., N. Bardeesy, R.A. DePinho, and J.B. Green. 2003. LKB1 (XEEK1) regulates Wnt signalling in vertebrate development. *Nat Cell Biol*. 5:889-94.
- Palazzo, A.F., T.A. Cook, A.S. Alberts, and G.G. Gundersen. 2001a. mDia mediates Rho-regulated formation and orientation of stable microtubules. *Nat Cell Biol*. 3:723-9.
- Palazzo, A.F., H.L. Joseph, Y.J. Chen, D.L. Dujardin, A.S. Alberts, K.K. Pfister, R.B. Vallee, and G.G. Gundersen. 2001b. Cdc42, dynein, and dynactin regulate MTOC reorientation independent of Rho-regulated microtubule stabilization. *Curr Biol*. 11:1536-41.
- Piehl, M., and L. Cassimeris. 2003. Organization and dynamics of growing microtubule plus ends during early mitosis. *Mol Biol Cell*. 14:916-25.
- Pollard, T.D., and G.G. Borisy. 2003. Cellular motility driven by assembly and disassembly of actin filaments. *Cell*. 112:453-65.
- Polleux, F., R.J. Giger, D.D. Ginty, A.L. Kolodkin, and A. Ghosh. 1998. Patterning of cortical efferent projections by semaphorin-neuropilin interactions. *Science*. 282:1904-6.
- Prasad, B.C., and S.G. Clark. 2006. Wnt signaling establishes anteroposterior neuronal polarity and requires retromer in *C. elegans*. *Development*. 133:1757-66.
- Preuss, U., J. Biernat, E.M. Mandelkow, and E. Mandelkow. 1997. The 'jaws' model of tau-microtubule interaction examined in CHO cells. *J Cell Sci*. 110 ( Pt 6):789-800.
- Rakic, P., E. Knyihar-Csillik, and B. Csillik. 1996. Polarity of microtubule assemblies during neuronal cell migration. *Proc Natl Acad Sci U S A*. 93:9218-22.
- Raynaud-Messina, B., and A. Merdes. 2007. Gamma-tubulin complexes and microtubule organization. *Curr Opin Cell Biol*. 19:24-30.
- Reed, N.A., D. Cai, T.L. Blasius, G.T. Jih, E. Meyhofer, J. Gaertig, and K.J. Verhey. 2006. Microtubule acetylation promotes kinesin-1 binding and transport. *Curr Biol*. 16:2166-72.
- Reichardt, L.F. 2006. Neurotrophin-regulated signalling pathways. *Philos Trans R Soc Lond B Biol Sci*. 361:1545-64.
- Reynolds, C.H., J.C. Betts, W.P. Blackstock, A.R. Nebreda, and B.H. Anderton. 2000. Phosphorylation sites on tau identified by nanoelectrospray mass spectrometry: differences in vitro between the mitogen-activated protein kinases ERK2, c-Jun N-terminal kinase and P38, and glycogen synthase kinase-3beta. *J Neurochem*. 74:1587-95.

- Ricos, M.G., N. Harden, K.P. Sem, L. Lim, and W. Chia. 1999. Dcdc42 acts in TGF-beta signaling during *Drosophila* morphogenesis: distinct roles for the Drac1/JNK and Dcdc42/TGF-beta cascades in cytoskeletal regulation. *J Cell Sci.* 112 ( Pt 8):1225-35.
- Riederer, B.M., V. Pellier, B. Antonsson, G. Di Paolo, S.A. Stimpson, R. Lutjens, S. Catsicas, and G. Grenningloh. 1997. Regulation of microtubule dynamics by the neuronal growth-associated protein SCG10. *Proc Natl Acad Sci U S A.* 94:741-5.
- Riento, K., and A.J. Ridley. 2003. Rocks: multifunctional kinases in cell behaviour. *Nat Rev Mol Cell Biol.* 4:446-56.
- Rosales, C.R., K.D. Osborne, G.V. Zuccarino, P. Scheiffele, and M.A. Silverman. 2005. A cytoplasmic motif targets neuroligin-1 exclusively to dendrites of cultured hippocampal neurons. *Eur J Neurosci.* 22:2381-6.
- Rösner, H., W. Möller, T. Wassermann, J. Mihatsch, and M. Blum. 2007. Attenuation of actinomyosinII contractile activity in growth cones accelerates filopodia-guided and microtubule-based neurite elongation. *Brain Res.* 1176:1-10.
- Sampo, B., S. Kaech, S. Kunz, and G. Banker. 2003. Two distinct mechanisms target membrane proteins to the axonal surface. *Neuron.* 37:611-24.
- Saneto, R.P., and J. de Vellis. 1987. Neuronal and glial cells: cell culture of the central nervous system. *In Neurochemistry-A Practical Approach.* A.J. Turner and H.S. Bachelard, editors. IRL Press, Washington. 27-63.
- Saraste, M., and M. Hyvonen. 1995. Pleckstrin homology domains: a fact file. *Curr Opin Struct Biol.* 5:403-8.
- Schiff, P.B., J. Fant, and S.B. Horwitz. 1979. Promotion of microtubule assembly in vitro by taxol. *Nature.* 277:665-7.
- Schiff, P.B., and S.B. Horwitz. 1980. Taxol stabilizes microtubules in mouse fibroblast cells. *Proc Natl Acad Sci U S A.* 77:1561-5.
- Schwamborn, J.C., M. Muller, A.H. Becker, and A.W. Puschel. 2007. Ubiquitination of the GTPase Rap1B by the ubiquitin ligase Smurf2 is required for the establishment of neuronal polarity. *Embo J.* 26:1410-22.
- Schwamborn, J.C., and A.W. Puschel. 2004. The sequential activity of the GTPases Rap1B and Cdc42 determines neuronal polarity. *Nat Neurosci.* 7:923-9.
- Seeds, N.W., and S.C. Haffke. 1978. Cell junction and ultrastructural development of reaggregated mouse brain cultures. *Dev Neurosci.* 1:69-79.
- Segal, M. 1983. Rat hippocampal neurons in culture: responses to electrical and chemical stimuli. *J Neurophysiol.* 50:1249-64.
- Setou, M., T. Nakagawa, D.H. Seog, and N. Hirokawa. 2000. Kinesin superfamily motor protein KIF17 and mLin-10 in NMDA receptor-containing vesicle transport. *Science.* 288:1796-802.
- Shahar, A., J. de Vellis, A. Vernadakis, and B. Haber. 1989. *A Dissection and Tissue Culture Manual of the Nervous System.* Alan R. Liss, New York.
- Shelly, M., L. Cancedda, S. Heilshorn, G. Sumbre, and M.M. Poo. 2007. LKB1/STRAD promotes axon initiation during neuronal polarization. *Cell.* 129:565-77.
- Shi, S.H., T. Cheng, L.Y. Jan, and Y.N. Jan. 2004. APC and GSK-3beta are involved in mPar3 targeting to the nascent axon and establishment of neuronal polarity. *Curr Biol.* 14:2025-32.

- Shi, S.H., L.Y. Jan, and Y.N. Jan. 2003. Hippocampal neuronal polarity specified by spatially localized mPar3/mPar6 and PI 3-kinase activity. *Cell*. 112:63-75.
- Siegrist, S.E., and C.Q. Doe. 2006. Extrinsic cues orient the cell division axis in *Drosophila* embryonic neuroblasts. *Development*. 133:529-36.
- Smith, C.L. 1994. Cytoskeletal movements and substrate interactions during initiation of neurite outgrowth by sympathetic neurons in vitro. *J Neurosci*. 14:384-98.
- Sperber, B.R., S. Leight, M. Goedert, and V.M. Lee. 1995. Glycogen synthase kinase-3 beta phosphorylates tau protein at multiple sites in intact cells. *Neurosci Lett*. 197:149-53.
- Spitzer, N.C., and J.E. Lamborghini. 1976. The development of the action potential mechanism of amphibian neurons isolated in culture. *Proc Natl Acad Sci U S A*. 73:1641-5.
- Steffen, A., K. Rottner, J. Ehinger, M. Innocenti, G. Scita, J. Wehland, and T.E. Stradal. 2004. Sra-1 and Nap1 link Rac to actin assembly driving lamellipodia formation. *Embo J*.
- Stein, R., S. Orit, and D.J. Anderson. 1988. The induction of a neural-specific gene, SCG10, by nerve growth factor in PC12 cells is transcriptional, protein synthesis dependent, and glucocorticoid inhibitable. *Dev Biol*. 127:316-25.
- Stepanova, T., J. Slemmer, C.C. Hoogenraad, G. Lansbergen, B. Dortland, C.I. De Zeeuw, F. Grosveld, G. van Cappellen, A. Akhmanova, and N. Galjart. 2003. Visualization of microtubule growth in cultured neurons via the use of EB3-GFP (end-binding protein 3-green fluorescent protein). *J Neurosci*. 23:2655-64.
- Stowell, J.N., and A.M. Craig. 1999. Axon/dendrite targeting of metabotropic glutamate receptors by their cytoplasmic carboxy-terminal domains. *Neuron*. 22:525-36.
- Südhof, T.C. 2008. Neurotransmitter release. *Handb Exp Pharmacol*:1-21.
- Sumi, T., K. Matsumoto, and T. Nakamura. 2001. Specific activation of LIM kinase 2 via phosphorylation of threonine 505 by ROCK, a Rho-dependent protein kinase. *J Biol Chem*. 276:670-6.
- Suter, D.M., L.D. Errante, V. Belotserkovsky, and P. Forscher. 1998. The Ig superfamily cell adhesion molecule, apCAM, mediates growth cone steering by substrate-cytoskeletal coupling. *J Cell Biol*. 141:227-40.
- Tanaka, E., T. Ho, and M.W. Kirschner. 1995. The role of microtubule dynamics in growth cone motility and axonal growth. *J Cell Biol*. 128:139-55.
- Tang, B.L. 2001. Protein trafficking mechanisms associated with neurite outgrowth and polarized sorting in neurons. *J Neurochem*. 79:923-30.
- Tararuk, T., N. Ostman, W. Li, B. Bjorkblom, A. Padzik, J. Zdrojewska, V. Hongisto, T. Herdegen, W. Konopka, M.J. Courtney, and E.T. Coffey. 2006. JNK1 phosphorylation of SCG10 determines microtubule dynamics and axodendritic length. *J Cell Biol*. 173:265-77.
- Tolias, K.F., L.C. Cantley, and C.L. Carpenter. 1995. Rho family GTPases bind to phosphoinositide kinases. *J Biol Chem*. 270:17656-9.
- Trapp, B.D., P. Honegger, E. Richelson, and H.D. Webster. 1979. Morphological differentiation of mechanically dissociated fetal rat brain in aggregating cell cultures. *Brain Res*. 160:117-30.
- Trenkner, E., and R.L. Sidman. 1977. Histogenesis of mouse cerebellum in microwell cultures. Cell reaggregation and migration, fiber and synapse formation. *J Cell Biol*. 75:915-40.

- Trinczek, B., J. Biernat, K. Baumann, E.M. Mandelkow, and E. Mandelkow. 1995. Domains of tau protein, differential phosphorylation, and dynamic instability of microtubules. *Mol Biol Cell*. 6:1887-902.
- Trivedi, N., P. Marsh, R.G. Goold, A. Wood-Kaczmar, and P.R. Gordon-Weeks. 2005. Glycogen synthase kinase-3 $\beta$  phosphorylation of MAP1B at Ser1260 and Thr1265 is spatially restricted to growing axons. *J Cell Sci*. 118:993-1005.
- Vale, R.D. 2003. The molecular motor toolbox for intracellular transport. *Cell*. 112:467-80.
- van Horck, F.P., M.R. Ahmadian, L.C. Haeusler, W.H. Moolenaar, and O. Kranenburg. 2001. Characterization of p190RhoGEF, a RhoA-specific guanine nucleotide exchange factor that interacts with microtubules. *J Biol Chem*. 276:4948-56.
- Vasquez, R.J., B. Howell, A.M. Yvon, P. Wadsworth, and L. Cassimeris. 1997. Nanomolar concentrations of nocodazole alter microtubule dynamic instability in vivo and in vitro. *Mol Biol Cell*. 8:973-85.
- Verhey, K.J., D. Meyer, R. Deehan, J. Blenis, B.J. Schnapp, T.A. Rapoport, and B. Margolis. 2001. Cargo of kinesin identified as JIP scaffolding proteins and associated signaling molecules. *J Cell Biol*. 152:959-70.
- Vignal, E., A. Blangy, M. Martin, C. Gauthier-Rouviere, and P. Fort. 2001. Kinectin is a key effector of RhoG microtubule-dependent cellular activity. *Mol Cell Biol*. 21:8022-34.
- Votin, V., W.J. Nelson, and A.I. Barth. 2005. Neurite outgrowth involves adenomatous polyposis coli protein and  $\beta$ -catenin. *J Cell Sci*.
- Walker, R.A., N.K. Pryer, and E.D. Salmon. 1991. Dilution of individual microtubules observed in real time in vitro: evidence that cap size is small and independent of elongation rate. *J Cell Biol*. 114:73-81.
- Watabe-Uchida, M., K.A. John, J.A. Janas, S.E. Newey, and L. Van Aelst. 2006. The Rac activator DOCK7 regulates neuronal polarity through local phosphorylation of stathmin/Op18. *Neuron*. 51:727-39.
- Waterman-Storer, C.M., and E.D. Salmon. 1997. Actomyosin-based retrograde flow of microtubules in the lamella of migrating epithelial cells influences microtubule dynamic instability and turnover and is associated with microtubule breakage and treadmilling. *J Cell Biol*. 139:417-34.
- Weiner, O.D., P.O. Nielsen, G.D. Prestwich, M.W. Kirschner, L.C. Cantley, and H.R. Bourne. 2002. A PtdInsP(3)- and Rho GTPase-mediated positive feedback loop regulates neutrophil polarity. *Nat Cell Biol*. 4:509-13.
- Weisenberg, R.C., G.G. Borisy, and E.W. Taylor. 1968. The colchicine-binding protein of mammalian brain and its relation to microtubules. *Biochemistry*. 7:4466-79.
- Wen, Y., C.H. Eng, J. Schmoranzer, N. Cabrera-Poch, E.J. Morris, M. Chen, B.J. Wallar, A.S. Alberts, and G.G. Gundersen. 2004. EB1 and APC bind to mDia to stabilize microtubules downstream of Rho and promote cell migration. *Nat Cell Biol*. 6:820-30.
- West, A.E., R.L. Neve, and K.M. Buckley. 1997. Identification of a somatodendritic targeting signal in the cytoplasmic domain of the transferrin receptor. *J Neurosci*. 17:6038-47.
- Westermann, S., and K. Weber. 2003. Post-translational modifications regulate microtubule function. *Nat Rev Mol Cell Biol*. 4:938-47.
- Whitford, K.L., P. Dijkhuizen, F. Polleux, and A. Ghosh. 2002. Molecular control of cortical dendrite development. *Annu Rev Neurosci*. 25:127-49.

- Wisco, D., E.D. Anderson, M.C. Chang, C. Norden, T. Boiko, H. Folsch, and B. Winckler. 2003. Uncovering multiple axonal targeting pathways in hippocampal neurons. *J Cell Biol.* 162:1317-28.
- Witte, H., and F. Bradke. 2005. Guidance of Axons to Targets in Development and in Disease. *In* Peripheral Neuropathy. Vol. 1. P.J. Dyck and P.K. Thomas, editors. Elsevier Inc., Philadelphia. 447-481.
- Wodarz, A. 2002. Establishing cell polarity in development. *Nat Cell Biol.* 4:E39-44.
- Xie, H., J.M. Litersky, J.A. Hartigan, R.S. Jope, and G.V. Johnson. 1998. The interrelationship between selective tau phosphorylation and microtubule association. *Brain Res.* 798:173-83.
- Yamada, M., H. Ohnishi, S. Sano, A. Nakatani, T. Ikeuchi, and H. Hatanaka. 1997. Insulin receptor substrate (IRS)-1 and IRS-2 are tyrosine-phosphorylated and associated with phosphatidylinositol 3-kinase in response to brain-derived neurotrophic factor in cultured cerebral cortical neurons. *J Biol Chem.* 272:30334-9.
- Yap, C.C., D. Wisco, P. Kujala, Z.M. Lasiecka, J.T. Cannon, M.C. Chang, H. Hirling, J. Klumperman, and B. Winckler. 2008. The somatodendritic endosomal regulator NEEP21 facilitates axonal targeting of L1/NgCAM. *J Cell Biol.* 180:827-42.
- Yavin, Z., and E. Yavin. 1977. Synaptogenesis and myelinogenesis in dissociated cerebral cells from rat embryo on polylysine coated surfaces. *Exp Brain Res.* 29:137-47.
- York, R.D., H. Yao, T. Dillon, C.L. Ellig, S.P. Eckert, E.W. McCleskey, and P.J. Stork. 1998. Rap1 mediates sustained MAP kinase activation induced by nerve growth factor. *Nature.* 392:622-6.
- Yoshida, H., C.J. Hastie, H. McLauchlan, P. Cohen, and M. Goedert. 2004. Phosphorylation of microtubule-associated protein tau by isoforms of c-Jun N-terminal kinase (JNK). *J Neurochem.* 90:352-8.
- Yoshimura, T., N. Arimura, Y. Kawano, S. Kawabata, S. Wang, and K. Kaibuchi. 2006. Ras regulates neuronal polarity via the PI3-kinase/Akt/GSK-3beta/CRMP-2 pathway. *Biochem Biophys Res Commun.* 340:62-8.
- Yoshimura, T., Y. Kawano, N. Arimura, S. Kawabata, A. Kikuchi, and K. Kaibuchi. 2005. GSK-3beta regulates phosphorylation of CRMP-2 and neuronal polarity. *Cell.* 120:137-49.
- Zeitelhofer, M., J.P. Vessey, Y. Xie, F. Tubing, S. Thomas, M. Kiebler, and R. Dahm. 2007. High-efficiency transfection of mammalian neurons via nucleofection. *Nat Protoc.* 2:1692-704.
- Zeringue, H.C., and M. Constantine-Paton. 2004. Post-transcriptional gene silencing in neurons. *Curr Opin Neurobiol.* 14:654-9.
- Zhang, Y., S. Kwon, T. Yamaguchi, F. Cubizolles, S. Rousseaux, M. Kneissel, C. Cao, N. Li, H.L. Cheng, K. Chua, D. Lombard, A. Mizeracki, G. Matthias, F.W. Alt, S. Khochbin, and P. Matthias. 2008. Mice lacking HDAC6 have hyperacetylated tubulin but are viable and develop normally. *Mol Cell Biol.*
- Zhou, F.Q., and W.D. Snider. 2005. Cell biology. GSK-3beta and microtubule assembly in axons. *Science.* 308:211-4.
- Zhou, F.Q., J. Zhou, S. Dedhar, Y.H. Wu, and W.D. Snider. 2004. NGF-induced axon growth is mediated by localized inactivation of GSK-3beta and functions of the microtubule plus end binding protein APC. *Neuron.* 42:897-912.
- Zmuda, J.F., and R.J. Rivas. 1998. The Golgi apparatus and the centrosome are localized to the sites of newly emerging axons in cerebellar granule neurons in vitro. *Cell Motil Cytoskeleton.* 41:18-38.

Zumbrunn, J., K. Kinoshita, A.A. Hyman, and I.S. Nathke. 2001. Binding of the adenomatous polyposis coli protein to microtubules increases microtubule stability and is regulated by GSK3 beta phosphorylation. *Curr Biol.* 11:44-9.



# 7. Appendix – Source codes of Scion Image macros

## Source codes of Scion image (version Beta 4.0.2) macros

(see 5.2.2.4 Scion image macros for image acquisition and analysis, p. 80)

### 7.1 Triple stain image acquisition

```
{ Global variables }
var
mag, barlength: real; { objective magnification, size of scale bar to
use (µm) }
camerapid: integer; { PID of camera window }
bgpid: integer; { background window }
bgsb: boolean; { whether to subtract background }
tsoff: boolean; { whether to omit timestamp from captured
images }
asoff: boolean; { whether the AutoShutter feature is off }
shopen: boolean; { whether we think the shutter is open }
tperiod: real; { timelapse period }
n: integer; {Global variable used by integration macros}
hour1,mini,sec1:integer;
timeron:boolean;
nframes, nframes1, nframes2, nframes3, pframes, pframes2,
tframes:integer;
name, wavelength, wavelength1, wavelength2, wavelength3:integer;
antigen, antigen1, antigen2, antigen3, annotation, framenummer: string;
Settings, Settings1, Settings2, Settings3, generalsettings, nophase:
boolean;
NumberofStainings, magnification: integer;
TimelapseSet, annotateon, annotateon2: boolean;
year,month,day,hour,min,sec,minute,second,DoW:integer;
roundnumber: integer;

{ Error(s) issues the error message S and terminates the macro. }
procedure Error(s:string);
begin
PutMessage(s); exit;
end;

procedure ResetTimer
var
year,month,day,hour,min,sec,DoW:integer;
begin
GetTime(year,month,day,hour,min,sec,DoW);
timeron:=True;
hour:=hour;
mini:=min;
sec:=sec;
end;

procedure Timer;
var
year,month,day,hour,min,sec,hourC,minC,secC,DoW:i
neger;
year2,month2,day2,hour2,min2,sec2,hourC2,minC2,se
cC2,DoW2:integer;
l,t,w,h:integer;
begin
GetRoi(l,t,w,h);
If (w=0) then Error("Select an ROI First");
If timeron then begin
GetTime(year,month,day,hour,min,sec,DoW);
if (sec>=sec1) then secC:=sec-sec1 else begin
secC:=(sec+60)-sec1;
min:=min-1;
end;
if (min>=mini) then minC:=min-mini else begin
minC:=min+60-mini;
hour:=hour-1;
end;
hourC:=hour-hour1;
MoveTo(665,559);
SetForegroundColor(0);
SetFont('Helvetica');SetFont(14);
GetTime(year2,month2,day2,hour2,min2,sec2,D
oW2);
write("Time: ",hour2:2,',');
```

```
if (min2<10) then
Write('0',min2:1,',') else Write(min2:2,',');
if (sec2<10) then
Write('0',sec2:1) else Write(sec2:2);
MoveTo(665, 547);
write("Date: ", year:4, '-');
if (month<10) then
write ('0', month:1, '-') else write (month:2, '-');
if
(day<10) then write ('0', day:1) else write (day:2);
MoveTo(560,547);
Write("Timer: ",hourC:2,',');
if (minC <10) then
Write('0',minC:1,',') else Write(minC:2,',');
if (secC<10) then
Write('0',secC:1) else Write(secC:2);
RestoreRoi;
end else begin
ResetTimer;
Timer;
end;
```

```
procedure OpenShutter;
begin
scion[4]:=0;
shopen:=true;
end;
```

```
macro 'Open Shutter [1]';
begin
OpenShutter;
end;
```

```
procedure CloseShutter;
begin
scion[4]:=15;
shopen:=false;
end;
```

```
macro 'Close Shutter [2]';
begin
CloseShutter;
end;
```

```
macro'(-' begin end; {Menu divider}
```

```
macro 'Reset Timer [R]';
begin
ResetTimer;
end;
```

```
macro 'Timer [T]';
begin
Timer;
end;
```

```
{
These two macros continuously integrate and display frames either off-
chip, using the Scion AG-5, or on-clip, using the
Scion LG-3 and a Coho 4910 series camera. Press and
hold the mouse button near the top of the Camera
window to decrease the number of frames integrated.
Press near the bottom to increase the number of
frames integrated. Press above or to the left of the
Camera window to stop integrating.
}
```

```
procedure Integrate (mode:string);
var
x,y,delta:integer;
begin
if n=0 then n:=6;
repeat
```

```

if button then begin
  GetMouse(x,y);
  if (x<0) or (y<0) then begin
    closeShutter;
    exit;
  end;
  delta:=round(0.333*n);
  if delta<1 then delta:=1;
  if y<220 then begin
    n:=n-delta;
    if n<1 then n:=1;
  end else begin
    n:=n+delta;
    if n>127 then n:=127;
  end;
end;
AverageFrames(mode, n);
until false;
end;

macro '-' begin end; {Menu divider}

macro 'Counter +1 [+]';
begin
  name:=name+1;
  ShowMessage('Counter: ',name);
end;

macro 'Counter -1 [-]';
begin
  name:=name-1;
  ShowMessage('Counter: ',name);
end;

macro 'Picture number +1 [B]';
begin
  roundnumber:=roundnumber+1;
  ShowMessage('Picture number:\',roundnumber);
end;

macro 'Picture number -1 [V]';
begin
  roundnumber:=roundnumber-1;
  ShowMessage('Picture number:\',roundnumber);
end;

macro '-' begin end; {Menu divider}

macro 'Antigen1 frames +1 [I]';
begin
  nframes1:=nframes1+1;
  ShowMessage('Antigen1:\Number of
frames\integrated: ',nframes1);
end;

macro 'Antigen1 frames -1 [J]';
begin
  nframes1:=nframes1-1;
  ShowMessage('Antigen1:\Number of
frames\integrated: ',nframes1);
end;

macro 'Antigen2 frames +1 [O]';
begin
  nframes2:=nframes2+1;
  ShowMessage('Antigen2:\Number of
frames\integrated: ',nframes2);
end;

macro 'Antigen2 frames -1 [K]';
begin
  nframes2:=nframes2-1;
  ShowMessage('Antigen2:\Number of
frames\integrated: ',nframes2);
end;

macro 'Antigen3 frames -1 [6]';
begin
  nframes3:=nframes3-1;
  ShowMessage('Antigen3:\Number of
frames\integrated: ',nframes3);
end;

macro 'Antigen3 frames +1 [7]';
begin
  nframes3:=nframes3+1;
  ShowMessage('Antigen3:\Number of
frames\integrated: ',nframes3);
end;

macro '-' begin end; {Menu divider}

procedure FluorescenceSettings;
begin
  NumberofStainings:=GetNumber('Enter Number of
Stainings -1 to 3-:', NumberofStainings);
  if NumberofStainings <> 1 then
    if NumberofStainings <> 2 then
      if NumberofStainings
<> 3 then
        Exit('Only 1, 2 or 3 allowed!');
      if NumberofStainings=1 then Settings1:=true
        else Settings1:=false;
      if NumberofStainings=2 then Settings2:=true
        else Settings2:=false;
      antigen1:=GetString('Name of Staining 1 / Antigen 1:',
antigen1);
      if antigen1='Global String' then Exit('Please
enter name!');
      wavelength1:=GetNumber('Excitation wavelength of
Antigen 1 in nm:', wavelength1);
      if (nframes1=0) then nframes1:=4;
      nframes1:=GetNumber('Number of Fluorescence-
Frames (Antigen 1):', nframes1);
      if Settings1=true then begin
        settings := true;
        Exit;
      end;
      antigen2:=GetString('Name of Staining 2 / Antigen 2:',
antigen2);
      if antigen2='Global String' then Exit('Please
enter name!');
      wavelength2:=GetNumber('Excitation wavelength of
Antigen 2 in nm:', wavelength2);
      if (nframes2=0) then nframes2:=4;
      nframes2:=GetNumber('Number of Fluorescence-
Frames (Antigen 2):', nframes2);
      if Settings2=true then begin
        Settings1 := true;
        Settings2 := true; {only necessary if
number of stainings is changed later}
        Settings := true;
        Exit;
      end;
      antigen3:=GetString('Name of Staining 3 / Antigen 3:',
antigen3);
      if antigen3='Global String' then Exit('Please
enter name!');
      wavelength3:=GetNumber('Excitation wavelength of
Antigen 3 in nm:', wavelength3);
      if (nframes3=0) then nframes3:=4;
      nframes3:=GetNumber('Number of Fluorescence-
Frames (Antigen 3):', nframes3);
      Settings1 := true;
      Settings2 := true;
      Settings3 := true;
      Settings := true;
    end;
  end;
end;

procedure Annotate;
begin
  if generalsettings=true then
  begin
    MoveTo(10,547);
    SetForegroundColor(0); SetFont('Helvetica');
    SetFontSize(14);
    write(annotation);
    MoveTo(10,559);
    write('Magnification:', magnification, 'x');
    if (nophase=true) then begin
      write ('
', antigen, ' ', wavelength, 'nm ', nframes);
      if
(nframes>1) then framenummer:= 'frames' else
framenummer:= 'frame';
      write(' ',
framenummer);
    end;
    if (nophase=false) then begin write
(' Phase contrast ', pframes);
  end;
end;
end;

```

```

        if
        (pframes>1) then framenumbers:=frames' else
        framenumbers:=frame';
        framenumbers);
        end;
        MoveTo(665,547);
        SetForegroundColor(0); SetFont('Helvetica');
        SetFontSize(14);
        GetTime(year,month,day,hour,min,sec,DoW);
        write('Date: ', year:4, '-');
        if (month<10) then write ('0',
        month:1, '-') else write (month:2, '-');
        if (day<10) then write ('0', day:1)
        else write (day:2);
        MoveTo(665,559);
        write('Time: ',hour:2,':');
        if (min<10) then Write('0',min:1,':')
        else Write(min:2,':');
        if (sec<10) then Write('0',sec:1)
        else Write(sec:2);
        end;
end;

macro 'Fluorescence Settings [N]';
begin
    FluorescenceSettings;
end;

macro 'Phase contrast settings [M]';
begin
    if (pframes=0) then pframes:=2;
    pframes:=GetNumber('Number of Phase contrast-
    Frames to integrate:', pframes);
end;

macro 'General settings [0]';
begin
    annotation:=GetString('Date and/or Type of
    experiment:', annotation);
    magnification:=GetNumber('Magnification:',
    magnification);
    ShowMessage('Date and/or Type of experiment:',
    annotation, '\Magnification:', magnification, 'x');
    generalsettings:=true;
end;

macro 'Annotation on/off [A]';
begin
    annotateon2:=annotateon;
    if (annotateon=true) then annotateon:=false;
    if (annotateon2=false) then annotateon:=true;
    if (annotateon=true) then begin
        ShowMessage('Annotation on');
    end else begin ShowMessage('Annotation off');
    end;
end;

macro 'Save As "Window Title.tif" [S]';
begin
    SetSaveAs('TIFF');
    SaveAs;
End;

Macro 'Make Standard ROI [Q]';
begin
    MakeRoi(0,34,767,512);
end;

macro '(-' begin end; {Menu divider}

macro 'Integrate Phase [P]';
begin;
    nopphase:=false;
    GetTime(year,month,day,hour,minute,second,DoW);
    StartCapturing;
    StopCapturing;
    StartCapturing;
    name:=name+1;
    if (pframes=0) then pframes:=2;
    AverageFrames('Integrate',pframes);

    if (annotateon=true) then Annotate;
    if (pframes>1) then framenumbers:=frames' else
    framenumbers:=frame';
    SetPicName(name:3, '_', roundnumber:2, '_1p_',
    year:4, '-', month:2, '-', day:2, '_', hour:2, '-', minute:2,
    '-', second:2, '-', pframes:1, framenumbers);
    duplicate(name:3, '_', roundnumber:2, '_1p_', year:4, '-',
    month:2, '-', day:2, '_', hour:2, '-', minute:2, '-',
    second:2, '-', pframes:1, framenumbers);
end;

procedure IntegrateFluorescent;
begin;
    if (nframes>1) then framenumbers:=frames' else
    framenumbers:=frame';
    if (annotateon=true) then begin
        if (settings=false) then FluorescenceSettings;
        if (nframes<1) then FluorescenceSettings;
        nopphase:=true;

        GetTime(year,month,day,hour,minute,second,D
        oW);
        StartCapturing;
        StopCapturing;
        StartCapturing;
        OpenShutter;
        AverageFrames('Integrate On-chip',nframes);
        Annotate;
        SetPicName(name:3, '_',
        roundnumber:2, '_2f_', antigen, '_', nframes:1,
        framenumbers, '_', year:4, '-', month:2, '-', day:2, '_',
        hour:2, '-', minute:2, '-', second:2, '-',
        CloseShutter;
        duplicate(name:3, '_', roundnumber:2, '_2f_',
        antigen, '_', nframes:1, framenumbers, '_', year:4, '-',
        month:2, '-', day:2, '_', hour:2, '-', minute:2, '-',
        second:2, '-',
        nopphase:=false;
    end else begin
        if (nframes<1) then nframes:=1;

        GetTime(year,month,day,hour,minute,second,D
        oW);
        StartCapturing;
        StopCapturing;
        StartCapturing;
        OpenShutter;
        AverageFrames('Integrate On-chip',nframes);
        SetPicName(name:3, '_',
        roundnumber:2, '_', year:4, '-', month:2, '-',
        day:2, '_', hour:2, '-', minute:2, '-', second:2, '_',
        nframes:1, framenumbers);
        CloseShutter;
        duplicate(name:3, '_',
        roundnumber:2, '_', year:4, '-', month:2, '-',
        day:2, '_', hour:2, '-', minute:2, '-', second:2, '_',
        nframes:1, framenumbers);
        end;
    end;

macro 'Integrate Fluorescent (Antigen 1) [F]';
begin
    settings:=settings1;
    antigen:=antigen1;
    wavelength:=wavelength1;
    nframes:=nframes1;
    IntegrateFluorescent;
end;

macro 'Integrate Fluorescent (Antigen 2) [G]';
begin
    settings:=settings2;
    antigen:=antigen2;
    wavelength:=wavelength2;
    nframes:=nframes2;
    IntegrateFluorescent;
end;

macro 'Integrate Fluorescent (Antigen 3) [H]';
begin
    settings:=settings3;
    antigen:=antigen3;
    wavelength:=wavelength3;
    nframes:=nframes3;
    IntegrateFluorescent;
end;

macro 'Integrate On-chip Using CoHu [C]';
begin
    StartCapturing;
    OpenShutter;
    Integrate('integrate on-chip');
    CloseShutter;
end;

```

## 7.2 Intensity or ratio measurements

```
{global variables}
```

```
var
    n,mean,mode,min,max:integer;
    left,top,width,height:integer;
    left2,top2,width2,height2:integer;
    x, y, xcorrection, ycorrection, leftRoi, topRoi:integer;
    total:integer;
```

```
macro 'Synchronize mouse and window coordinates [W]';
```

```
begin
    MoveWindow (100, 90);
    {getmouse(x, y);
    showmessage('X: ', x, ' Y: ', y);}
end;
```

```
procedure PositionROI;
```

```
begin
    GetMouse(x,y);
    if (width2=0) then width2:=5;
    leftRoi:=x+xcorrection-(width2/2);
    {xcorrection needed as the mouse position
    ScionImage considers x=0 depends on the
    position
    of the picture window for unknown reasons}
    left2:=leftRoi;
    if (height2=0) then height2:=5;
    topRoi:=y+ycorrection-(height2/2);
    {ycorrection needed as the mouse position
    ScionImage considers y=0 depends on the
    position
    of the picture window for unknown reasons}
    top2:=topRoi;
    MakeRoi(leftRoi,topRoi,width2,height2);
end;
```

```
procedure OvalROI;
```

```
begin
    GetMouse(x,y);
    if (width2=0) then width2:=5;
    leftRoi:=x+xcorrection-(width2/2);
    {xcorrection needed as the mouse position
    ScionImage considers x=0 depends on the
    position
    of the picture window for unknown reasons}
    left2:=leftRoi;
    if (height2=0) then height2:=5;
    topRoi:=y+ycorrection-(height2/2);
    {ycorrection needed as the mouse position
    ScionImage considers y=0 depends on the
    position
    of the picture window for unknown reasons}
    top2:=topRoi;
    MakeOvalRoi(leftRoi,topRoi,width2,height2);
end;
```

```
macro 'Define Size of rectangular Region of Interest (ROI) by keyboard [N]';
```

```
begin
    if (width2=0) then width2:=5;
    if (height2=0) then height2:=5;
    width2:=GetNumber('Width:', width2);
    height2:=GetNumber('Height:', height2);
    PositionROI;
end;
```

```
macro 'Define ROI by mouse [D]';
```

```
begin
    GetRoi(left,top,width,height);
    left2:=left; top2:=top; width2:=width; height2:=height;
    KillRoi;
    RestoreRoi;
end;
```

```
macro '(-' begin end; {Menu divider}
```

```
macro 'Position Oval ROI at mouse position (no zoom) [K]';
```

```
begin
    xcorrection:=100;
    ycorrection:=64;
    OvalROI;
end;
```

```
macro 'Position ROI at mouse position (no zoom) [P]';
```

```
begin
    xcorrection:=100;
    ycorrection:=64;
    PositionROI;
end;
```

```
macro 'Position ROI at mouse position (2:1 zoom) [6]';
```

```
begin
    xcorrection:=49;
    ycorrection:=32;
    PositionROI;
end;
```

```
macro 'Position ROI at mouse position (3:1 zoom) [7]';
```

```
begin
    xcorrection:=32;
    ycorrection:=20;
    PositionROI;
end;
```

```
macro 'Position ROI at mouse position (4:1 zoom) [8]';
```

```
begin
    xcorrection:=24;
    ycorrection:=15;
    PositionROI;
end;
```

```
macro 'Position ROI at mouse position (8:1 zoom) [9]';
```

```
begin
    xcorrection:=12;
    ycorrection:=7;
    PositionROI;
end;
```

```
macro '(-' begin end; {Menu divider}
```

```
macro 'Restore ROI [R]';
```

```
begin
    RestoreRoi;
end;
```

```
macro 'Total and Average density of selection [T]';
```

```
begin
    GetRoi(left,top,width,height);
    measure;
    GetResults(n,mean,mode,min,max);
    total:=n*mean;
    ShowMessage('Total density of selection: ', total,
    'Average:', mean, '\Pixels:', n);
end;
```

```
macro '(-' begin end; {Menu divider}
```

```
macro 'Display Mouse Position [M]';
```

```
begin
    GetMouse(x,y);
    ShowMessage('x: ', x, ', y: ', y);
end;
```

```
macro 'Correct X-Y coordinates manually [C]';
```

```
begin
    GetMouse(x,y);
    xcorrection:=GetNumber('Correction of x-coordinates:',
    xcorrection);
    ycorrection:=GetNumber('Correction of y-coordinates:',
    ycorrection);
end;
```

```
macro 'Convert to Binary Image [V]';
```

```
begin
    MakeBinary;
end;
```

```
macro '(-' begin end; {Menu divider}
```

```
macro 'Invert Picture [I]';
```

```
begin
    MakeRoi(0,34,767,512);
    Invert;
    KillROI;
end;
```

```
procedure CheckForStack;
```

```
begin
```

```

if nPics=0 then begin
  PutMessage("This macro requires a stack!");
  exit;
end;
if nSlices=0 then begin
  PutMessage("This window is not a stack!");
  exit;
end;
end;

macro 'Invert Stack [O]';
var
  i:integer;
begin
  CheckForStack;
  for i:= 1 to nSlices do begin
    SelectSlice(i);
    MakeRoi(0,34,767,512);
    Invert;
  end;
  SelectSlice(1);
  KillROI;
end;

Macro 'Make Standard ROI [Q]';
begin
  MakeRoi(0,34,767,512);
end;

macro '(-' begin end; {Menu divider}

macro 'Move ROI 1 Pixel left [G]';
begin
  MoveRoi(-1,0);
  {MoveRoi(dx,dy); Moves ROI right dx pixels and down dy
pixels.}
end;

macro 'Move ROI 1 Pixel right [H]';
begin
  MoveRoi(1,0);
end;

macro 'Move ROI 1 Pixel up [Z]';
begin
  MoveRoi(0,-1);
end;

macro 'Move ROI 1 Pixel down [B]';
begin
  MoveRoi(0,1);
end;

{ macro '(-' begin end; {Menu divider} }

macro 'GoTo Slice Number... [G]';
var
  j:integer;
begin
  CheckForStack;
  j:=GetNumber("Go to slice number...", j);
  SelectSlice(j);
end;

macro 'Slice Number -5 [K]';
begin
  CheckForStack;
  If (SliceNumber-5>0) then SelectSlice(SliceNumber-5)
  Else
  SelectSlice(1);
end;

macro 'Slice Number +5 [L]';
begin
  CheckForStack;
  If (SliceNumber+5<nSlices) then SelectSlice(SliceNumber+5)
  Else
  SelectSlice(nSlices);
end;

```

## 7.3 Shutter control during uncaging experiments

```
{ Global variables }
var
mag, barlength: real; { objective magnification, size of scale bar to
use (µm) }
camerapid: integer; { PID of camera window }
bgpid: integer; { background window }
bgsb: boolean; { whether to subtract background }
tsoff: boolean; { whether to omit timestamp from
captured images }
asoff: boolean; { whether the AutoShutter feature
is off }
PhaseOpen, FluorescOpen: boolean; { whether we think the
shutter is open }
tperiod: real; { timelapse period }
n: integer; {Global variable used by integration macros}
hour1, mini, sec1, ticksuncaging1, ticksuncaging2: integer;

frequency, duration, WaitBetweenPics: integer; {Uncaging parameters}
xcoord, ycoord : integer; {coordinates of uncaged area}
UncagingSet, Uncaging, AimSet: Boolean;
left, top, width, height: integer; {parameters of fluorescence iris ROI}

extension: string; {variable for extension of window title}

timeron: boolean;
nframes, nframes1, nframes2, nframes3, pframes, pframes2,
tiframes: integer;
name, wavelength, wavelength1, wavelength2: integer;
antigen, antigen1, antigen2, annotation, annotation2, annotation3,
framenummer: string;
Settings, Settings1, Settings2, generalsettings, nophase: boolean;
NumberofStainings, magnification: integer;
TimelapseSet, annotatoon, annotatoon2: boolean;
year, month, day, hour, min, sec, minute, second, DoW: integer;
roundnumber: integer;

{ Error(s) issues the error message S and terminates the macro. }
procedure Error(s: string);
begin
PutMessage(s); exit;
end;

procedure ResetTimer
var
year, month, day, hour, min, sec, DoW: integer;

begin
GetTime(year, month, day, hour, min, sec, DoW);
timeron:=True;
hour:=hour;
mini:=min;
seci:=sec;

end;

procedure Timer;
var
year, month, day, hour, min, sec, hourC, minC, secC, DoW: integer
;
year2, month2, day2, hour2, min2, sec2, hourC2, minC2, secC2, D
oW2: integer;
l, t, w, h: integer;
begin
GetRoi(l, t, w, h);
If (w=0) then Error('Select an ROI First');
If timeron then begin
GetTime(year, month, day, hour, min, sec, DoW);
if (sec>=sec1) then secC:=sec-sec1 else begin
secC:=(sec+60)-sec1;
min:=min-1;
end;
if (min>=mini) then minC:=min-mini else begin
minC:=min+60-mini;
hour:=hour-1;
end;
hourC:=hour-hour1;
MoveTo(665, 559);
SetFont('Helvetica'); SetFontSize(14);

GetTime(year2, month2, day2, hour2, min2, sec2, DoW2);
write('Time: ', hour2:2, ':', min2:2, ':', sec2:2, ' ');
if (min2<10) then
Write('0', min2:1, ':') else Write(min2:2, ':');
if (sec2<10) then
Write('0', sec2:1) else Write(sec2:2);
MoveTo(665, 547);
write('Date: ', year:4, '-');
```

```
if (month<10) then
write ('0', month:1, '-') else write (month:2, '-');
if (day<10) then write ('0', day:1) else write (day:2);
MoveTo(560, 547);
Write('Timer: ', hourC:2, ':');
if (minC <10) then
Write('0', minC:1, ':') else Write(minC:2, ':');
if (secC<10) then
Write('0', secC:1) else Write(secC:2);
RestoreRoi;
end else begin
ResetTimer;
Timer;
end;

end;

procedure OpenFluorescenceShutter;
begin
{Uniblitz Shutters are routinely set to active-low, i.e. an input
signal means no output, no input signal means output}
if (PhaseOpen=true) then scion[4]:= 12 {shutter 0 & 1 open}
else
scion[4]:=13; {Shutter 0 closed & 1 open}
FluorescOpen:=true;

end;

procedure CloseFluorescenceShutter;
begin
if (PhaseOpen=false) then scion[4]:= 15 {all shutters closed}
else
scion[4]:=14; {Shutter 0 closed & 1
open}
FluorescOpen:=false;

end;

procedure OpenPhaseShutter;
begin
if (FluorescOpen=true) then scion[4]:= 12 {shutter 0 & 1
open} else
scion[4]:=14; {Shutter 0 open & 1
closed}
PhaseOpen:=true;

end;

procedure ClosePhaseShutter;
begin
if (FluorescOpen=false) then scion[4]:= 15 {all shutters
closed} else
scion[4]:=13; {Shutter 0 closed & 1
open}
PhaseOpen:=false;

end;

macro 'Open Fluorescence Shutter [1]';
begin
OpenFluorescenceShutter;
end;

macro 'Close Fluorescence Shutter [2]';
begin
CloseFluorescenceShutter;
end;

macro 'Open Phase Shutter [3]';
begin
OpenPhaseShutter;
end;

macro 'Close Phase Shutter [4]';
begin
ClosePhaseShutter;
end;

macro '-' begin end; {Menu divider}

macro 'Reset Timer [R]';
begin
ResetTimer;
end;

macro 'Timer [T]';
```

```

begin
  Timer;
end;

{
  These two macros continuously integrate and display frames either off-
  chip, using the Scion AG-5, or on-clip, using the Scion LG-3 and a Coho
  4910 series camera. Press and hold the mouse button near the top of the
  Camera window to decrease the number of frames integrated. Press near
  the bottom to increase the number of frames integrated. Press above or
  to the left of the Camera window to stop integrating.
}

procedure Integrate (mode:string);
var
  x,y,delta:integer;
begin
  if n=0 then n:=6;
  repeat
    if button then begin
      GetMouse(x,y);
      if (x<0) or (y<0) then begin
        CloseFluorescenceShutter;
        exit;
      end;
      delta:=round(0.333*n);
      if delta<1 then delta:=1;
      if y<220 then begin
        n:=n-delta;
        if n<1 then n:=1;
      end else begin
        n:=n+delta;
        if n>127 then n:=127;
      end;
      end;
      AverageFrames(mode, n);
    until false;
  end;
end;

macro 'Counter +1 [+];'
begin
  name:=name+1;
  ShowMessage('Counter: ',name);
end;

macro 'Counter -1 [-];'
begin
  name:=name-1;
  ShowMessage('Counter: ',name);
end;

macro 'Picture number +1 [B]';
begin
  roundnumber:=roundnumber+1;
  ShowMessage('Picture number:\',roundnumber);
end;

macro 'Picture number -1 [V]';
begin
  roundnumber:=roundnumber-1;
  ShowMessage('Picture number:\',roundnumber);
end;

macro 'Antigen1 frames +1 [I]';
begin
  nframes1:=nframes1+1;
  ShowMessage('Antigen1:\Number of frames\integrated:
',nframes1);
end;

macro 'Antigen1 frames -1 [J]';
begin
  nframes1:=nframes1-1;
  ShowMessage('Antigen1:\Number of frames\integrated:
',nframes1);
end;

macro 'Antigen2 frames +1 [O]';
begin
  nframes2:=nframes2+1;
  ShowMessage('Antigen2:\Number of frames\integrated:
',nframes2);
end;

macro 'Antigen2 frames -1 [K]';
begin
  nframes2:=nframes2-1;
  ShowMessage('Antigen2:\Number of frames\integrated:
',nframes2);
end;

```

```

macro '(-' begin end; {Menu divider}

procedure FluorescenceSettings;
begin
  NumberofStainings:=GetNumber('Enter Number of Stainings
-1 or 2-:', NumberofStainings);
  if NumberofStainings <> 1 then
    if NumberofStainings <> 2 then
      Exit('Only 1 or 2 allowed!');
    if NumberofStainings=1 then Settings1:=true
    else Settings1:=false;

    antigen1:=GetString('Name of Staining 1 / Antigen 1:
antigen1);
    if antigen1='Global String' then Exit('Please
enter name!');
    wavelength1:=GetNumber('Excitation wavelength of Antigen
1 in nm:', wavelength1);
    if (nframes1=0) then nframes1:=4;
    nframes1:=GetNumber('Number of Fluorescence-Frames
(Antigen 1):', nframes1);
    if Settings1=true then begin
      settings := true;
      Exit;
    end;

    antigen2:=GetString('Name of Staining 2 / Antigen 2:
antigen2);
    if antigen2='Global String' then Exit('Please
enter name!');
    wavelength2:=GetNumber('Excitation wavelength of Antigen
2 in nm:', wavelength2);
    if (nframes2=0) then nframes2:=4;
    nframes2:=GetNumber('Number of Fluorescence-Frames
(Antigen 2):', nframes2);
    Settings1 := true;
    Settings2 := true;
    Settings := true;

    exit;
  end;

procedure Annotate;
begin
  if generalsettings=true then
    begin
      MoveTo(10,547);
      SetForegroundColor(0); SetFont('Helvetica');
      SetFontSize(14);
      write(annotation);
      MoveTo(10,559);
      write('Magnification:', magnification, 'x');
      if (nophase=true) then begin
        write (
', antigen, ' ', wavelength, 'nm ', nframes);
        if
(nframes>1) then framenumbers:='frames' else framenumbers:='frame';
        write(' ',
framenumbers);
      end;
      if (nophase=false) then begin write
(' Phase contrast ', pframes);
      if
(pframes>1) then framenumbers:='frames' else framenumbers:='frame';
      write(' ',
framenumbers);
      end;
      MoveTo(665,547);
      SetForegroundColor(0); SetFont('Helvetica');
      SetFontSize(14);
      GetTime(year,month,day,hour,min,sec,DoW);
      write('Date: ', year:4, '-');
      if (month<10) then write ('0',
month:1, '-') else write (month:2, '-');
      if (day<10) then write ('0', day:1)
else write (day:2);
      MoveTo(665,559);
      write('Time: ',hour:2,':');
      if (min<10) then Write('0',min:1,':')
else Write(min:2,':');
      if (sec<10) then Write('0',sec:1)
else Write(sec:2);
      end;
    end;
  end;

macro 'Fluorescence Settings [N]';
begin
  FluorescenceSettings;
end;

macro 'Phase contrast settings [M]';
begin
  if (pframes=0) then pframes:=2;
  pframes:=GetNumber('Number of Phase contrast-Frames to
integrate:', pframes);
end;

```

```

macro 'General settings [0]';
begin
    annotation:=GetString('Annotation 1: Date and/or Type of
experiment:', annotation);
    annotation2:=GetString('Annotation 2: Date and/or Type of
experiment:', annotation2);
    magnification:=GetNumber('Magnification:', magnification);
    ShowMessage('Date and/or Typelof experiment:',
annotation, '\Magnification:', magnification, 'x');
    generalsettings:=true;
end;

```

```

macro 'Annotation on/off [A]';
begin
    annotatoon2:=annotatoon;
    if (annotatoon=true) then annotatoon:=false;
    if (annotatoon2=false) then annotatoon:=true;
    if (annotatoon=true) then begin
        ShowMessage('Annotation on');
    end else begin ShowMessage('Annotation off');
    end;
end;

```

```

macro 'Toggle annotation';
begin
    annotation3:=annotation;
    annotation:=annotation2;
    annotation2:=annotation3;
    ShowMessage('Annotations switched');
end;

```

```

Procedure SaveAsTitle;
begin
    SetSaveAs('TIFF');
    SaveAs;
End;

```

```

macro 'Save As "Window Title.tif" [S]';
begin
    SaveAsTitle;
End;

```

```

Macro 'Make Standard ROI [Q]';
begin
    MakeRoi(0,34,767,512);
end;

```

```

macro '(' begin end; {Menu divider}

```

```

Macro 'Make Standard Fluorescence Iris ROI [D]';
begin
    MakeOvalRoi(335,235,80,80);
end;

```

```

macro 'Correct Aim [W]';
var
a, b, c, d: integer;
begin
    GetRoi(a,b,c,d); {a=left; b=top; c=width; d=height}
    If (c<>0) then begin
        KillROI;
        StartCapturing;
        Exit;
        end;
    If (c=0) then StopCapturing;
    If (AimSet = true) then begin
        MakeOvalRoi(xcoord, ycoord, width, height);
    end else begin
        MakeOvalRoi(335,235,80,80);
    end;
end;

```

```

macro 'Set Iris ROI [E]';
var
a, b, c, d: integer;
begin
    GetRoi(a, b, c, d); {a=left; b=top; c=width; d=height}
    If (c = 0) then begin
        Exit('Please use "Correct Aim [W]" or define Iris
ROI first!');
    end;
    xcoord := a; {values of local position variables are copied to
global position variables}

```

```

ycoord := b; {without local variables, there is no ROI any
more after setting the Iris ROI}
width := c; {when nothing is selected, even if an error is
displayed}
height := d;
AimSet := true;
end;

```

```

procedure DisplayIris;
begin
    MakeOvalRoi(xcoord, ycoord, width, height);
    SetLineWidth(2);
    DrawBoundary;
    KillRoi;
end;

```

```

macro 'Display Iris ROI [X]';
begin
    If (AimSet = false) then Exit('Please set Iris ROI using "Set
Iris ROI [E]" first!');
    DisplayIris;
end;

```

```

macro 'Show Iris Parameters [5]';
begin
    PutMessage('X-coord.: ', xcoord, ' Y-coord.: ', ycoord, '
Width: ', width, ' Height: ', height);
end;

```

```

macro '(' begin end; {Menu divider}

```

```

procedure SetUncagingParameters;
begin
    frequency := GetNumber('Time between pulses in seconds
(fractions allowed):', frequency);
    duration := GetNumber('Duration of pulses in seconds
(fractions allowed):', duration);
    If duration >= frequency then Exit('Duration too long for this
frequency!');
    UncagingSet := true;
end;

```

```

macro 'Set Uncaging parameters [Z]';
begin
    SetUncagingParameters;
end;

```

```

procedure IntegratePhase;
begin;
    nopphase:=false;
    GetTime(year,month,day,hour,minute,second,DoW);
    If (Uncaging=false) then begin
        StartCapturing;
        StopCapturing;
        StartCapturing;
        end;
    roundnumber:=roundnumber+1;
    if (pframes=0) then pframes:=1;
    AverageFrames('Integrate',pframes);

    if (annotatoon=true) then Annotate;
    if (pframes>1) then framenumber:='frames' else
framenumber:='frame';
    SetPicName(name:3, '_', roundnumber:2, '_1p_', year:4, '-',
month:2, '-', day:2, '_', hour:2, '-', minute:2, '-', second:2, '_',
framenumber);
end;

```

```

macro 'Start uncaging [Y]';
var
i, StartTick, StopTick, NoROI, WithROI:integer;
begin
    If UncagingSet=false then SetUncagingParameters;
    PutMessage('To stop, press "Esc" or hold down "Shift" until
pulsing ceases!');
    i:=0;
    wait(2);
    repeat
        OpenFluorescenceShutter;
        wait(duration);
        CloseFluorescenceShutter;
        Wait(frequency-duration);
    until KeyDown ('Shift');
end;

```



```

{ start at the next multiple of tperiod }
GetTime(year,month,day,hour,minute,second,DoW);
time:=second+60*(minute+60*hour);
if (tperiod<60) then next:=time+tperiod
else next:=time+(60-second);
last:=time;

while true do begin
  while (time<next) do begin
    GetTime(year,month,day,hour,minute,second,DoW);
    time:=second+60*(minute+60*hour);
    if (time>last) then begin
      ShowMessage(hour:2,':',minute:2,':',second:2,'\',next-time);
      last:=time;
    end;
  end;
end;
{take phase picture}
  TimelapsePhase;

  GetTime(year,month,day,hour,minute,second,DoW);
  RestoreROI;
  Timer;
  RestoreROI;

{save phase image}
  SetSaveAs('TIFF');
  SaveAs;

  if (w>0) then begin
    SetLineWidth(1);
    DrawBoundary;
  end;
  RestoreROI;
  next:=next+tperiod;
end;
end;

macro '(-' begin end; {Menu divider}

procedure ExtendWindowtitle;
begin
  duplicate(windowtitle);
  SetPicName(windowtitle, extension);
end;

macro 'Add "_before uncaging" to window title [6]';
begin
  extension:='_before uncaging';
  ExtendWindowtitle;
end;

macro 'Add "_after uncaging" to window title [7]';
begin
  extension:='_after uncaging';
  ExtendWindowtitle;
end;

macro 'Add "_ROI" to window title [8]';
begin
  extension:='_ROI';
  ExtendWindowtitle;
end;

macro 'Shorten window title by one character [9]';
var
  picnamelength: integer;
  picname: string;
begin
  picname:=windowtitle;
  picnamelength:=length(windowtitle);
  Delete(picname, picnamelength, 1); {removes last character
from picture name}
  SetPicName(picname);
end;

macro '(-' begin end; {Menu divider}

macro 'Add "_1 day recovery" to window title [3]';
begin
  extension:='_1 day recovery';
  ExtendWindowtitle;
end;

```

## 7.4 Time lapse imaging

```
{ Global variables }
var
mag, barlength: real; { objective magnification, size of scale bar to
use (µm) }
camerapid: integer; { PID of camera window }
bgpid: integer; { background window }
bgsub: boolean; { whether to subtract background }
tsoff: boolean; { whether to omit timestamp from
captured images }
asoff: boolean; { whether the AutoShutter feature
is off }
PhaseOpen, FluorescOpen: boolean; { whether we think the shutters are
open }
tperiod: real; { timelapse period }
n: integer; {Global variable used by integration macros}
hour,mini,seci:integer;
timeron:boolean;
nframes, nframes1, nframes2, nframes3, pframes, pframes2:integer;
name, wavelength, wavelength1, wavelength2:integer;
antigen, antigen1, antigen2, annotation, annotation2, annotation3,
framenumber: string;
Settings, Settings1, Settings2, generalsettings, nophas: boolean;
NumberofStainings, magnification: integer;
TimelapseSet, annotateon, annotateon2: boolean;
KindOfTimelapse: integer;
year,month,day,hour,min,sec,minute,second,DoW:integer;
roundnumber: integer;
```

```
{ Error(s) issues the error message S and terminates the macro. }
procedure Error(s:string);
begin
PutMessage(s); exit;
end;
```

```
procedure ResetTimer
var
```

```
year,month,day,hour,min,sec,DoW:integer;
begin
GetTime(year,month,day,hour,min,sec,DoW);
timeron:=True;
hour:=hour;
mini:=min;
seci:=sec;
end;
```

```
procedure Timer;
var
```

```
year,month,day,hour,min,sec,hourC,minC,secC,DoW:integer
;
year2,month2,day2,hour2,min2,sec2,hourC2,minC2,secC2,D
oW2:integer;
l,t,w,h:integer;
begin
GetRoi(l,t,w,h);
If (w=0) then Error("Select an ROI First");
if timeron then begin
GetTime(year,month,day,hour,min,sec,DoW);
if (sec>=sec1) then secC:=sec-sec1 else begin
secC:=(sec+60)-sec1;
min:=min-1;
end;
if (min>=mini) then minC:=min-mini else begin
minC:=min+60-mini;
hour:=hour-1;
end;
hourC:=hour-houri;
MoveTo(665,559);
SetForegroundColor(0);
SetFont('Helvetica');SetFont(14);
GetTime(year2,month2,day2,hour2,min2,sec2,DoW2);
write("Time: ",hour2:2,',');
if (min2<10) then
Write('0',min2:1,',') else Write(min2:2,',');
if (sec2<10) then
Write('0',sec2:1) else Write(sec2:2);
MoveTo(665, 547);
write("Date: ", year:4, '-');
if (month<10) then
write ('0', month:1, '-') else write (month:2, '-');
if (day<10) then write ('0', day:1) else write (day:2);
MoveTo(580,559);
Write("Timer: ",hourC:2,',');
if (minC <10) then
Write('0',minC:1,',') else Write(minC:2,',');
```

```
if (secC<10) then
Write('0',secC:1) else Write(secC:2);
RestoreRoi;
end else begin
ResetTimer;
Timer;
end;
end;
```

```
procedure OpenFluorescenceShutter;
begin
```

```
{Uniblitz Shutters are routinely set to active-low, i.e. an input
signal means no output, no input signal means output}
if (PhaseOpen=true) then scion[4]:= 12 {shutter 0 & 1 open}
else
scion[4]:=13; {Shutter 0 closed & 1 open}
FluorescOpen:=true;
end;
```

```
procedure CloseFluorescenceShutter;
begin
```

```
if (PhaseOpen=false) then scion[4]:= 15 {all shutters closed}
else
scion[4]:=14; {Shutter 0 closed & 1
open}
FluorescOpen:=false;
end;
```

```
procedure OpenPhaseShutter;
begin
```

```
if (FluorescOpen=true) then scion[4]:= 12 {shutter 0 & 1
open} else
scion[4]:=14; {Shutter 0 open & 1
closed}
PhaseOpen:=true;
end;
```

```
procedure ClosePhaseShutter;
begin
```

```
if (FluorescOpen=false) then scion[4]:= 15 {all shutters
closed} else
scion[4]:=13; {Shutter 0 closed & 1
open}
PhaseOpen:=false;
end;
```

```
macro 'Open Fluorescence Shutter [1]';
begin
OpenFluorescenceShutter;
end;
```

```
macro 'Close Fluorescence Shutter [2]';
begin
CloseFluorescenceShutter;
end;
```

```
macro 'Open Phase Shutter [3]';
begin
OpenPhaseShutter;
end;
```

```
macro 'Close Phase Shutter [4]';
begin
ClosePhaseShutter;
end;
```

```
macro '-' begin end; {Menu divider}
```

```
macro 'Reset Timer [R]';
begin
ResetTimer;
end;
```

```
macro 'Timer [T]';
begin
Timer;
end;
```

```
{
These two macros continuously integrate and display frames either off-
chip, using the Scion AG-5, or on-clip, using the Scion LG-3 and a Coho
```

4910 series camera. Press and hold the mouse button near the top of the Camera window to decrease the number of frames integrated. Press near the bottom to increase the number of frames integrated. Press above or to the left of the Camera window to stop integrating.

```

}

procedure Integrate (mode:string);
var
  x,y,delta:integer;
begin
  if n=0 then n:=6;
  repeat
    if button then begin
      GetMouse(x,y);
      if (x<0) or (y<0) then begin
        closeFluorescenceShutter;
        exit;
      end;
      delta:=round(0.333*n);
      if delta<1 then delta:=1;
      if y<220 then begin
        n:=n-delta;
        if n<1 then n:=1;
      end else begin
        n:=n+delta;
        if n>127 then n:=127;
      end;
      end;
      AverageFrames(mode, n);
    until false;
  end;

macro 'Counter +1 [+];'
begin
  name:=name+1;
  ShowMessage('Counter: ',name);
end;

macro 'Counter -1 [-];'
begin
  name:=name-1;
  ShowMessage('Counter: ',name);
end;

macro 'Picture number +1 [B]';
begin
  roundnumber:=roundnumber+1;
  ShowMessage('Picture number:\',roundnumber);
end;

macro 'Picture number -1 [V]';
begin
  roundnumber:=roundnumber-1;
  ShowMessage('Picture number:\',roundnumber);
end;

macro 'Antigen1 frames +1 [I]';
begin
  nframes1:=nframes1+1;
  ShowMessage('Antigen1:\Number of frames\integrated:
',nframes1);
end;

macro 'Antigen1 frames -1 [J]';
begin
  nframes1:=nframes1-1;
  ShowMessage('Antigen1:\Number of frames\integrated:
',nframes1);
end;

macro 'Antigen2 frames +1 [O]';
begin
  nframes2:=nframes2+1;
  ShowMessage('Antigen2:\Number of frames\integrated:
',nframes2);
end;

macro 'Antigen2 frames -1 [K]';
begin
  nframes2:=nframes2-1;
  ShowMessage('Antigen2:\Number of frames\integrated:
',nframes2);
end;

macro '(-' begin end; {Menu divider}

procedure FluorescenceSettings;
begin
  NumberOfStainings:=GetNumber('Enter Number of Stainings
-1 or 2-:', NumberOfStainings);

```

```

  if NumberOfStainings <> 1 then
    if NumberOfStainings <> 2 then
      Exit('Only 1 or 2 allowed!');
    if NumberOfStainings=1 then Settings1:=true
      else Settings1:=false;

  antigen1:=GetString('Name of Staining 1 / Antigen 1:');
  antigen1);
  if antigen1='Global String' then Exit('Please
enter name!');
  wavelength1:=GetNumber('Excitation wavelength of Antigen
1 in nm:', wavelength1);
  if (nframes1=0) then nframes1:=4;
  nframes1:=GetNumber('Number of Fluorescence-Frames
(Antigen 1):', nframes1);
  if Settings1=true then begin
    settings := true;
    Exit;
  end;

  antigen2:=GetString('Name of Staining 2 / Antigen 2:');
  antigen2);
  if antigen2='Global String' then Exit('Please
enter name!');
  wavelength2:=GetNumber('Excitation wavelength of Antigen
2 in nm:', wavelength2);
  if (nframes2=0) then nframes2:=4;
  nframes2:=GetNumber('Number of Fluorescence-Frames
(Antigen 2):', nframes2);
  Settings1 := true;
  Settings2 := true;
  Settings := true;

  exit;
end;

procedure Annotate;
begin
  if generalsettings=true then
  begin
    MoveTo(10,547);
    SetForegroundColor(0); SetFont('Helvetica');
    SetFontSize(14);
    write(annotation);
    MoveTo(10,559);
    write('Magnification:', magnification, 'x');
    if (nophase=true) then begin
      write (
', antigen, ' ', wavelength, 'nm ', nframes);
      if
(nframes>1) then framenummer:='frames' else framenummer:='frame';
      write(' ',
framenummer);
    end;
    if (nophase=false) then begin write
(' Phase contrast ', pframes);
    if
(pframes>1) then framenummer:='frames' else framenummer:='frame';
    write(' ',
framenummer);
    end;
    MoveTo(665,547);
    SetForegroundColor(0); SetFont('Helvetica');
    SetFontSize(14);
    GetTime(year,month,day,hour,min,sec,DoW);
    write('Date: ', year:4, '-');
    if (month<10) then write ('0',
month:1, '-') else write (month:2, '-');
    if (day<10) then write ('0', day:1)
else write (day:2);
    MoveTo(665,559);
    write('Time: ',hour:2,':');
    if (min<10) then Write('0',min:1,':')
else Write(min:2,':');
    if (sec<10) then Write('0',sec:1)
else Write(sec:2);
    end;
  end;

macro 'Fluorescence Settings [N]';
begin
  FluorescenceSettings;
end;

macro 'Phase contrast settings [M]';
begin
  if (pframes=0) then pframes:=1;
  pframes:=GetNumber('Number of Phase contrast-Frames to
integrate:', pframes);
end;

macro 'General settings [0]';
begin
  annotation:=GetString('Annotation 1: Date and/or Type of
experiment:', annotation);
  annotation2:=GetString('Annotation 2: Date and/or Type of
experiment:', annotation2);
  magnification:=GetNumber('Magnification:', magnification);

```

```

        ShowMessage('Date and/or Type of experiment:\',
annotation, '\Magnification:', magnification, 'x');
        generalSettings:=true;
end;

macro 'Annotation on/off [A]';
begin
    annotateon2:=annotateon;
    if (annotateon=true) then annotateon:=false;
    if (annotateon2=false) then annotateon:=true;
    if (annotateon=true) then begin
        ShowMessage('Annotation on');
    end else begin ShowMessage('Annotation off');
    end;
end;

macro 'Toggle annotation [7]';
begin
    annotation3:=annotation;
    annotation:=annotation2;
    annotation2:=annotation3;
    ShowMessage('Annotations switched');
end;

macro 'Save As "Window Title.tif" [S]';
begin
    SetSaveAs('TIFF');
    SaveAs;
end;

Macro 'Make Standard ROI [Q]'
begin
    MakeRoi(0,34,767,512);
end;

macro '(-' begin end; {Menu divider}

macro 'Integrate Phase [P]';
begin;
    nophase:=false;
    GetTime(year,month,day,hour,minute,second,DoW);
    StartCapturing;
    StopCapturing;
    StartCapturing;
    name:=name+1;
    if (pframes=0) then pframes:=2;
    AverageFrames('Integrate',pframes);

    if (annotateon=true) then Annotate;
    if (pframes>1) then framenumbers:='frames' else
framenumbers:='frame';
        SetPicName(name:3, '_', roundnumber:2, '_1p_', year:4, '-',
month:2, '-', day:2, '-', hour:2, '-', minute:2, '-', second:2, '-', pframes:1,
framenumbers);
        duplicate(windowtitle);
end;

procedure IntegrateFluorescent;
begin;
    if (nframes>1) then framenumbers:='frames' else
framenumbers:='frame';
    if (annotateon=true) then begin
        if (settings=false) then FluorescenceSettings;
        if (nframes<1) then FluorescenceSettings;
        nophase:=true;

        GetTime(year,month,day,hour,minute,second,DoW);
        StartCapturing;
        StopCapturing;
        StartCapturing;
        OpenFluorescenceShutter;
        AverageFrames('Integrate On-chip',nframes);
        Annotate;
        SetPicName(name:3, '_',
roundnumber:2, '_2f_', antigen, '-', nframes:1, framenumbers, '-', year:4, '-',
'-', month:2, '-', day:2, '-', hour:2, '-', minute:2, '-', second:2);
        closeFluorescenceShutter;
        duplicate(name:3, '-', roundnumber:2, '_2f_',
antigen, '-', nframes:1, framenumbers, '-', year:4, '-', month:2, '-', day:2, '-',
hour:2, '-', minute:2, '-', second:2);
        nophase:=false;
    end else begin
        if (nframes<1) then nframes:=1;

        GetTime(year,month,day,hour,minute,second,DoW);
        StartCapturing;
        StopCapturing;
        StartCapturing;
        OpenFluorescenceShutter;
        AverageFrames('Integrate On-chip',nframes);
        SetPicName(name:3, '_',
roundnumber:2, '-', year:4, '-', month:2, '-', day:2, '-',
second:2, '-', nframes:1, framenumbers);
        closeFluorescenceShutter;
        duplicate(name:3, '-',
roundnumber:2, '-', year:4, '-', month:2, '-', day:2, '-',
second:2, '-', nframes:1, framenumbers);
    end;

macro 'Integrate Fluorescent (Antigen 1) [F]';
begin
    settings:=settings1;
    antigen:=antigen1;
    wavelength:=wavelength1;
    nframes:=nframes1;
    IntegrateFluorescent;
end;

macro 'Integrate Fluorescent (Antigen 2) [G]';
begin
    settings:=settings2;
    antigen:=antigen2;
    wavelength:=wavelength2;
    nframes:=nframes2;
    IntegrateFluorescent;
end;

macro 'Integrate On-chip Using Cohu [C]';
begin
    StartCapturing;
    OpenFluorescenceShutter;
    Integrate('integrate on-chip');
    closeFluorescenceShutter;
end;

macro 'Integrate InvertedÉ';
{
    Inverts captured video to allow more than 128 frames to be
    integrated without overflow. For example, the sum of 256 pixels
    with an average value of 200(very dark) is 51,200, which is
    greater than the 32,767 maximum, but the sum of 256 pixels
    with an average value of 55(200 inverted) is 14,080.
}
begin
    nframes:=GetNumber('Number of Frames:', 200);
    SetVideo('Invert');
    AverageFrames('Integrate', nframes);
    SetVideo(''); {Don't invert}
    Invert;
end;

macro '(-' begin end; {Menu divider}

procedure SetTimelapse;
begin
    if (tperiod=0) then tperiod:=5;
    tperiod:=GetNumber('Seconds between pictures:',tperiod);
    KindOfTimelapse:= GetNumber('Timelapse: 1=Phase; 2=
Fluorescence; 3=both', KindOfTimelapse);
    if ((KindOfTimelapse<=1) AND
(KindOfTimelapse<=2) AND (KindOfTimelapse<=3)) then Exit('Only 1, 2
or 3 allowed!');
    PutMessage ('Your current integration settings for phase
and fluorescence will be used for the time lapse. ');
    TimelapseSet:=true;
end;

macro 'Set Timelapse [8]';
begin
    SetTimelapse;
end;

{Timelapse starts taking a timelapse series of pictures, every tperiod
seconds (use Set Timelapse to set this period). Use command-period to
abort the series.

Note: the timing loop doesn't handle the transition over midnight.}

procedure TimelapsePhase;
begin
    nophase:=false;
    GetTime(year,month,day,hour,minute,second,DoW);
    StartCapturing;
    OpenPhaseShutter;
    name:=name+1;
    if (pframes=0) then pframes:=1;
    AverageFrames('Integrate',pframes);
    ClosePhaseShutter;
    if (annotateon=true) then Annotate;

```

```

        if (pframes>1) then framenumbers:=frames' else
framenumbers:=frame';
        SetPicName(name:3, '_', roundnumber:2, '_1p_', year:4, '-',
month:2, '-', day:2, '_', hour:2, ':', minute:2, ':', second:2, '_', pframes:1,
framenumbers);
end;

procedure InsertTimer;
begin
    GetTime(year,month,day,hour,minute,second,DoW);
    RestoreROI;
    Timer;
    RestoreROI;
end;

procedure TimelapseFluorescent;
begin;
    if (nframes>1) then framenumbers:=frames' else
framenumbers:=frame';
    if (annotateon=true) then begin
        if (settings=false) then FluorescenceSettings;
        if (nframes<1) then FluorescenceSettings;
        nophase:=true;

        GetTime(year,month,day,hour,minute,second,DoW);
        StartCapturing;
        StopCapturing;
        StartCapturing;
        OpenFluorescenceShutter;
        AverageFrames('Integrate On-chip',nframes);
        Annotate;
        SetPicName(name:3, '_',
roundnumber:2, '_2f_', antigen, '-', nframes:1, framenumbers, '-', year:4,
'-', month:2, '-', day:2, '_', hour:2, ':', minute:2, ':', second:2);
        closeFluorescenceShutter;
        nophase:=false;
    end else begin
        if (nframes<1) then nframes:=1;

        GetTime(year,month,day,hour,minute,second,DoW);
        StartCapturing;
        StopCapturing;
        StartCapturing;
        OpenFluorescenceShutter;
        AverageFrames('Integrate On-chip',nframes);
        SetPicName(name:3, '_',
roundnumber:2, '_1', year:4, '-', month:2, '-', day:2, '_', hour:2, ':', minute:2, ':',
second:2, '_', nframes:1, framenumbers);
        closeFluorescenceShutter;
        end;
end;

end;

procedure AcquireImages;
begin
    if (KindOfTimelapse<=2) then begin { KindOfTimelapse<=2
means 'NOT "fluorescence only", but phase (1) or phase/fluorescence
(3)' }
        TimelapsePhase; { take phase picture }
        InsertTimer;
        { save phase image }
        SetSaveAs('TIFF');
        SaveAs;
    end;

    if (KindOfTimelapse<=1) then begin { 'KindOfTimelapse<=1
means NOT "phase only", but fluorescence (2) or phase/fluorescence (3)'
}
        TimelapseFluorescent; { take fluorescence
picture }
        InsertTimer;
        { save fluorescence image }
        SetSaveAs('TIFF');
        SaveAs;
        end;
end;

macro 'Timelapse [9]';
var
    l, t, w, h, round1: integer;
    year, month, day, hour, minute, second, DoW: integer;
    time, time2, next,last:real;

begin
    if (WindowTitle<>'Camera') then Startcapturing;
    if TimelapseSet=false then
        SetTimelapse;

    if (KindOfTimelapse<=1) then begin { settings for
fluorescence (2) or phase/fluorescence (3) timelapse }
        settings:=settings1;
        antigen:=antigen1;
        wavelength:=wavelength1;
        nframes:=nframes1;
    end;

    {wait(1);} { to avoid instant start }

    GetROI(l,t,w,h);
    if (w=0) then SelectAll;
    KillROI;
    RestoreROI; { save ROI for future RestoreROIs }
    StopCapturing; { in case we're live }
    if (tperiod=0) then tperiod:=5;

    AcquireImages; {First image is acquired "outside" the while
loop to allow instant start}

    { start at the next multiple of tperiod }
    GetTime(year,month,day,hour,minute,second,DoW);
    time:=second+60*(minute+60*hour); { time is converted into
seconds }
    if (tperiod<60) then next:=time+tperiod
    else next:=time+(60-second);
    last:=time;

    while true do begin
        while (time<next) do begin

            GetTime(year,month,day,hour,minute,second,DoW);
            time:=second+60*(minute+60*hour);
            if (time>last) then begin

                ShowMessage(hour:2, ':', minute:2, ':', second:2, '\', next-time);
                last:=time;
            end;
        end;

        AcquireImages;

        if (w>0) then begin
            SetLineWidth(1);
            DrawBoundary;
        end;

        RestoreROI;
        next:=next+tperiod;
    end;
end;

```

## 7.5 Kymograph building and analysis

```
{global variables}
var
i, bigger, BiggerStack, OldStack, OldStackSize: integer;
angle, magnif, picscale, number, i, SourceWindow, intermediate, root:
integer;
a, b, c, d, left, top, width, height, FirstSlice, LastSlice: integer;
AngleSet, MagnifSet, StackPresent, ProcSelect, ProcSelect2, SelectSet:
boolean;
Stack, Stack2, Kymograph, Stacksize, Stack2Size: integer;
timescalepix, timescalesec, picscale, measurecount: integer;
xfix, yfix, down, right, xy, SecondSelect, ROIwidth: integer;
PicScaleSet, TimeScaleSet, ROIset, AnchorDef, FirstSliceAdded,
SecondSlice, SecondSlice2: boolean;
extension, custextensio: string;

macro 'Set rotation angle [1]';
begin
    If (angleset=false) then angle:=90;
    angle:=Getnumber('Please enter rotation angle (-180 <= x <=
180):', angle, 0);
    if (angle>=-180) then
        if (angle<=180) then
            AngleSet:=true
        else Exit('Not a valid angle!');
    end;
end;

macro 'Set magnification [2]';
begin
    If (MagnifSet=false) then magnif:=1;
    magnif:=Getnumber('Enter magnification (0.05 <= scale <=
25.0):', magnif);
    if (magnif>=0.05) then
        if (magnif<=25) then
            MagnifSet:=true
        else Exit('Not a valid Scale!');
    end;
end;

macro 'Set Slice Selection [3]';
begin
    FirstSlice:=GetNumber('Enter number of first slice to be
processed:', FirstSlice, 0);
    LastSlice:=GetNumber('Enter number of last slice to be
processed:', LastSlice, 0);
    SelectSet:=true;
end;

macro 'Process Slice Selection only on/off [4]';
begin
    ProcSelect2:=ProcSelect;
    if (ProcSelect=true) then ProcSelect:=false;
    if (ProcSelect2=false) then ProcSelect:=true;
    if (ProcSelect=true) then begin
        ShowMessage('Slice Selection active');
    end else begin ShowMessage('Slice Selection inactive');
    end;
end;

procedure SetPicScale;
begin
    If picscale=0 then picscale:=3.856;
    picscale:=GetNumber('Please enter scale (pixel/μm):',
picscale, 3);
    SetScale(picscale,'μm');
    PicScaleSet:=true;
end;

macro 'Set picture scale (pixel/μm) [5]';
begin
    SetPicScale;
end;

procedure SetTimeScale;
begin
    If TimeScaleSec=0 then TimeScaleSec:=5;
    If TimeScalePix=0 then TimeScalePix:=4;

    timescalesec:=GetNumber('Please enter seconds between
frames:', timescalesec, 0);
```

```
timescalepix:=GetNumber('Pixel width of 1 frame in the
kymograph:', timescalepix, 0);
    TimeScaleSet:=true;
end;

macro 'Set time scale [6]';
begin
    SetTimeScale;
end;

macro '-'; {menu divider}
begin
end;

Macro 'Make Standard ROI [Q]';
var
a,b,c,d: integer;
begin
    SelectAll;
    GetROI(a,b,c,d); {a=left, b=top, c=width, d=height}
    if (c=768) then begin
        MakeROI(0,34,767,512)
    end else begin
        MakeROI(100, 100, 768, 576);
    end;
end;

Macro 'Set width of ROI [C]';
var
a,b,c,d: integer;
begin
    GetROI(a,b,c,d);
    if (c=0) then exit;
    if (ROIWidth=0) then ROIWidth:=c;
    ROIWidth:=GetNumber('Enter width of ROI:', ROIWidth, 0);
    MakeROI(a,b,ROIWidth, d);
end;

macro 'Define ROI [D]';
begin
    GetROI(a, b, c, d); {a=left, b=top, c=width, d=height}
    If (c=0) then Exit('Please define ROI first!');
    ROISet:=true;
end;

macro 'Show defined ROI [F]';
begin
    if (ROISet=false) then Exit('Define ROI first!');
    MakeROI(a,b,c,d);
end;

macro 'Rotate ROI [R]';
var
RotatedPic: integer;
begin
    SourceWindow:=PidNumber;
    KillROI;
    RestoreROI;
    GetROI(left,top,width,height);
    Copy;
    Root:=Sqrt(width*width+height*height);
    SetNewSize(Root,Root);
    MakeNewWindow('Intermediate');
    Intermediate:=PidNumber;
    Paste;
    SelectAll;
    SetScaling('Bilinear, New Window');
    if (MagnifSet=false) then Magnif:=1;
    if (AngleSet=false) then Angle:=90;
    ScaleAndRotate(Magnif,Magnif,angle);
    RotatedPic:=PidNumber;
    SelectPic(Intermediate);
    Dispose;
    SelectPic(RotatedPic);
    SetForegroundColor(0);
    MakeROI(root/2-50,0, 100, 14);
    Fill;
    MoveTo(root/2-42,0);
    SetForegroundColor(255);
    Write(Angle, ' degree turned');
    MakeROI(root/2-2, 30, 4, 100);
end;

macro 'Rotate ROI with various angles [V]';
var
RotatedPic, FlexAngle, AngleStack: integer;
```

```

begin
    SourceWindow:=PidNumber;
    KillROI;
    RestoreROI;
    GetROI(left,top,width,height);
    Copy;
    SetForegroundColor(255);
SetFont('Helvetica');SetFontSize(14);
    Root:=Sqrt(width*width+height*height);
    SetNewSize(Root,Root);
    MakeNewStack('Tested angles');
    AngleStack:=PidNumber;
    SetScaling('Bilinear, New Window');
    if (MagnifSet=false) then Magnif:=1;
    if (AngleSet=false) then Angle:=90;
    for i:=0 to 10 do begin
        SelectPic(SourceWindow);
        Copy;
        MakeNewWindow('Intermediate');
        Intermediate:=PidNumber;
        Paste;
        SelectAll;
        FlexAngle:=angle-10+i*2;
        ScaleAndRotate(Magnif,Magnif,FlexAngle);
        RotatedPic:=PidNumber;
        SelectAll;
        Copy;
        Dispose;
        SelectPic(Intermediate);
        Dispose;
        SelectPic(AngleStack);
        Paste;
        MoveTo(0,0);
        Write(FlexAngle, ' degree turned');
        If (i<10) then AddSlice;
        SelectPic(SourceWindow);
        MakeROI(left,top,width,height);
        Copy;
        Paste;
    end;
    SelectPic(AngleStack);
    MakeROI(root/2-2, 30, 4, 100);
end;

macro 'Dispose window [+];
begin
    Dispose;
end;

procedure CheckStack1;
begin
    StackPresent:=false;
    if nPics=0 then begin
        PutMessage('This macro requires a stack.');
```

exit;

```

    end;
    if nSlices=0 then begin
        PutMessage('This window is not a stack.');
```

exit;

```

    end;
    StackPresent:=true;
end;

procedure CheckStack2;
begin
    if nSlices=0 then StackPresent:=false
    else StackPresent:=true;
end;

macro 'Rotate ROI in stack [T]';
var
    FirstSlice2: integer;
begin
    CheckStack1;
    SetScaling('Bilinear, New Window');
    if (MagnifSet=false) then Magnif:=1;
    if (AngleSet=false) then Angle:=90;
    Stack:=PidNumber;
    StackSize:=nSlices;
    if (ProcSelect=true) then begin
        if LastSlice<Stacksize then
            StackSize:=LastSlice;
        FirstSlice2:=FirstSlice;
    end else begin
        FirstSlice2:=1;
    end;
    GetRoi(left,top,width,height);
    if width=0 then begin
        SelectAll;
        GetRoi(left,top,width,height);
    end;
    Root:=Sqrt(width*width+height*height);
    SetNewSize(Root,Root);
    MakeNewStack('Stack2');
    Stack2:=PidNumber;
    ChoosePic(Stack);
    for i:=FirstSlice2 to StackSize do begin
        ChoosePic(Stack);
        ChooseSlice(i);
        Copy;
        MakeNewWindow('Intermediate');
        Intermediate:=PidNumber;
        Paste;
        SelectAll;
        ScaleAndRotate(Magnif,Magnif,angle);
        SelectAll;
        Copy;
        Dispose;
        ChoosePic(Intermediate);
        Dispose;
        ChoosePic(Stack2);
        ChooseSlice(i);
        Paste;
        If (i<StackSize) then AddSlice;
    end;
    SelectSlice(1);
    SetForegroundColor(0);
    MakeROI(root/2-50,0, 100, 14);
    Fill;
    MoveTo(root/2-42,0);
    SetForegroundColor(255);
    Write(Angle, ' degree turned');
    MakeROI(root/2-2, 30, 4, 100);
end;

macro '(-); {menu divider}
begin
end;

procedure Measurement;
var
    left2,top2,width2,height2: integer;
    duration, distance: integer;
begin
    GetRoi(left2,top2,width2,height2);
    If (width2=0) then exit;
    If (PicScaleSet=false) then SetPicScale;
    If (TimeScaleSet=false) then SetTimeScale;
    SetOptions('User1; User2');
    SetPrecision(2);
    SetUser1Label('time_sec');
    SetUser2Label('dist_µm');
    duration:=trunc(width2/timescalepix+1.6)*timescalesec;
    {duration} is a good estimation for the number
of frames which are
crossed by the line selection. '+1.6'
compensates that one measures
from roughly the middle of one frame to
roughly the middle of another,
thereby missing more or less the width of one
frame (namely the first
half of the first and the second half of the last
frame). In addition
it compensates for the truncation of the
number.}
    distance:=height2/PicScale;
    rUser1[rcount+1]:=duration;
    rUser2[rcount+1]:=distance;
    Measure;
    SetForegroundColor(120);
    Setlinewidth(2);
    DrawBoundary;
end;

macro 'Measure [A]';
begin
    Measurement;
end;

macro 'Redo last measurement [L]';
begin
    SetCounter(rcount-1);
    Measurement;
end;

macro 'Reset measurement counter [0]';
begin
    ResetCounter;
end;

macro '(-); {Menu divider}

```

```

begin
end;

macro 'Make Kymograph [Y]';
begin
    CheckStack1;
    GetRoi(left,top,width,height);
    KillROI;
    RestoreROI;
    If (width=0) then Exit("Select ROI first!");
    Stack:=PidNumber;
    StackSize:=nsllices;
    SetNewSize(Stacksize*width,height);
    MakeNewWindow("Kymograph");
    Kymograph:=PidNumber;
    for i:=1 to StackSize do begin
        SelectPic(Stack);
        SelectSlice(i);
        Copy;
        SelectPic(Kymograph);
        MakeROI(((i-1)*width),0,width,height);
        Paste;
    end;
    KillROI;
end;

macro '(-'; {menu divider}
begin
end;

macro 'Crop area outside ROI';
var
name: string;
FirstSlice2: integer;

begin
    CheckStack2;
    GetRoi(left,top,width,height);
    name:=windowtitle;
    SetNewSize(width,height);
    If (StackPresent=false) then begin
        Copy;
        MakeNewWindow(name);
        Paste;
    end else begin
        Stack:=PidNumber;
        StackSize:=nsllices;
        if (ProcSelect=true) then begin
            if LastSlice<Stacksize
then StackSize:=LastSlice;

            FirstSlice2:=FirstSlice;
            end else begin
                FirstSlice2:=1;
            end;
            MakeNewStack(name);
            Stack2:=PidNumber;
            for i:=FirstSlice2 to StackSize do begin
                SelectPic(Stack);
                SelectSlice(i);
                Copy;
                SelectPic(Stack2);
                Paste;
                If (i<StackSize) then AddSlice;
            end;
            SelectSlice(1);
            end;
            KillROI;
end;

macro 'Outline ROI [O]';
begin
    SetForegroundColor(120);
    Setlinewidth(2);
    DrawBoundary;
end;

macro '(-'; {menu divider}
begin
end;

macro 'Save As "Window Title.tif" [S]';
begin
    SetSaveAs("TIFF");
    SaveAs;
end;

End;

procedure ExtendWindowtitle;
begin
    duplicate(windowtitle);
    SetPicName(windowtitle, extension);
end;

macro 'Add custom extension to window title [N]';
begin
    if (custextensio="Global String') then
    custextensio:='_o'clock';
    custextensio:=GetString("Enter custom file name
extension:");
    extension:=custextensio;
    ExtendWindowtitle;
end;

macro 'Add "_anterograde" to window title';
begin
    extension:='_anterograde';
    ExtendWindowtitle;
end;

macro 'Add "_retrograde" to window title';
begin
    extension:='_retrograde';
    ExtendWindowtitle;
end;

macro 'Shorten window title by one character [-]';
var
    picnamelength: integer;
    picname: string;

begin
    picname:=windowtitle;
    picnamelength:=length(windowtitle);
    Delete(picname, picnamelength, 1); {removes last character
from picture name}
    SetPicName(picname);
end;

macro '(-'; {Menu divider}
begin
end;

macro 'Define anchor point [7]';
begin
    GetMouse (xfix, yfix);
    showmessage('Anchorpoint defined:UX: ', xfix, ' Y: ', yfix);
    rUser1[1]:=xfix;
    rUser2[1]:=yfix;
    SetCounter(rcount+1);
    AnchorDef:=true;
end;

macro 'Switch process all slices/every second slice';
begin
    SecondSlice2:=SecondSlice;
    if (SecondSlice=true) then SecondSlice:=false;
    if (SecondSlice=false) then SecondSlice:=true;
    if (SecondSlice=true) then begin
        ShowMessage('Every second slice will be
processed');
    end else begin ShowMessage('Every slice will be
processed');
    end;
end;
SecondSelect

procedure MoveImage;
var
    xfix2, yfix2: integer;

begin
    if (AnchorDef=false) then Exit("Please define anchor point
first!");
    if (ROIset=false) then Exit("Please define ROI first!");
    getMouse (xfix2, yfix2);
    MakeROI(a, b, c, d);
    Copy;
    {DrawBoundary;}
    MoveROI(xfix-xfix2, yfix-yfix2); {MoveRoi(dx,dy) Moves ROI
right dx pixels and down dy pixels.}
    Paste;
    {DrawBoundary;}
end;

```

```

Macro 'Move image according to anchor point [8]';
begin
    SetForegroundColor(125);
    SetLineWidth(2);
    MoveImage;
end;

Macro 'Move remaining slices according to anchor point [X]';
var
i, Current, Last: integer;
begin
    for i:=SliceNumber to nSlices do begin
        SelectSlice(i);
        MoveImage;
    end;
end;

macro '(-'; {Menu divider}
begin
end;

procedure ROIStackMove;
begin
    CheckStack1;
    xy:=SliceNumber;
    i:=SliceNumber;
    if (SecondSlice=true) then SecondSelect:=2 else
SecondSelect:=1;
    while i<=nslices do begin
        SelectSlice(i);
        MakeROI(80, 80, 808, 616);
        Copy;
        MoveRoi(down, right); {MoveRoi(dx,dy) Moves
ROI right dx pixels and down dy pixels.}
        Paste;
        i:=i+SecondSelect;
    end;
    SelectSlice(xy);
end;

macro 'Move content of ROI in whole stack 1 pixel to the left [G]';
begin
    down:=-1;
    right:=0;
    ROIStackMove;
end;

macro 'Move content of ROI in whole stack 1 pixel to the right [H]';
begin
    down:=1;
    right:=0;
    ROIStackMove;
end;

macro 'Move content of ROI in whole stack 1 pixel up [Z]';
var
xy: integer;
begin
    down:=0;
    right:=-1;
    ROIStackMove;
end;

macro 'Move content of ROI in whole stack 1 pixel down [B]';
begin
    down:=0;
    right:=1;
    ROIStackMove;
end;

macro '(-'; {menu divider}
begin
end;

procedure ROI Move;
begin
{
    GetROI(a, b, c, d); {a=left, b=top, c=width, d=height}
    If (c=0) then Exit('Please make ROI first!');}
    MakeROI(70, 80, 808, 616);
    Copy;
    MoveRoi(down, right); {MoveRoi(dx,dy) Moves ROI right dx
pixels and down dy pixels.}
    Paste;
}

{
    MakeROI(a, b, c, d);}
end;

macro 'Move content of ROI 1 pixel to the left [J]';
begin
    down:=-1;
    right:=0;
    ROI Move;
end;

macro 'Move content of ROI 1 pixel to the right [K]';
begin
    down:=1;
    right:=0;
    ROI Move;
end;

macro 'Move content of ROI 1 pixel up [I]';
var
xy: integer;
begin
    down:=0;
    right:=-1;
    ROI Move;
end;

macro 'Move content of ROI 1 pixel down [M]';
begin
    down:=0;
    right:=1;
    ROI Move;
end;

macro '(-'; {menu divider}
begin
end;

macro 'Transfer Stack to bigger window';
begin
    SetNewSize(968, 776);
    OldStack:=PidNumber;
    OldStackSize:=nslices;
    MakeNewStack('Bigger Stack');
    BiggerStack:=PidNumber;
    for i:=1 to OldStackSize do begin
        SelectPic(OldStack);
        SelectSlice(i);
        SelectAll;
        Copy;
        SelectPic(BiggerStack);
        SelectSlice(i);
        MakeROI(100, 100, 768, 576);
        Paste;
        if (i<OldStackSize) then AddSlice;
    end;
end;

macro 'Select Image in Bigger Stack [P]';
begin
    MakeROI(100, 100, 768, 576);
end;

macro 'Add first slice after every slice';
begin
    CheckStack1;
    SelectSlice(1);
    SelectAll;
    Copy;
    i:=0;
    while i<nslices-2 do begin
        SelectSlice(i+2);
        AddSlice;
        SelectAll;
        Paste;
        i:=i+2;
    end;
    FirstSliceAdded:=true;
    SecondSlice:=true;
    SelectSlice(1);
end;

macro 'Remove added first slices';
begin
    CheckStack1;

```

```
{      If FirstSliceAdded=false then Exit("No slices have been
added to this stack.);}
      i:=1;
      while i<nslices-1 do begin
        SelectSlice(i+2);
        DeleteSlice;
        i:=i+1;
      end;
      FirstSliceAdded:=false;
      SecondSlice:=false;
      SelectSlice(1);
end;

macro '-'; {menu divider}
begin
end;

macro 'Goto first slice [W]';
begin
      CheckStack1;
      SelectSlice(1);
end;

macro 'Goto last slice [E]';
begin
      CheckStack1;
      SelectSlice(nslices);
end;
```



## **8. Acknowledgements**

First, I wish to thank my supervisor Dr. Frank Bradke for giving me the opportunity to do my PhD in his lab, for his support, his encouragement and his training in presentation and writing skills. The excellent working atmosphere in his lab has always made it a nice place to go to. Especially, I would like to express my gratitude to Dr. Bradke for his support not only in good but also more difficult times.

I am very grateful to Dr. Rüdiger Klein and Dr. Damian Brunner (EMBL) as members of my thesis committee for their efforts, their precious time and suggestions.

I am indebted to Dr. Joshua Sanes for providing SAD A/B knockout mice, Dr. Magdalena Götz for GFP-expressing mice, Drs. Anna Akhmanova and Vic Small for the EB3-GFP expression plasmid and Drs. Susanne Nagel and Erich Nigg for the Tubulin-GFP construct. I am very grateful to Dr. Michael Schleicher for kindly sharing the antibody against tyrosinated tubulin. I am also indebted to Ralf Zenke for help with setting up the FRAP experiments.

I am very grateful to Jonathan Mackinnon for critically reading and proof-reading this thesis. Thanks a lot!

Especially, the members of the fabulous Bradke lab deserve my deep gratitude for their support and friendship.

In particular, Liane Meyn, for help with neuronal cultures, for keeping lab and kitchen tidy, and for many delicious cakes. Susana Gomis-Rüth, my “little (PhD) sister”, for Salsa music, GFP-expressing neurons, for cheering me up and introducing me to the world of Jorge Cham’s PhD-comics, and for mutual understanding. Boyan Garvalov, for great support and good music, his excellent dry sense of humor, and for patiently reading my paper manuscript over and over again, giving priceless input. Ali Ertürk, for Borma, friendship, Cinema Clubs, and the best trip to the USA I have ever had – “*Thanks, man!*”. Farida Hellal, for discussions, guidance and encouragement on both a scientific and personal level, many smiles and invaluable help to shape my paper to be accepted. Joana Enes, for her unbreakable optimism, her cheerful nature, and her unmatched skills at preparing DRG neurons. Keep going! Sabina Tahirovic, for sharing reagents and equipment at the “socialistic bench”, moral support and true appreciation of gentlemen. Bhavna Ylera, for her calm nature, her initial recommendation to Frank, and her excellent working morale. Dorothee ‘Dodo’ Neukirchen, for joining me to ‘X-Ray World’, for friendship and support, for simply listening, and for countless smiles and jokes. Michael Stiess, for supply with all kinds of music, for keeping the stocks of sweets filled, and for many Kalauer and Schenkelklopfer. Finally, Frank, for his support, encouragement and patience, his

cheerful personality, and for carefully selecting all these wonderful people to become part of his lab. I would also like to thank some of the transient lab members, Andres Hortado and Kevin Flynn, and one of the best neighbors our lab ever had, Harry Schnürch, for bringing out the best in us.

I would also like to express my gratitude to the members of the animal facilities and the MPI workshops, our EDV group, and the members of the Photolab for continued support.

On a personal level, I would like to thank Sabine Seidel, Max Mühlhaus, and the members of the “Gentlemen’s Club”, Matthias Dax, Florian Kiesl and Sascha Kampf, for continued encouragement, inspiration and friendship over the years. I am also deeply indebted to S. Stallone for the “Rocky” series and Bill Conti for the respective soundtrack.

Annette Dell’Aere danke ich ganz besonders herzlich für ihre Unterstützung, ihre große Geduld und die vielen Aufmunterungen, womit sie im Speziellen zum Gelingen dieser Arbeit beigetragen hat.

Meinen Eltern und Großeltern gilt ebenfalls mein besonderer Dank. Während des Studiums und der Promotion konnte ich immer auf sie zählen und ihrer Unterstützung gewiß sein. Danke dafür und für so vieles mehr!

## **9. Curriculum vitae**

### **Personal details**

**Name:** Harald Witte  
**Date of birth:** July 3<sup>rd</sup>, 1976  
**Place of birth:** Munich, Germany  
**Citizenship:** German

### **Education**

**July 2003 to July 2008** Ph.D. thesis in the laboratory for „Axonal Growth and Regeneration“ of Dr. Frank Bradke at the Max-Planck-Institute of Neurobiology, Martinsried  
Title: “The role of microtubules in initial neuronal polarization“

**March 2002 – Feb. 2003** Diploma thesis in the laboratory of Prof. Rudolf Grosschedl at the Gene Center, Munich  
Title: “Identification of ‘Matrix Attachment Region’-binding proteins and cofactors in a Yeast-One-Hybrid screen“

**Nov. 1997 – Feb. 2002** Diploma in Biology, Ludwig-Maximilians-Universität, Munich  
Final grade: 1.1  
Major subject: Genetics  
Minor subjects: Biochemistry, Physiological Botany and Cell Biology  
Additional subject: Informatics

**Oct. 1996 – Nov. 1997** Civil service

**1983 – 1996** Primary and Secondary Education  
May 1996 University-entrance diploma (Abitur; final grade: 1.1)

### **Scientific communications and publications**

- **Witte, H.**, and F. Bradke. 2008. The Establishment of Neuronal Polarity. *Curr Opin Neurobiol.* (in preparation)
- **Witte, H.**, D. Neukirchen, and F. Bradke. 2008. Microtubule stabilization specifies initial neuronal polarization. *J Cell Biol.* 180:619-32.
- **Platform presentation (talk)** at Cold Spring Harbor Laboratory meeting „Axon Guidance, Synaptogenesis & Neural Plasticity“, Sept. 2006

- **Witte, H.**, and F. Bradke. 2005. Guidance of Axons to Targets in Development and in Disease. In *Peripheral Neuropathy*. Vol. 1. P.J. Dyck and P.K. Thomas, editors. Elsevier Inc., Philadelphia. 447-481.
- **International Patent:** Bradke, F., **Witte, H.**, Ertürk, A. Use of microtubule stabilizing compounds for the treatment of lesions of CNS axons (WO/2006/094811). Filed March 9<sup>th</sup>, 2004 / March 9<sup>th</sup>, 2006